FLOW MODELLING OF CYCLONES

A thesis

submitted in partial fulfilment

of the requirements for the Degree

of

Doctor of Philosophy in Chemical Engineering

in the

University of Canterbury

By

Jian Qiang Zhao

University of Canterbury

1999

ACKNOWLEDGEMENTS

I am very grateful to Dr John Abrahamson for his guidance and supervision of the work in this thesis. He has paid a lot of energy and time to check my work and make my thesis more readable. I am very appreciative of his efforts of personal support to my life.

I would like to express my appreciation for assistance given to me by the staff in the Department of Chemical and Process Engineering.

Finally I wish to thank my parents for their financial assistance and encouragement.

Abstract

Cyclones have simple structures, a long development history and extensive applications, but their design methods are empirical. More knowledge of cyclone mechanisms and more flexible and reliable design methods from first principles are needed.

In this thesis, I discuss the development processes of cyclone theory and design method, and find that suitably simplified analytical solutions of the motion equations for cyclones are both desirable and possible.

I study the solutions of the equations of motion with the assumption of tangential velocity not changing in axial direction, and find that they cannot describe the normal cyclone flowfield.

I find and study some solutions of the equations of motion with the inviscid assumption, and use them to compare some experimental findings of other researchers, and analyse the flowfield of cyclone. Some findings are that:

The solutions of the Eular's equations with some assumptions can describe the flowfields of cyclones fairly well.

The flowfields can be classified by several kinds of patterns. The distribution of vorticity across streamlines determines the flow patterns. It is very important to control this distribution to obtain the required flowfields.

The phenomenon of tangential velocity being self-similar at high value is explained from first principles.

The mechanism and calculation of the central isolated region in high efficiency cyclones are given.

The mechanism and control means of "shortcut and eddy flows" are given.

Based on understanding the flowfield of cyclones, a new concept cyclone for clarification is described. A preliminary scheme of design is given.

TABLE OF CONTENTS

NOTATION

a_i	polynomial coefficients of 'circulation term'
A_i	series expansion coefficient of Ψ_4^*
b_i	polynomial coefficients of 'total pressure'
B_i	series expansion coefficient of Ψ_4^*
c	arbitrary constant
c_1	arbitrary constant
c_2	arbitrary constant
c_3	arbitrary constant
c_4	arbitrary constant
C_a	calculation constant
C_i	constant of integration
D	constant of integration
h	total pressure, atm
H	dimensionless total pressure
p	static pressure, atm
$p_i(\cos\theta)$	the first kind of Legendre function
p_i^*	a part of eigenfunction
P	dimensionless static pressure
$q_i(\cos\theta)$	the second kind of Legendre function
q_i^*	a part of eigenfunction
r	radius vector, m
R	dimensionless radius vector
R_0	reference length, m
R_c	dimensionless cylindrical radius
r_e	upper boundary radius vector, m
R_e	dimensionless upper boundary radius vector
r_s	lower boundary radius vector, m
R_s	Dimensionless lower boundary radius vector

Q	Dimensionless volume flow rate
Q_I	Dimensionless input volume flow rate
Q_N	Dimensionless net volume flow rate
V_0	arbitrary velocity
v_i	ith eigenvalue
$V_{\max 0}$	reference velocity, m/s
v_r	fluid velocity in radius direction, m/s
V_r	dimensionless fluid radial velocity (cylindrical radius)
V_R	dimensionless fluid velocity in radius direction (spherical radius)
v_ϑ	fluid velocity in colatitude direction, m/s
V_ϑ	dimensionless fluid velocity in colatitude direction
V_x	dimensionless fluid vertical velocity
V_{xu}	dimensionless fluid vertical velocity at upstream boundary
v_φ	fluid velocity in longitude direction, m/s
V_φ	dimensionless fluid velocity in longitude direction
$V_{\varphi u}$	dimensionless fluid tangential velocity at upstream boundary
$Z_i(\theta)$	ith eigenfunction
Z_{ig}	calculation constant
Z_{1ig}	calculation constant
Z_{2ig}	calculation constant
Z_{3ig}	calculation constant
Z_{4ig}	calculation constant

Greek letters

α	half angle of conical wall
γ	circulation, m^2/s
Γ	dimensionless circulation
θ	colatitude
ρ	fluid density, kg/m^3
φ	longitude

ψ	streamfunction, m^3/s
Ψ	dimensionless streamfunction
Ψ_I	dimensionless input streamfunction
Ψ_N	dimensionless net streamfunction
Ψ_1^*	a part of the solution of this problem
Ψ_2^*	a part of the solution of this problem
Ψ_3^*	a part of the solution of this problem
Ψ_4^*	a part of the solution of this problem
ω_φ	dimensionless fluid vorticity in longitude direction
ω_R	dimensionless fluid vorticity in radius direction (spherical radius)
ω_θ	dimensionless fluid vorticity in colatitude direction
Ω	angular velocity

Chapter 1

Introduction

1.1 CYCLONE—A BASIC DESCRIPTION

In THE OXFORD ENGLISH DICTIONARY (1933) the word "Cyclone" is explained as:

> A name introduced in 1848 by H. Piddington, as a general term for all storms or atmospheric disturbances in which the wind has a circular or whirling course. Its Greek meaning is "the coil of a serpent".

In THE NEW SHORTER OXFORD ENGLISH DICTIONARY (1993) a further explanation is:

> A pressure system characterised by a low central barometric pressure and circulation.
>
> A centrifugal machine for separating solids.

The former describes a natural phenomenon; the latter describes a cyclone separator, which was first patented in 1884. It can be conceived from this naming that a cyclone separator, a wonderful invention, might be inspired by the natural phenomenon. People must think that there are some relationships between the natural phenomenon and the equipment; both should possess some common characteristics. Knowledge about these common characteristics may be the original theory of the cyclone separator.

The main objective of a cyclone separator is to create a vortex, which will centrifuge the heavier materials to the walls where they can be transported into the collecting hopper. Unlike centrifuges, cyclone separators have no moving parts and the fluid itself performs the necessary spinning motion. There are many different types of cyclone separators. We can describe them from their basic function then the necessary structure.

The cyclone separator, often simply called a cyclone, is a device that redistributes fluid total pressure energy to create rotational fluid motion. This rotational motion causes relative movement of materials suspended in the fluid thus permitting separation of these materials, one from another or from the fluid. The rotation is produced by tangential injection of the fluid into a vessel or by guiding vanes at the entry. The vessel can be cylindrical or conical, but more usual it is the combination: an upper cylindrical portion and a lower conical portion.

The nearer to the axis, for equilibrium among different fluids the lighter the fluid will be. The outlet for the bulk of the fluid is usually located near to or on the axis of the vessel such that the rotating lighter fluid can escape directly. A rotational motion has thus built into it an inward radial motion somewhere within the vessel. Particles of a suspended material have two opposing forces acting on them in the radial direction, one in an outward radial direction due to the centrifugal acceleration, and one in an inward radial direction due to the drag force between the particles and fluid.

The magnitude of these forces is dependent on the flowfield and the physical properties of both the fluid and the suspended material (eg. size of particles, shape of particles, densittes of particles and fluid, and viscosity of fluid).

In the separation process the heavier product moves radially outwards, while the lighter moves radially inwards. It is therefore necessary to provide two outlets. One outlet is normally axial for the lighter product; the other outlet may be peripheral or axial. There are two major types of cyclone separators: direct-through cyclones and return flow cyclones. In the direct-through cyclone, the feed enters at the top, the lighter product leaves from the bottom and the heavier product at the lower periphery; in the return-flow cyclone, the feed enters at the upper periphery, the lighter product leaves overhead and the heavier product leaves from the bottom.

The return-flow cyclone offers higher collection efficiency, and is the more widely used by far. However, the direct-through cyclone has a high fluid-handling capacity and incurs a low pressure drop, so it is appropriate for large fluid flow rates and for situations where pressure drop must be minimised, as in fly-ash collectors. In this

work, the return-flow cyclone is the main object to study, but some ideas and methods can be used for the straight-through cyclone.

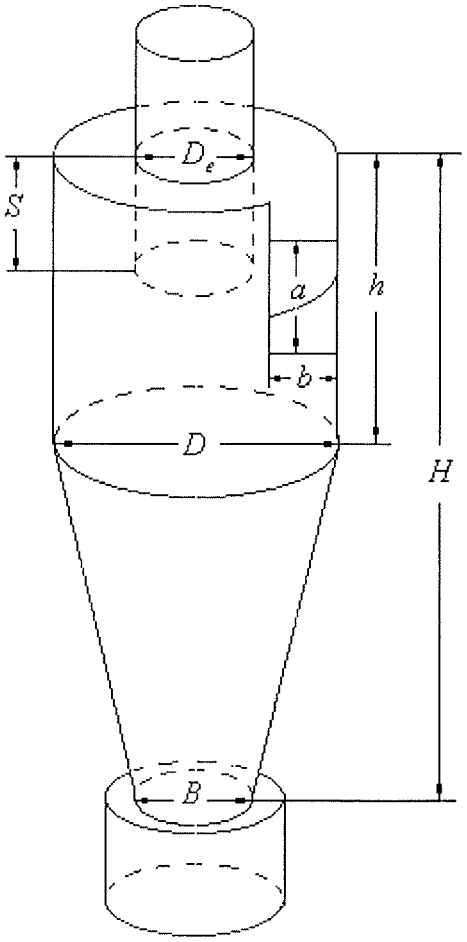

Fig, 1-1. Cyclone with tangential gas inlet and notations of dimensions

The typical returned flow cyclone possesses eight dimensions: inlet height a, inlet width b, lighter fluid outlet diameter D_e, outlet duct length S, cylinder diameter D, cylinder height h, cyclone height H, and heavier product outlet diameter B; see Fig. 1-1.

Each application has its particular requirements and goals, and it calls for changes in design and operation of the cyclone to make the cyclone most suitable for each case. Determining the eight dimensions is the task of design.

1.2 APPLICATIONS OF CYCLONES

Cyclones can be used to separate almost any phase from another phase. If there is a difference in size, density or shape between the phases, cyclones can be used to separate:

- solid from gas, such as particles from flue gases, fibre from air
- solid from liquid, such as sands from oil
- solid from solid, such as shale from coal, broken palm kernels from shells
- liquid from gas, such as paint droplets from air in panel beating workshop
- liquid from liquid, such as oil from water
- gas from liquid, such as gas from crude oil

Applications of cyclones fall into several broad categories, and we introduce some of them as following.

Clarification

The aim is to produce clear overflow, which is the same as to maximise the mass recovery of solids from the feed. The cyclone is therefore to be designed to give a maximum efficiency for all sizes of particle that will be fed to it. The feed should be dilute, otherwise the overflow could not be clear due to diffusion and crowding in particle exit. Normally a high efficiency design with small diameter cyclones nested in parallel in multi-cyclone arrangements is adopted. A high pressure is associated with high collection efficiency.

Applications include recovery of catalyst in the oil and chemical industries; separation of corrosion products in circulating systems in the nuclear power industry; removal of sand, scale and other organic or inorganic particles to protect heat exchangers, boilers, glands and seals; cleaning washwater in coal or ore processing plants; removal of drill chips from drill mud; degritting of milk of lime.

Thickening

This is for separating solids from liquids. The required duty in this case is to produce a high concentration of solids in the underflow and any loss of solids to the overflow is undesirable but of secondary importance. The feed solid concentrations in thickening applications are usually higher than in clarification duties. If the feed is too dilute, the connection of cyclones in series may be needed since the underflow liquid volume in normal cyclone practice is not less than about $1/50^{th}$ of the feed volume. Less than $1/50^{th}$ can only be achieved by impractically small underflow apertures, very large overflow apertures or high backpressure at the underflow. All these measures will decrease efficiency. Actually, if thick underflows are pursued, the total mass recovery of the feed solids in a cyclone must be sacrificed because throttling the underflow orifice leads to some loss of solids to the overflow.

A cyclone as a single unit cannot therefore be used for both clarification and thickening at the same time. If cyclones are to perform both thickening and clarification simultaneously, two or more units have to be connected in series, with one cyclone operated as a thickener and the other or others as a clarifier.

The applications include: thickening of the waste product from flue-gas desulphurization systems where cyclones are used to replace the more costly gravity thickeners; dewatering of mine back-fill; dewatering of silt in dredging operations; densification of the recovered and cleaned medium in medium recovery plants in dense medium separation; recovery and concentration of ammonium choride crystals or sodium bicarbonate.

Cyclone solid-gas separator (Dust collector)

Cyclones are the most widely used industrial dust collectors. The aim is to produce clearer gas or collect particles. Since no underflow needs to be concerned with, both aims require the same design to maximise the mass recovery of particles from the feed under certain requirements such as size of the particles to be collected or emission

regulation. Three general classes of cyclones can be considered. High-efficiency cyclones are designed primarily to provide high collection efficiency, but at the expense of high pressure drop or low gas flow. General-purpose designs aim for a compromise between efficiency, pressure drop, and gas flow. With high-throughout cyclones the emphasis is on handling a large gas volume with a reasonable pressure drop, and efficiency is sacrificed. The cyclones are designed to balance the number of cyclones and the gas throughput per cyclone with pressure drop and efficiency requirements.

Cyclone dust collectors are used to control emissions from cement, lime, and clay kilns; grain elevators; grain drying and milling; thermal coal driers; rotary rock driers; sawmills and other woodworking operations; ore beneficiation; sinter plants; and coffee roasting, amongst others.

Provided that a suitable construction material is used, cyclones can be built for any conditions of dust concentration or gas temperature, pressure, and corrosivity. In some applications, the nature and quantity of dust to be collected or the severity of operating conditions make cyclones the only practical choice for a collector. Cyclones are used frequently in applications where a dry collected dust is recycled. In the food industry, for example, fabric filters cannot be used to control some processes because cloth fibres might contaminate the recycled dust.

During the last decade cyclone collectors received new attention as a result of developments in fluidised bed combustion technology. In atmospheric pressure fluidised bed combustors, one or two stages of cyclone collectors are used to capture elutriated fines of coal and limestone. To increase thermal efficiency, unburned coal particles thus captured are often recycled to the combustor or burned in a separate unit. Captured limestone particles are also returned to the combustor to reduce loss of limestone. In pressurised combustors there is a greater need to clean the high temperature combustion gas before it passes through downstream gas turbines. Such applications currently require several stages of hot cyclones, together with a stage of filtration by either granular bed or ceramic filters. The newer technology of combustion in circulating fluidised beds places an even more stringent demand on the particulate collection system. In CFBC the bed material (limestone and coal) often

recycles hundreds to thousands of times through the fluidised bed combustor during its residency before being discharged as spent bed material.

Classification of solids according to size

This application of cyclone is for solid-solid separation by particle size. As the grade efficiency of a cyclone increases with particle size, it can be used to split the feed solids into fine and coarse fractions. The required duty in this case is maximum removal of suspended solids, which are above a give size, and minimum removal of those below this size. A cyclone used for this duty is usually referred to as a classifier and is not designed for maximum efficiency for all sizes of solid fed to it. Low efficiency of particles below the desired "cut point" and high efficiency above it are required.

Two extreme cases can be recognised in the general requirement of classification. These are, "desliming", and "degritting". The former refers to the removal of fines from a coarse fraction product and is of wide interest in the treatment of mined products. The latter refers to removal of coarse particles from a fine fraction product. For example, the removal of oversize foreign matter from many chemical products.

Some examples of cyclone in duty of classification by size are: desliming prior to filtration equipment to reduce the cake resistance to flow; separation of clay from barytes in drilling muds for control of specific gravity; degritting of underground water prior to pumping; classification of 'raw' cement slurries before kilning; classification of iron ore into coarse fraction and fine fraction; recovery of filter aid.

Sorting according to solids density (washer)

This use of a cyclone is for solid-solid separation by solid density. The sorting of mineral, industrial rocks and coal by cyclones is commonly accomplished by the dense medium cyclone. In dense medium cyclones, the density of the suspending medium is chosen to be between the densities of the two minerals to be separated and the cyclone is then used as a 'sink-and-float' separator. In the cyclone the heavier

components will "sink" to the underflow, the lighter components will "float" to the overflow. This application catalogue includes separating shale from coal.

Sorting according to particle shape and density

The mechanism of separation is on the particle differences in shape and density and, therefore, differences in their terminal settling velocities. By far the largest application in this category is cleaning of pulp prior to papermaking. Some other examples include sorting of cracked shells from kernels of palm nuts; separation of flat impurities from the globular grains of starch in the potato and corn starch industries.

Cyclone liquid-liquid separator

It is more difficult to separate two immiscible liquids in the cyclone. The reasons are that density differences are generally smaller and the existence of shear can cause the break-up rather than the coalescence of droplets of the dispersed phase. However specially adapted cyclones can be successfully applied to the separation of two immiscible liquids. Such cyclones can separate oil from water, dewater light oils and produce highly concentrated samples of a lighter dispersed phase.

Cyclone gas-liquid separator

Due to the low static pressure at the axial core area in a hydraulic cyclone, the gas dissolved in liquid can be released to form 'gas core', and then can be removed. There is a difference from conventional cyclone design due to necessary for non-axial removal of the liquid or destruction of the gas core at the point of an axial exit so to avoid re-entrainment of gas with discharging liquid. Some techniques have been developed for particular problems. An application is the degassing of crude oil. Many potential uses of this system also exist in the chemical industry where degassing of liquids is necessary.

Analytical tool (Sample cyclone)

The principle is based on the concept of cut size, which is in direct analogy with sieving. The cut size of the cyclone has to be known for the operating conditions under which the sample is processed by the cyclone, and the mass recovery under those conditions represents the percentage oversize in the sample at that cut size. From one measurement point some information about the size distribution is known. If more information is needed, the sample may be passed through the same cyclone under different operating conditions or through a number of different cyclones, singly or in series.

Dryer

Drying is a unit operation frequently used in the production of fine-grained materials, such as polymer powders, pharmaceuticals, foodstuffs and dyes. Many products can be dried by convection systems, particularly pneumatic conveyors. But these systems have very short residence time of solids, and therefore, only surface moisture is removed. A MST cyclone drying system is a "medium-residence time dryer" with the solids retained for 5 to 30 Min. It is based on the classifying effect: the residence time increases with particle size. The main advantages are low drying temperatures and low heat consumption.

Reactor

The cyclone seems to ensure excellent heat transfer efficiencies between carrier gas, solid particles and heated walls. Moreover, residence times in cyclones are generally of the order of or lower than a few seconds. The interest in the cyclone is consequently to obtain a system where contact, extraction, and separation all take place in a small volume and within a short time. Consequently, it can be anticipated that cyclones would be well suited for carrying out fast reactions of solid particles requiring high heat fluxes. It would be expected that, at the same time, solid by-products and unreacted particles would be automatically separated from gaseous products.

An example is flash pyrolysis of wood sawdust, in which heating, reaction and gas solid separation occur in the same vessel; another example is a cyclone as a continuous crystalliser.

With the better designs, more applications can be developed.

The merits of cyclones can be summarised as follows:

1. They are simple to produce, cheap to purchase, install, and run.

2. They have extensive applications in that they can be used to collect particles, clarify liquids and solids, sort solids according to density or shape, concentrate slurries, separate two immiscible liquids, and degas liquids.

3. They are small relative to other separators, thus saving space and also giving low residence times, which in turn needs less capital.

The main disadvantages of cyclones are that:

1. They are somewhat inflexible once installed and operated, giving low turndown ratios, due to the strong dependence of their separation performance on flow rate and feed concentration. They are also inflexible due to their general sensitivity to fluctuations in feed flowrate and solids concentration.

2. There are limitations on their separation performance in terms of sharpness of cut, range of operating cut size, de-watering performance or clarification power. Some of these characteristics may be improved in multi-stage arrangements, but at additional costs of power and investment.

3. They are susceptible to abrasion, but steps can be taken to reduce these effects.

1.3 CYCLONE DESIGN THEORY AND METHOD

The simplicity of structure, the long developing history and extensive applications would suggest that the principles underlying the performance would be well understood. But many mysteries are still puzzling cyclone designers.

Swift (1969) explains the cyclone developing process as ".. cyclones have been developed almost wholly by experiment, and it would be difficult to prove mathematically that [they] are of the best design...".

When the students in Chemical and Process Department of Canterbury University carry out their experiment of cyclone dust collector, they can find the statement in the experiment brief sheet "Although they (cyclone separators) have been used since 1890 it is not possible to predict the efficiency of collection from first principles. Instead the cyclone designer copies the geometry of a cyclone whose performance has been tested. ..."

Day, R. W. and Grichar, C. N. stated in their chapter on hydrocyclone separation that "..The suitability of a hydrocyclone to a given process must depend upon existing information known from past experience or upon results developed by laboratory or field testing.."

Dirgo, J. and Leith, D. describe the 'Standard Designs' in their manual that " ..extensive experience and testing on cyclones have resulted in practical design guidelines....Many of these considerations are embodied in "standard" cyclone design that have appeared in the literature. Some of the designs were developed through trial and error, the result of 'hunches' or effects to overcome operating difficulties. Nevertheless, standard designs represent accepted engineering practice"... .

Wakelin, R.F. (1992) summarised that "... research has tended to take an empirical, 'black-box' approach. ...Studies of cyclone performance have concentrated on the

measurement of the collection efficiency for various designs, resulting in an empirically determined 'optimum' design, but adding little to the understanding of the collection mechanism. It has not been possible to generalise the empirical correlations of cyclone performance to fit the wide range of geometrical parameters. The prediction of the efficiency for new designs is not possible, nor is it possible to suggest (with confidence) remedies for cyclones with poor performance. To optimise the cyclone design at present involves the testing of a large number of cyclones to cover the possible variations of the geometrical parameters. These parameters can have conflicting effects and confuse the findings... ."

Design of cyclones at present is based on empirical correlations but the knowledge on cyclone mechanism is improving with continuous effort. As is the case with the development of other devices, people understand cyclones gradually and, step by step, form improved cyclone theories.

1.3.1 Cyclone theory

In THE NEW SHORTER OXFORD ENGLISH DICTIONARY (1993) theory is explained as:

> "A system of ideas or statements explaining something
>
> A hypothesis that has been confirmed or established by observation or experiment and is accepted as accounting for known facts
>
> Systematic conception of something.
>
> Abstract knowledge or speculating thought"

Perhaps we can say that a design theory is: an expression of the relationships between the structures, dimensions as well as operating conditions, and the phenomena and performance of a device, taking account of working mechanisms.

In different developing stages, for different aims, at different conditions, from different investigation angles, on different emphasis points, to different objects, with different methods, different people can obtain different theories.

The primary theories were sketchy, superficial and qualitative. The relationships expressed were indistinct. With more studies, the sequence of ideas has become clearer, more relationships found, and the relationships expressed more accurately.

1.3.1.1 General study methodology

All the dimensions and operating conditions affect the performance of a cyclone; the relationships between the variables and the performance are very complex. To understand all the important relationships, some strategies have to be used.

Although all the dimensions and operating conditions will affect the performance of cyclones, they are not in equal position. In certain conditions some variables have great effect on the performance of cyclones, others not. The dominant factors can determine the performance, the trivial factors can be ignored. This is a common phenomenon in the universe. For example, when two iron balls with different diameter, one is several times bigger than another, fall from Pizza Leaning Pagoda, they will touch the earth with almost same velocity at almost the same time. Since their travelling velocities are limited, the drag effect can be ignored, they fall down as free falling objects. People can calculate the travelling time according to the free falling rule. The problem is simplified. In many cases a complex problem can be simplified by investigating the conditions carefully.

When operating conditions are varied the relationships between the variables and performance may change. These factors, which were dominant, may become trivial; the trivial may become dominant. If those two iron balls fall down from an aeroplane cruising 10,000 meters height, the two balls will fall down in different constant velocities respectively. Since the terminal velocities are large enough, the drag forces cannot be ignored. The drag forces will balance the gravity force, and will be the dominant factor to determine the terminal velocities. With the conditions varied, the different dominant factors should be distinguished.

The variables may affect the performance indirectly. They can produce some sub-results, and the sub-results will in turn affect the performance of cyclones. People can study and control the performance by studying and controlling the relationships between variables and sub-results. For example, if we express the saltation velocity as: the minimum velocity that picks up deposited particles and transports them without settling, we can study the relationship between dimensions, operating condition and saltation velocity. This background may be helpful in a cyclone to control particle reentrainment, then improve the separation efficiency of cyclones.

In summary, a complex problem can be decomposed and simplified by some methods as: find the dominant factors in certain conditions, and study the relationships between the factors and the performance; investigate more typical conditions and find new dominant factors, then the new relationships; study the relationship between sub-results and variables, then final performance and variables. At last, those isolated, unilateral and semi-stage knowledge areas should be synthesised systematically to form comprehensive knowledge.

To understand the relationships, two main methods, experiment induction and theory deduction, are employed. The latter can be classified into two kinds: numerical and analytical.

1.3.1.2 Experiment induction method

Experimental study is still the basic means of developing cyclones. In fact most abstract thought of human is based on observation, and theoretical studies cannot usefully begin without a limited body of knowledge derived from observation. Experiments provide us with the opportunity to acquire knowledge, skills and understanding through investigating the 'real world'. Science and technical advances rely heavily on the support that a critical experiment, or series of experiments, can give.

However, the flowfield and the particle movement inside the cyclone are too complex for people to study in their entirety by experiment. It would be a huge task to design

cyclones by trial and error with very little analytical work. For example, if we try to find the optimum design by changing the eight dimensions as well as the flowrate step by step with 5 levels for each variable, the number of tests will be 5^9 (1,953,125). So it is normal either to examine some particular variables such as the diameter of cyclone vortex finder alone, or to focus attention on some special problems such as shortcut flow. We then use this unilateral knowledge deliberately in the procedure of cyclone design.

If only one variable is examined under the condition of no other variables varied, its effect to the performance of a cyclone will be clear.

But if the condition changed, ie other variables are varied, new relationships between this same variable and the performance will be established. The new relationships may be really different from the old one, either in quantity or in tendency. If we want to know all the relationships under all possible conditions (say 5 options for each variable), we have to change the conditions as many as 5^8 (390,625) times, and 5^8 relationships are obtained through 5^8 tests. It is practically impossible to do so many tests and handle so many relationships for the designers.

It is obviously that designers cannot determine the optimum dimensions by a few relationships coming from limited casual tests. There are so many other options in which the optimum structure may hide.

An optimum experimental method, orthogonal experiment, has been used to find the optimum geometry (Zhou 1988). This is a technique that little mechanism may be considered but interactions between the geometry parameters will be recorded and analysed. This may be called as a black box method. This method can reduce the number of experiments dramatically, but the task is still huge. In fact, Zhou (1988) carried out his experiments with help from theory.

If designers do not have insight in to the mechanisms of cyclones, even after they have done many experiments, they cannot create new concepts and new structures.

The aim of modern design is to determine the optimum dimensions and operating conditions according to the requirements of performance. The simple experimental method is incompetent.

In fact some abstract thoughts of human may be "induced" from simple experimental results. These thoughts can express more general relationships, and be used to develop design theory.

1.3.1.3 Theory deduction method

The thoughts of human, in forms of concept, theory, idea and conjecture, can be deducted to produce new thoughts. No matter where the old thoughts come from, "induced" from new observations or deduced from other thoughts. Deduction can be carried out through logical operation or mathematical operation. If there is any fault in the old theories, the new observations or the deduction operations, the new thoughts should have a fault.

The design theory of cyclones can be developed by deductions from old theories or new observations.

Another resource of design theory is the deduction from basic principles. We are so lucky for the sake of the work of many great pioneer scientists. They have induced or deduced the basic principles, which never were violated before, and give us enough basic knowledge on the macro-mechanics to describe the general motion of matter. Any motion of a macro object will follow the basic principle: conservation of mass, conservation of momentum and conservation of energy .... If we know the initial status of an object and forces on it, we can predict principally its motion by these basic principles.

For the fluid flows in a practical device, if all the initial, boundary and operation conditions are determined, the fluid has to follow these principles and flows in a determined way. All the relationships between dimensions, operating conditions and the fluid status will be determined. This process can be described mathematically by the motion equations with their boundary conditions. Any relationships, such as

dimensions vs pressure-field, and vs velocity-field, can be obtained by solving the mathematical problem. These relationships should be very reliable under these conditions, if there is no fault in the mathematical operation.

These conservation motion equations seem very simple, but they may describe very complex motion of fluid. It is impossible to express all the complex cases, unlimited kind of cases, with our limited simple basic mathematical functions in analytical solutions. There is no analytical general solution for the equations in all situations. Even if we focus on a particular case, the complex flow status may not be expressed by the known basic mathematical functions. In this meaning, the analytical solution for the case does not exist. For some lucky cases, the solution can be expressed by the combination of basic mathematical functions, but in a very abstruse form to study the relationships.

1.3.1.3.a Numerical method

Again we are lucky, this time for the sake of the development of computer and numerical method. During the last half-century, computers have done so well, and are offering incredible aid to understand the universe. We can use a computer to solve the motion equations and then study the relationships between variables and performance of cyclones.

The calculation of cyclone performance, normally the separation efficiency, can be divided into two parts: the flowfield and particle trajectory.

The calculation of a two-phase flowfield is complex. If the particle concentration is not high, the particles will not affect the flowfield very much, and the flowfield can be calculated as fluid only. CFD (Computational Fluid Dynamics) techniques have been developed very fast during last 20 years. Much experience in giving boundary conditions, choosing turbulence models and calculation schemes has been accumulated through practical calculation for the cyclone flowfield by trial and error.

The calculation of a single particle trajectory is comparatively simple. Little difficulty is found in the calculation schemes, but the flowfield fluctuation makes the particle

trajectory uncertain. Determining the fluctuation of the flowfield needs so much detailed information, it is practically impossible. Cyclone designers are not concerned with the behaviour of a simple particle, they want to know the macro behaviour of many particles. The fluctuation is treated by statistical methods , and the trajectory can be calculated by numerical tests. The effects between particles can be treated by statistical method also.

I calculated the cyclone flowfield and particle trajectory with FLUENT for some particular cases, and good results were obtained in 1992. Some researchers (Yoshida, 1991), (Wolbert, 1995),(Hoffmann, 1996), (Sevilla, 1997), published their works on cyclone simulations, and indicated that they can calculate separation efficiency very well.

Though much experience has been accumulated, the CFD techniques are far from perfection. The theory of CFD has not been well developed. It is difficult to judge the reliability for a particular problem. People can not be sure whether a calculated result for a new case is reliable or not.

The normal calculation strategy is to calculate the flowfield from initial and boundary conditions and then study the calculated flowfield. The optimum method is to calculate many cases, and compare the performance of these cases, then determine the optimum variable values. Different optimum methods choose the calculating cases by different techniques. This strategy normally does not suggest new structures and concepts directly. Perhaps a new strategy can be developed in future, in which the flowfield can be given, then study the relationships between the variables.

The calculating time is still too long for a practical optimisation problem. People have to find better numerical methods with less iteration time. The development of a super computer will help to decrease the calculating time.

Sometimes it is more convenient to get the relationships between variables and flowfield with CFD than experiment. The results of CFD are clearer and easier to handle. Furthermore CFD has given people more information of the flowfield which was difficult to get with experiments.

It is predictable that with the increase of calculating speed of computer and the improvement of CFD techniques and optimum methods, people will find the optimum variable groups of given structures with numerical method. This should be a main direction, maybe the inevitable way, for the modern design method of cyclones.

1.3.1.3.b Analytical method

Although the analytical solutions of motion equations are very limited, they are very desirable. A device with good design should have the best performance with least cost. The optimum design is a quantitative procedure, and the quantitative relationships between variables and performance or any key function are needed. This calls for the general formula expressing the essential relationships.

As the analytical solution can express the essential relationships between variables and functions compactly and clearly, it can be very helpful for understanding the operation process and mechanism. It also can express and handle the complex relationships of multi-variables with functions, which cannot be obtained by several experiments. These relationships normally have common sense, and are valid for not only a few cases. Even if these relationships are valid only for some certain not simplified cases, the conditions to use should be clear. People can use these relationships correctly with confidence. Since it is very easy to check the solution with simple operations, if there is a lack of ability to describe the real world, it must be in the wrong conditions only. Sometimes people can deduce directly the necessary boundary conditions from the required performance functions with these clear relationships. This strategy may suggest new concepts and structures. The findings of analytical solutions may bring great progress in design methods.

To find these solutions should be an important direction to work in, but during the long developing history of cyclones only a few analytical solutions have been found. In fact this is a very arduous way. As we mentioned above, the solutions of motion equations are limited, and the effort to find more general analytical solutions seems doomed to futility. Some analytical solutions for particular cases do exist, but no well-trained right people work on them or the people are not so lucky to have found them,

and the solutions remain hidden. Some mathematicians may know what the solutions for a particular problem should be, but no engineers use the solutions to study cyclones. A complex problem can be decomposed and simplified into some simple problems, where the solutions for these simple problems still express the essential relationships and are very desirable. To find these solutions, people need accumulated experience to decompose and simplify the complex problem, this may be a process taking a long time. Since the high risk and difficulty, less investment (both financial support or time) are attracted to this area. People tend to drill a hole on a wood plate at the flimsy point, experimental and numerical methods are regard as more practical; even some practical designers think that mathematical deduction is a useless game, and this in turn decreases the opportunity to find analytical solutions.

Since last century, many important inventions result from theoretical deductions such as the electrical generator (1872) from electromagnet theory (1831), broadcasting station (1921) from electric-magnet wave theory (1895), radar station (1935) from radar theory (1925), atom bomb (1945) from atom fission theory (1938)..... Now some important disciplines have developed tremendously based on the deduction of principles, people can exploit into microcosmic world, DNA structure, outer space. The development of cyclones is inferior by comparison. People do not understand cyclone mechanism clearly and thoroughly from the first principles, and even do not know what is the best design. This fact would suggest that people should possess the ability to deduce the performance of cyclones from first principles; and that there might be some fruits of theory deduction on cyclone design to be picked up.

As we know that there must be some relationships between dominant variables and performance, the difficulty is how to find and express them. With the computer, we can express complex functions in more flexible forms such as series, we even can produce new functions easily if necessary. So many successful examples of methodology in other area broaden our experience, that we should be more skilful in decomposing and simplifying a complex problem and in finding the dominant factors. The rich experience on cyclone performance by experiments could make the assumptions to simplify a complex problem more reasonable.

Practice shows that we can often express an essential relationship in a simple form. It is natural to reach an empirical relationship from well-accumulated experiences. This empirical relationship should not be inconsistent with the basic principles. If we find an empirical relationship between variables or reference variables and performance or semi-results for a mechanical problem, and this relationship can be expressed in a formula, we should able to deduce it from the basic principles by decomposing, simplifying, synthesising and approximating. During this 'deduction' process, we could find the dominant factors and make the conditions clear, then understand the operation mechanism. If all the basic essential relationships for an object have been 'proved', the design theory of the object should be mature. This is an ideal situation.

To summarise, the suitably simplified analytical solutions of the motion equations for cyclones are desirable, possible and inevitable.

1.3.1.4. The developing process of cyclone theory

To develop cyclone theory both experimental and deductive methods are needed. An improved cyclone theory can come from the old theories, the new inductions from experimental observations and the deductions of principles.

It is generally accepted that the old theories and the new inductions from experimental observations should not violate the principles or their correct deductions. An attempt to challenge the principles in their suitable conditions will generally be proved to be futile. For example, an attempt to produce a working engine without energy consumption will generally be rejected.

Sometimes, the experimental observations are the only advisable resource of a theory, and the only means to design a cyclone. Normally, an experimental observation can improve the old theories, even might seldom 'break' a principle (We should bear it in mind that all principles should be used in certain conditions).

New and old theories are 'put to the test' through experiments. Devising and executing an experiment that provides a thorough test of a theory may not be easy, but

until such a test is undertaken, and the results confirmed independently by others, the theory is unlikely to gain complete acceptance. Additionally, carefully performed experiments may reveal new effects that require existing explanations to be modified.

The analytical solutions from the equations of principles are very desirable, but very difficult to obtain. Using the old theories and the new inductions from experimental observations, a complex problem may be simplified or decomposed, then a suitable solution may be obtained.

An experiment can be organised under the guidance of the old theories and the deductions of principles to develop an improved theory.

An experimental result can be analysed according to the old theories and the deductions of principles to induce an improved theory.

A cyclone theory can be improved gradually with help of the old theories, the new inductions from experimental observations and the deductions of principles, from superficial to essential, from unilateral to comprehensive, from isolated to interrelated.

1.3.1.5. Existing cyclone theory

The cyclone design theory is for expressing the relationships between the structures, dimensions as well as operating conditions, and the phenomena and performance of a cyclone.

To increase separation efficiency, the motion of particles in cyclone should be studied. A simplified analysis can be carried out. Separation of particles in the cyclone occurs the centrifugal force caused by the spinning fluid stream. For a particle rotating with the same speed as the tangential fluid velocity at radial position r, the centrifugal force is

$$F_c = \frac{\pi \rho_p d^3 v_t^2}{6r}$$

where v_t is the tangential velocity of fluid.

Opposing the outward particle motion resulting from centrifugal force is an inward drag force.

$$F_d = 3\pi\mu d(u_r - v_r)$$

where u_r is the outward radial velocity of particle while v_r is the fluid radial velocity directed toward the cyclone axis. This force can be calculated from Stokes' law.

The sum of these two opposing forces will equal the mass of the particle times its radial acceleration.

$$\frac{\pi \rho_p d^3 v_t^2}{6r} - 3\pi\mu d(u_r - v_r) = \frac{\pi \rho_p d^3}{6} \frac{d^2 r}{dt^2} \qquad (1\text{-}1)$$

From experimental observations, in the separation region, the tangential velocity of fluid can be expressed as

$$v_t r^n = v_{tw} r_w^n$$

where n is a constant, footnote w indicates the wall of the cyclone.

This substitution, expressing u_r in different form, and combining other terms in equation (1-1) yields an expression to describe the radial motion of a particle in the cyclone vortex as a function of time.

$$\frac{d^2 r}{dt^2} + \frac{18\mu}{p_p d^2} \frac{dr}{dt} - [\frac{v_{tw}^2}{r^{2n+1}} + \frac{18\mu v_r}{\rho_p d^2}] = 0 \qquad (1\text{-}2)$$

This equation can be solved, if the radial velocity of fluid v_r is known. Some researchers have arrived at various approximate solutions by making different

assumptions about fluid flow through the cyclone. Some of approaches are described in the following.

1.3.1.5.a Theories from particle motion

i. The equilibrium orbit theory

This theory determines the particle diameter for which centrifugal force is exactly balanced by the drag force from fluid that flows radially inward to the cyclone core. For these particles, radial acceleration and velocity are zero, so the particles should rotate indefinitely around the edge of the core. Drag force on smaller particles exceeds centrifugal force so they are carried into the core and out of the cyclone. Larger particles spin out toward the cyclone wall for collection. The radial velocity of fluid is assumed as an average constant, it depends on the length of separation region and the radius of the up-flow core. The equation (1-2) is simplified. To determine the length and the radius brings some sub-theories.

The equilibrium orbit theory predicts a sharp increase in cyclone efficiency from zero for particles smaller than the critical diameter to unity for larger particles. In practice, such a sharp separation is never observed because of fluctuations in radial and tangential fluid velocity over the height of the cyclone. The efficiency for the critically sized particle is often assumed to be 50%.

This theory does not establish directly the relationships between the structures, dimensions as well as operating conditions, and the phenomena and performances of a cyclone. But it indicates how the length of separation region and radius of up-flow core affect efficiency in the assumed flowfield. People can use the information indirectly to understand the relationships.

ii. The residence-time theory

This theory assumes that both radial acceleration of particles in the vortex and radial fluid velocity into the core are zero. The equation (1-2) is simplified. An inter-most radial position (usually the width or half-width of the cyclone inlet) is assumed for

particles entering the cyclone. Particles must travel from this position to the cyclone wall to be collected; the critical particle is that travels exactly this distance during its residence time in the cyclone. Different assumptions about initial radial position, the value of the vortex exponent n, and residence time lead to different approximate solution.

Again, this theory does not establish directly the relationships between the structures, dimensions as well as operating conditions, and the phenomena and performances of a cyclone. But it can provide some useful information to design cyclones.

iii. Fractional efficiency theory

These theories use more complex assumptions of the flowfield and dust distribution in the cyclone. One of these theories, by Leith and Licht assumed that radial acceleration and radial fluid velocity in the cyclone can be neglected. Their model accounts for turbulent fluid flow by assuming that at any height in the cyclone, uncollected dust is completely and uniformly mixed. An average residence time for fluid in the cyclone is determined from cyclone dimensions and gas throughput.

Some experimental findings confirmed the predictions of this theory , but some of the assumptions made by Leith and Licht are not valid. Although fluid flow in industrial cyclones is always turbulent, this turbulence is not sufficient to produce the complete radial mixing of uncollected particles that the theory assumes. Measurements of dust concentrations in cyclones have shown that although smaller particles may be uniformly distributed, larger particles are concentrated near the cyclone wall.

Other theories that direct calculation of cyclone fractional efficiency have been published by Beeckmans (1972,1973), by Dietz (1981) and by many others. The Beeckmans theories are considerably more complex than the Leith and Licht method, requiring a computer for solution, and do not predict efficiency as accurately. Compared to the Leith and Licht theory, Dietz's theory uses a more realistic description of fluid flow and dust distribution in cyclone. However, based on limited

comparisons of the two approaches with experimental data, the Dietz theory does a poorer job of predicting efficiency.

1.3.1.5.b Theories about flowfield modelling

It is obvious that the relationships between the structures and the flowfields are the key factors to understand the relationships between the structures and performance of cyclones. Most work on flowfield in cyclones have been done by experiments. A huge of experiences have been accumulated, but the knowledge are unilateral, isolated, and sometimes contradicted. . Most relationships between the structures and the flowfields are empirical. In any case, an empirical description is likely to be valid only over the range of geometry that it was based on.

More general essential relationships from first principles are needed. The solution of the motion equations for swirling flow cannot be solved completely, but Burgers (1948) and Bloor and Ingham (1987) have solved some simplified cases. In Burgers' solution, the radial and azimuthal velocities only depend on the radius. Rott (1958) and Bellamy-Knights (1970), and Donaldson & Sullivan (1960) explored the solutions with the same assumption. These kind of solution cannot be used to describe the flowfield of cyclones, but the tangential velocity can fit experimental findings fairly well.

Bloor and Ingham did extensive analytical studies on the flow modelling in cyclones. In their early work (1975), they assumed that the tangential velocity (in cylindrical coordinates) is a function of radius alone, the flow is inviscid along radial and axial directions, and the leading term of the distribution of vorticity behaves only like $F\Psi^{\delta}$, where Ψ is the Stokes stream function, and F and δ are constants. Their results show surprisingly good agreement with some velocity data of Kelsall(1952). However, their results have not so good an agreement with all velocity data in the whole flow field.

After 12 years, Bloor and Ingham (1987) obtained a simple mathematical model for the flow in a conical cyclone, which allows a solution to be obtained in closed form. The flow in the main body of the cyclone is regarded as inviscid but the nature of the

fluid entry to the device and the conical geometry ensure that secondary flows develop which make the flow highly rotational. The results of the theory are compared with data from two quite different experimental investigations, and good agreements are obtained in some range. Again, their results cannot fit the whole flowfield, especially at the boundary regions.

Various polynomial approximations to the experimentally measured velocity profiles in vortex flow have been made (Mager, 1972), (Tran, 1981), (Reyna and Menne, 1988), (Zhou and Soo, 1990). All of these are not the exact solutions of the motion equations). Some of them can satisfy individual equations such as the continuity equation, as did the solution by Soo(1989). It is difficult to reveal the nature of the flow using this group of solutions.

1.3.1.5.c Theories for some particular problems

Since some phenomena or dimensions can heavily affect the performance of cyclone, they were studied with special attention. Corresponding concepts and theories may be risen, for example, "Shortcut flow", "Air core", "Re-entrainment of particle", "Diffusion theory", "Crowding theory", "Natural length" and "Vortex breakdown theory".

1.3.2. Cyclone design methods

A cyclone design method is the application of the knowledge and theories, which the designer accepted. With the improvement of the knowledge and theories, the method should also be developed.

Existing design method include 3 categories:

- Regression method

These methods base almost entirely on regression analysis of test data, applicable only to the specific system tested. They are concerned with the two main performance

characteristics of cyclones, the pressure drop and the separation efficiency in the form of the cut size.

- Dimensionless group method

Basically, these methods are the mathematical operations, which based on dimensional analysis. If people find a "optimum design", which has been found with experiments by stairmand (1951), Rietema (1961) and Bradley (1959) for example, then its flowfield and particle motion should able to be described by the motion equations with special boundary conditions. It is expected that the same solution will describe the motions with same essential characteristics. If some norm numbers can remain the same in the alternations of equations and conditions, the same solutions can be obtained. A "optimum design" can be alternated to another one, which can remain the same characteristics, if some norms are observed.

This method simplifies cyclone design and allows the designer to select the "best" compromise between cyclone performance and the design and operating conditions likely to achieve it. Since it is difficult to prove that the original "optimum design" is the best, and some "good" characteristics may be lost during the similar alteration, and an opportunity to find the best design in new conditions is given up, the new design may not the "best".

- Data synthesis method

This is a rough empirical method, it gives the ranges of dimensions and operating conditions. It needs lot of experimental work and experience to complete a good design.

In summary, the development of a new design method depends heavily on the improvement of theories. The knowledge on the relationship between the structures and the flowfields is insufficient, and suitably simplified analytical solutions of the motion equations for cyclones are both desirable and possible.

Chapter 2

Some Analytical Results on Swirling Flow in Cyclones

Abstract

A theoretical investigation into the fluid flow within a dust collection cyclone has been carried out. Some analytical results have been obtained, for both viscous and inviscid models. The results provide insight into the relationships between boundary conditions, geometry and the flow pattern in cyclones. Most previous models have assumed that radial and axial velocities are not linked to the tangential vortex profile. In this work, the interdependence of axial velocity and radial velocity with tangential velocity is fully explored. These results are compared with experimental investigations by R.F. Wakelin (1993). Their application is discussed.

2.1 INTRODUCTION

The cyclone separator has been used extensively in industry to separate dust and condensed-phase pollutants from gas streams, since its first application for dust collection purposes in 1885. Most attention has been paid to find new techniques to reduce the pressure drop and to increase the collection efficiency. The simple design of this device makes its principle of operation seem straightforward. But because of the complexity of very strongly swirling turbulent fluid-solid flows in a cyclone, much mechanism remains to be understood.

Optimisations of cyclone dimensions are mainly determined by experiment, since the analysis of fluid flow and particle motions is very complicated. Most experimental studies omitted the investigation of interactions among the structure parameters as well as the flow parameters, and hence the results were limited and sometimes contradictory.

Numerical calculations of fluid flow and particle motion in the cyclone have been conducted for about 20 years. Although some computed results satisfactorily compare with experimental data in some range, they result in limited information with regard to design improvements. Analytical solutions can offer clearer insight into the underlying physical mechanisms operating and provide well-defined special cases against which numerical procedures can be tested.

It is impossible to describe all features of flow pattern in cyclones with analytical solutions, but some special cases have been obtained, notably by Burgers (1948) and Bloor and Ingham (1987).

In early efficiency prediction models, the radial distribution of tangential velocity was described by empirically fitting

$$v_\varphi = \frac{C}{r^n}$$

where v_φ is tangential velocity, C is a constant and r is the cylindrical radius.

The range of exponent n summarised from experiments are 0.5-0.88 for gas cyclones and 0.5-1.0 for hydraulic cyclones (Gupta, 1984).

A typical analytical solution for vortex flow is that due to Burgers (1948).

$$v_x = 2ax$$

$$v_r = -ar$$

$$v_\varphi = \frac{\Gamma_0}{r}(1 - e^{-\frac{ar^2}{2\upsilon}})$$

where v_x is axial velocity, v_r is radial velocity and v_φ is tangential velocity. The a is a constant, x is the axial distance from some origin and r is the radius. υ is the turbulent or eddy viscosity; Γ_0 is the circulation at large radius($\Gamma_0 = \lim_{r\to\infty}(r.v_\varphi)$).

It is an exact solution of equations of motion. The solution fails to describe the flowfield in reverse flow cyclones, because the axial velocity possesses only one direction, not being consistent with reverse flow. Also the radial velocity at the

cyclone wall cannot be zero, which means that the fluid would flow into the cyclone through the wall from outside. However, it is widely used to calculate the tangential velocity in cyclones, and shows good agreement with experiments (Wakelin 1993).

Many researchers (Rott, 1958), (Ogawa, 1987), (Phillips, 1991) studied the development and improvement of the Burger's vortex. Most of them concentrated on adding terms to fit the profile of tangential velocity from experiments.

Most previous models have assumed that the tangential velocity profiles are a function of cylindrical radius alone and can be modelled separately without considering the relationships with radial and axial velocities, Vatistas (1991) and Leibovich (1984). In this work, I will give the general form of the viscous solution under the assumption of tangential velocity being a function of radius alone. Then I will give an exact solution of equations of motion with the inviscid assumption. The interdependence of axial velocity and radial velocity with tangential velocity will be fully explored.

2.2 ANALYSIS

We use cylindrical co-ordinates (x, r, φ), with corresponding velocity components (v_x, v_r, v_φ). p is static pressure and both density ρ and kinematic viscosity υ are constants. The equation of motion for steady axisymmetric flow of viscous incompressible fluid are,

$$v_x \frac{\partial v_x}{\partial x} + v_r \frac{\partial v_x}{\partial r} = -\frac{1}{\rho}\frac{\partial p}{\partial x} + \upsilon \nabla^2 v_x \qquad (2\text{-}1)$$

$$v_x \frac{\partial v_r}{\partial x} + v_r \frac{\partial v_r}{\partial r} - \frac{v_\varphi^2}{r} = -\frac{1}{\rho}\frac{\partial p}{\partial r} + \upsilon(\nabla^2 v_r - \frac{v_r}{r^2}) \qquad (2\text{-}2)$$

$$v_x \frac{\partial v_\varphi}{\partial x} + v_r \frac{\partial v_\varphi}{\partial r} + \frac{v_\varphi v_r}{r} = \upsilon(\nabla^2 v_\varphi - \frac{v_\varphi}{r^2}) \tag{2-3}$$

where $\nabla^2 = \frac{\partial^2}{\partial x^2} + \frac{\partial^2}{\partial r^2} + \frac{1}{r}\frac{\partial}{\partial r}$

The equation of continuity is

$$\frac{\partial v_x}{\partial x} + \frac{1}{r}\frac{\partial (rv_r)}{\partial r} = 0 \tag{2-4}$$

If we assume that tangential velocity is the function of radius alone, the solution of equations (2-1)-(2-4) is

$$v_\varphi(r) = \frac{1}{r}\int re^{\int \frac{v_r}{\upsilon} dr} dr \tag{2-5}$$

$$v_r(r) = \upsilon \frac{d\ln(\frac{d(rv_\varphi)}{rdr})}{dr} \tag{2-6}$$

$$v_x(r,x) = -\frac{1}{r}\frac{d(rv_r)}{dr}x + C_x(r) \tag{2-7}$$

where $C_x(r)$ is an arbitrary function, and the radial velocity must satisfy the following equation

$$(-\frac{1}{r}\frac{d(rv_r)}{dr})^2 + v_r \frac{d(-\frac{1}{r}\frac{d(rv_r)}{dr})}{dr} - \frac{\upsilon}{r}\frac{d(r\frac{d(-\frac{1}{r}\frac{d(rv_r)}{dr})}{dr})}{dr} = const \tag{2-8}$$

It is easy to make out that a particular solution of equation (2-8) can be obtained from

$$\frac{1}{r}\frac{d(rv_r)}{dr} = const = 2A$$

so

$$v_r = Ar + \frac{B}{r} \tag{2-9}$$

Both A and B are constants. From equations (2-5) and (2-7),

$$v_x(r,x) = -2Ax + C_x(r) \tag{2-10}$$

$$v_\varphi(r) = \frac{C}{2r}\int e^{\frac{A}{2\upsilon}r^2} r^{\frac{B}{\upsilon}} d(r^2) \tag{2-11}$$

C is a constant.

If we take B=0, A=-a, and $C_x(r)$=0; and consider the boundary conditions: v_φ=0 on r=0, $\underset{r\to\infty}{Lim}(r.v_\varphi) = \Gamma_0$, equations (2-9)-(2-11) become the Burgers' solution:

$$v_x = 2ax \tag{2-12}$$

$$v_r = -ar \tag{2-13}$$

$$v_\varphi = \frac{\Gamma_0}{r}(1 - e^{-\frac{ar^2}{2\upsilon}}) \tag{2-14}$$

$$(\Gamma_0 = \frac{C\upsilon}{a} = \text{const})$$

If we consider the flow is inviscid and the tangential velocity is a function of radius alone, then equation (2-3) becomes

$$v_r(\frac{dv_\varphi}{dr} + \frac{v_\varphi}{r}) = 0 \tag{2-15}$$

Equation (2-15) has two solutions, $v_r = 0$ and $v_\varphi = \frac{D}{r}$ (D is a constant). The corresponding solutions of inviscid motion are:

Solution 1

$$v_r = 0$$

Equation (2-4) becomes $\frac{\partial v_x}{\partial x} = 0$

v_φ and v_x are arbitrary functions of radius r alone. Equation (2-1) becomes $\frac{1}{\rho}\frac{\partial p}{\partial x} = 0$, so p is a function of r alone.

From equation (2-2), $p = \int \rho \frac{v_\varphi^2}{r} dr$

Solution 2

$$v_\varphi = \frac{D}{r}$$

With the inviscid assumption, the relationship between v_r and v_φ by equation (2-5) is broken, v_r and v_x may be functions of axial distance x and radius r.

In practice, the Reynolds number of the main flow in cyclones is generally very large, the flow is turbulent, in which case the flow in the main body of the cyclone can be described by a mean flow, approximately inviscid (Bloor and Ingham (1987)). The solution of inviscid flow in the main body of the cyclone can allow the efficiency of collection of a suspended particle to be calculated.

I find a simple mathematical model for the inviscid reversed flow (the fluid flows into and out the cyclone from upper portion) in a cylindrical cyclone, which allows solutions to be obtained in exact solution form.

$$v_x = A(\frac{x}{H} - 1)\mu_{1i}(J_0(\mu_{1i}r) - \frac{J_1(\mu_{1i}R_c)}{Y_1(\mu_{1i}R_c)}Y_0(\mu_{1i}r)) \qquad (2\text{-}16)$$

$$v_r = A(\frac{J_1(\mu_{1i}R_c)}{Y_1(\mu_{1i}R_c)}Y_1(\mu_{1i}r) - J_1(\mu_{1i}r)) \tag{2-17}$$

$$v_\varphi = \frac{[(A(1-\frac{x}{H})\mu_{1i}r(J_1(\mu_{1i}r) - \frac{J_1(\mu_{1i}R_c)}{Y_1(\mu_{1i}R_c)}Y_1(\mu_{1i}r)))^2 + C]^{\frac{1}{2}}}{r} \tag{2-18}$$

This solution satisfies the boundary conditions:

$v_r = 0$ when $r = R_c$ and $r = R_0$, $v_x = 0$ when $x = H$. Please refer Fig. 2-6.

where

R_c is the radius of the central "air core" (central region of self-contained flow).

R_0 is the radius of the outer cylinder wall.

H is the height of the cylinder.

$J_1(\mu_{1i}r)$ is the first kind of Bessel function, of order 1.

$Y_1(\mu_{1i}r)$ is the second kind of Bessel function, of order 1.

μ_{1i} is the ith eigenvalue of equation $J_1(\mu_{1i}R_0) - \frac{J_1(\mu_{1i}R_c)}{Y_1(\mu_{1i}R_c)}Y_1(\mu_{1i}R_0) = 0$.

The above set of equations is an exact solution of equation (2-1)-(2-4) with the inviscid assumption.

It is well known that when the tangential velocity is small enough, the central 'air' core may not occur. In this case, the solution reduces to,

$$v_x = A(\frac{x}{H} - 1)\mu_{1i}J_0(\mu_{1i}r) \tag{2-19}$$

$$v_r = -AJ_1(\mu_{1i}r) \tag{2-20}$$

$$v_\varphi = A(\frac{x}{H} - 1)\mu_{1i} J_1(\mu_{1i} r) \qquad (2\text{-}21)$$

2.3 RESULTS AND DISCUSSION

Fig. 2-1 through Fig. 2-4 show the streamlines, the profiles of axial, radial and tangential velocities at seven heights respectively described by equations (2-19)-(2-21) with μ_{1i}=3.8317. The solution domain is below the lip of the vortex finder.

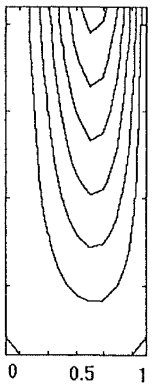

Fig. 2-1 Streamlines of low swirling flow in a cylindrical cyclone

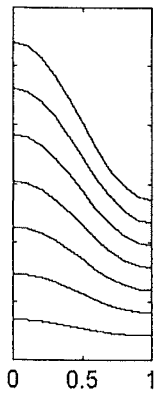

Fig. 2-2 Axial velocities at seven heights

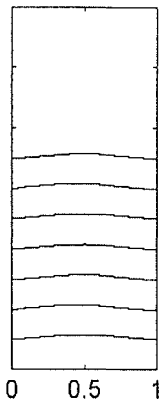

Fig. 2-3 Radial velocities at seven heights

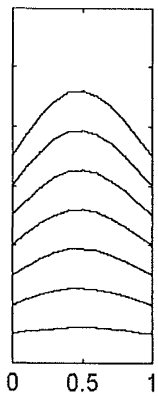

Fig. 2-4 Tangential velocities at seven heights

In this case the three components of velocity are related by follows,

$$v_x = \frac{1}{r\mu_{1i}} \frac{\partial\, rv_\varphi}{\partial\, r} \tag{2-22}$$

$$v_r = -\frac{H}{r\mu_{1i}} \frac{\partial\, rv_\varphi}{\partial\, x} \tag{2-23}$$

That is, the axial velocity at a point in the flowfield depends on the radial distribution of tangential velocity at the same point; and the radial velocity depends on the axial distribution of tangential velocity.

In most well designed cyclones, there appears a central core, into which the streamlines will not enter. Fig.2-5 shows the flow pattern from Stairmand (1951). Fig. 2-6 shows the streamlines in a cylindrical cyclone measured by Smith (1962).

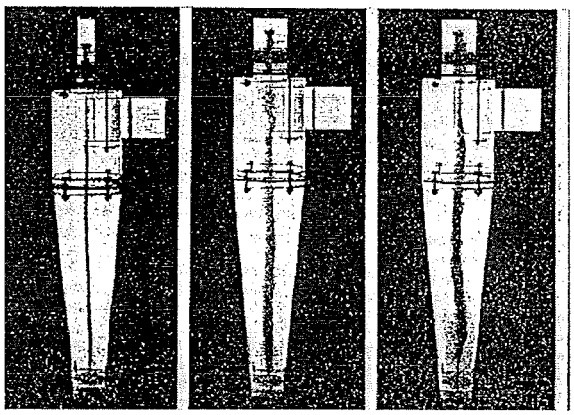

Fig. 2-5 Flow pattern in cyclones with central core

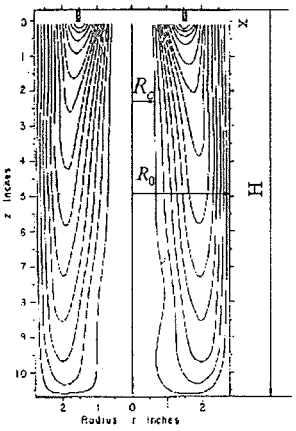

Fig. 2-6 Streamlines in a cylindrical cyclones

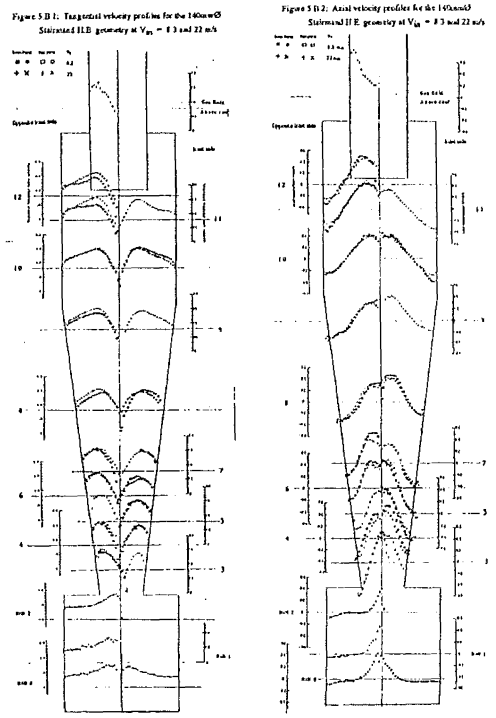

Fig. 2-7 Tangential velocity profile (left) and axial velocity profile (right), for a Stairmand cyclone measured by Wakelin.

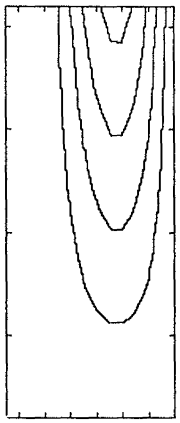

Fig. 2-8 Streamlines with a central core in a cylindrical cyclone calculated with equations (2-16)-(2-18).

In these cases, the magnitude of tangential velocity is much larger than that of axial velocity. Then, the equations (2-16)-(2-18) should be used to describe the flow in the upper cylindrical part of a cyclone. Fig. 2-7 shows a experimental result for a Stairmand cyclone measured by Wakelin(1993), Fig. 2-8 shows a calculated result for a cylindrical cyclone by the theory.

Fig. 2-9 shows the radial distributions of axial velocity in a Stairmand cyclone at different heights measured by Wakelin (1993), and Fig. 2-10 shows the corresponding calculated results by my theory. Though the axial velocity seems not change along the axis from Fig. 2-7, it does decline gradually in the barrel portion, because of the reduction of mass flux. In the conical portion, the axial velocity can remain unchanged because of the compensation of the reduction of cross area.

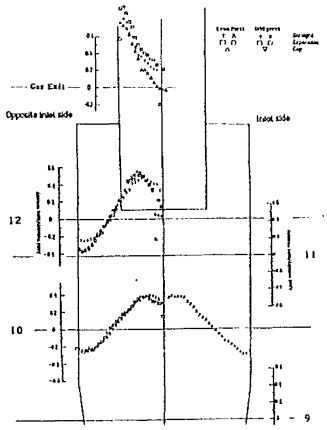

Fig. 2-9 Axial velocity profile in a Stairmand cyclone.

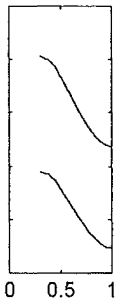

Fig 2-10 Calculated axial velocity profile for case of Fig. 2-9

The accurate measurement of radial velocity component has proved to be very difficult. Radial velocities were measured by Pervov (1974), Hejma (1971) and ter Linden (1953), and found to be directed inwards in the outer region, but outwards in the core. Fig. 2-11 shows the radial velocity profile in a Stairmand cyclone measured by Wakelin (1993); Fig. 2-12 shows the corresponding calculated results by my theory. The comparison seems quite reasonable.

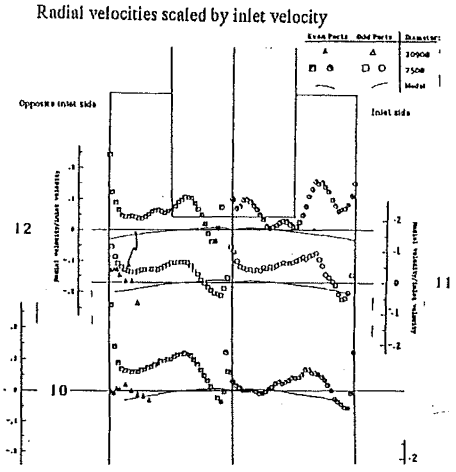

Fig. 2-11 Radial velocity profile in a Stairmand cyclone.

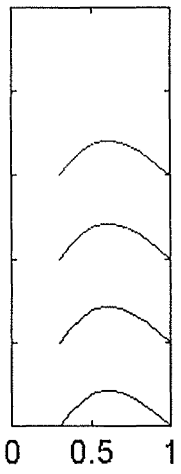

Fig. 2-12 Calculated radial velocity profile for case of Fig. 2-11

The modeling of radial velocity is essential to predict the efficiency of a cyclone. The static particle theory suggests that for a critical particle size at a particular radius a balance is achieved between the centrifugal force given to the particles by the spinning gas, and the drag force caused by the inward flowing gas. The equation of the force balance at the radius of the core r_c is

$$\frac{v_\varphi^2}{r_c} = \frac{18\mu}{d^2\rho} v_r$$

Barth (1956) assumed the inlet flow Q_0 is evenly distributed over the length of the cyclone, and obtained the radial velocity as

$$v_r = \frac{Q_0}{2\pi r_c L}$$

Dietz (1981) calculated the radial velocity as

$$v_r = \frac{Q_0(1-\frac{x}{L})}{2\pi r_c L}$$

It is obvious that the values of radial velocity depend on the determination of radius r_c. In fact the radial velocity would be zero at the annular interface of an 'air' core. At different annular areas, the mass flux Q_0 will vary. Hence we know that the above calculation for radial velocity is very rough. My theory will give a reasonable improvement for radial velocity calculation.

Fig. 2-13 shows the tangential velocity profile in a Stairmand cyclone measured by Wakelin (1993); Fig. 2-14 shows the corresponding calculated results by the theory. The calculated curves are higher than that of measurement near the core regime. This is due to the inviscid assumption, so that Kelvin's circulation theorem follows that the circulation will not change along the streamlines.

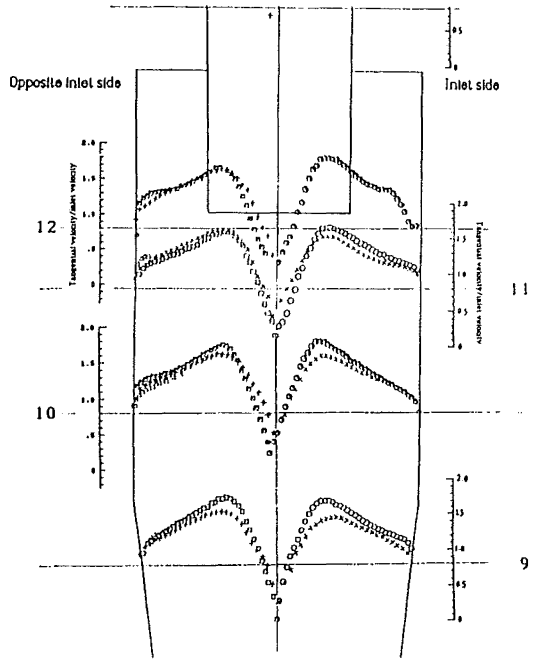

Fig. 2-13 Tangential velocity profile in a Stairmand cyclone measured by Wakelin (1993);

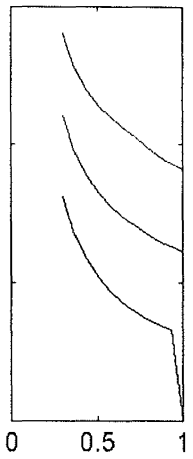

Fig 2-14 Calculated tangential velocity profile for case of Fig. 2-13

Both measurement and calculated results show that the tangential velocity profiles vary little along the axial direction. We can see the minor difference of tangential velocity profiles at different heights from Fig. 2-15. The axial and radial velocities are connected with tangential velocity in this case by the following equations respectively:

$$v_x = \frac{v_\varphi}{A(\frac{x}{H}-1)\mu_{1i}^2 r(J_1(\mu_{1i}r)-\frac{J_1(\mu_{1i}R_c)}{Y_1(\mu_{1i}R_c)}Y_1(\mu_{1i}r))}\frac{d(rv_\varphi)}{dr}$$

$$v_r = -\frac{v_\varphi}{A(\frac{x}{H}-1)\mu_{1i}^2 r(J_1(\mu_{1i}r)-\frac{J_1(\mu_{1i}R_c)}{Y_1(\mu_{1i}R_c)}Y_1(\mu_{1i}r))}\frac{d(rv_\varphi)}{dx}$$

As with the low spin case, the axial velocity at a point in the flowfield is connected with the radial distribution of tangential velocity at the same point; and the radial

velocity connected with the axial distribution of tangential velocity. In general, the three velocity components connected together by

$$v_x = \frac{\psi'(rv_\varphi)}{r}\frac{d(rv_\varphi)}{dr}$$

$$v_r = -\frac{\psi'(rv_\varphi)}{r}\frac{d(rv_\varphi)}{dx}$$

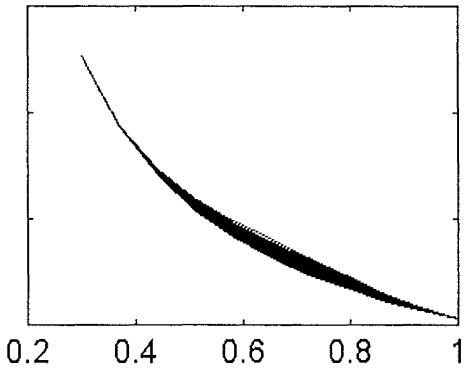

Fig. 2-15 The difference of tangential velocity profiles at different heights

where ψ is the Stokes stream-function, whose unique relationship with circulation rv_φ can be specified at the upstream boundary.

From the tangential velocity equation (2-18), we know that the tangential velocity can be divided into two parts, one related through r and x further to v_x and v_r, the other is a constant C in numerator. If the tangential velocity is not high, the first part will be the dominant term, and the tangential velocity profiles are as shown in Fig. 2-4; If the tangential velocity is high enough, the second part will be the dominant term, so that the tangential velocity profiles have a uniform shape with minor difference as shown in Fig. 2-15. In the second case, axial and radial velocities have little effect on tangential velocity. However the small variation in distributions of tangential velocity will determine the axial and radial velocities, and the variation is difficult to measure. In practice, the tangential velocity is seen to be self-similar, if it is high enough.

Most previous models have tried to include the main body flow and the central region of self-contained flow in a unified equation to describe one of velocity components, eg. using Burgers's tangential velocity equation to describe the tangential velocity in the two regions. This is an intractable task and may not reveal the flow nature. My model shows that when tangential velocity is small only one region can remain, when tangential velocity becomes larger enough two regions will occur. The two regions can be modelled separately. Generally collection models are concerned with the flow field beneath the gas exit tube and at larger radii. For an efficiency prediction, knowledge of the flow pattern in the main body of cyclone is important. Normally, the internal flow pattern of central 'air' core is expected to have little effect on the calculation of separation efficiency, because the streamlines do not enter the core while they pass through cyclone. The radius of the central region will have effect on the flowfield of main body. Some imperial relations can be used to estimate the radius for the purpose of efficiency prediction. The theoretical estimation of the radius of a central region is complex. For a flow pattern of the main body in a cyclone, several different flow patterns of central region can be matched, which depend on the tangential velocity, the structures of collection bin and exit tube. It is noted that sometimes the flow pattern of the central region may have effect on separation performance if the re-entrance of particles from collection bin occur.

My simple reverse swirling model can correctly describe the flowfield and the relationships between the velocity components.

2. 4 CONCLUSION

1. I have given the general flow patterns under the assumption of tangential velocity not varying along axial direction: For viscous flow, tangential and radial velocities are then functions of radius alone respectively, and axial velocity is a linear function of axial distance. For inviscid flow, if $v_r \neq 0$, the tangential velocity $v_\varphi = \frac{C}{r}$, and axial and radial velocities are the functions of radius and axial distance.

2. For the first time, I find a simple inviscid exact solution for the reverse swirling flow in a cylinder, which shows the natural features of the flow similar to those from experimental investigations, The results of this model show good tendency with experiments by Wakelin (1993).

3. Most previous models have assumed that radial and axial velocities are not linked to the tangential vortex profile. My theory shows that this can be tenable in a certain range. When tangential velocity is high enough, it will be insensitive to the variations of axial and radial velocities; but the small variation in distributions of tangential velocity will decide the axial and radial velocities.

4. Design practice and my theory prove that it is not necessary to include the two regions ('air' core and inviscid main body) in a unified equation to describe one of velocity components, it makes the task intractable and may not reveal the flow nature.

5. To predict the efficiency, thus to improve the cyclones, more detail about radial velocity is desired. Previous models have not paid enough attention to this velocity component, and provide rough equations only. My theory gives an improvement for this knowledge.

Chapter 3

Analysis of Inviscid Flow in Cyclones

Abstract

In this chapter, I give some solutions of the simplified equations of motion for incompressible, steady, axisymmetric and inviscid flow. The simplification made by the assumptions of different vorticity distributions over the streamlines. The problem domains are both conical and cylindrical, and the solution can be used to study the flow in cyclones.

3.1 INTRODUCTION

The analytical general solution of the general equations of motion does not exist. We have to simplify the problem by suitable assumptions.

Since the Reynols number in the main body of cyclones is normally large enough, the flow may be regarded as inviscid. Some models such as in Bloor and Ingham's work (1987), as well as the work of myself mentioned in the chapter 2 show that good agreement between theoretical results and experiments can be obtained.

It is timely here to defend the use of inviscid solutions as opposed to the more difficult viscous ones, for the design of cyclones. An inviscid solution is adequate for particle collective efficiency estimation provided one is aware of the extent of the central viscous region. Generally collection models are concerned with the flow field beneath the gas exit tube and at larger radii. Mayer and Powell (1992) have shown by their comparison of viscid and inviscid models that they show significant difference only for radii less than the core radius (where tangential velocity is a maximum). Inviscid

models show increasing tangential and axial velocities towards the centre, within this core region, whereas viscid models give decreasing tangential and constant axial velocities towards the centre. Return-flow cyclones generally have a core radius a little more than half the gas exit radius (Iozia D. L. and Leith D. (1989)). Thus an inviscid model is adequate for the region below the gas exit lip, and at larger radii, and useful for particle collection estimation.

Some important relationships between characteristics of inviscid flowfield can be revealed by the solutions with inviscid assumption. All the real flowfield are viscous, the relationships may be distorted in a real flowfield. The comparisons confirm that the relationships may remain if they are extended in suitable situations such as to the normal cyclones with high enough Reynods number.

3.2. THEORY

If we introduce the streamfunction ψ, the equation of motion for the incompressible, steady, axisymmetric and inviscid flow with uniform density can be written as,

$$\frac{\partial^2 \Psi}{\partial R^2} + \frac{\sin\theta}{R^2}\frac{\partial}{\partial \theta}\left(\frac{1}{\sin\theta}\frac{\partial \Psi}{\partial \theta}\right) = -\Gamma\frac{d\Gamma}{d\Psi} + R^2\sin^2\theta\frac{dH}{d\Psi} = -\omega R\sin\theta$$

$$V_R = \frac{1}{R^2\sin\theta}\frac{\partial \Psi}{\partial \theta}$$

$$V_\theta = -\frac{1}{R\sin\theta}\frac{\partial \Psi}{\partial R}$$

(Spherical polar co-ordinates (R, θ, φ))

or

$$\frac{\partial^2 \psi}{\partial X^2} + \frac{\partial^2 \psi}{\partial R^2} - \frac{1}{R}\frac{\partial \psi}{\partial R} = -\Gamma\frac{d\Gamma}{d\psi} + R^2\frac{dH}{d\psi} = -\omega R$$

$$V_x = \frac{1}{R}\frac{\partial \Psi}{\partial R}$$

$$V_r = -\frac{1}{R}\frac{\partial \Psi}{\partial X}$$

(Cylindrical co-ordinates (X, R, φ))

Γ is $(2\pi)^{-1}$ times the circulation round a symmetrically placed circle, and $H = \frac{p}{\rho} + \frac{V^2}{2}$ is ρ^{-1} times the total pressure. Both Γ and H are functions of ψ alone. ω is the vorticity in axisymmetric flow.

The vorticity can be divided into two parts, one related to circulation, another related to total pressure.

Each of these parts can be expanded by polynomials

$$\frac{\partial^2 \Psi}{\partial R^2} + \frac{\sin\theta}{R^2}\frac{\partial}{\partial \theta}\left(\frac{1}{\sin\theta}\frac{\partial \Psi}{\partial \theta}\right) = \sum_0^N a_i \Psi^i + R^2 \sin^2\theta \sum_0^N b_i \Psi^i \qquad (3\text{-}1)$$

(Spherical polar co-ordinates (R, θ, φ))

or

$$\frac{\partial^2 \Psi}{\partial X^2} + \frac{\partial^2 \Psi}{\partial R^2} - \frac{1}{R}\frac{\partial \Psi}{\partial R} = \sum_0^N a_i \Psi^i + R^2 \sum_0^N b_i \Psi^i \qquad (3\text{-}1a)$$

(Cylindrical co-ordinates (X, R, φ))

The different groups of parameters (a_i , b_i) correlate different flow patterns.

I will briefly give some of the solutions of the pattern equations (3-1) and (3-1a) here.

3.2.1 Flow patterns in conical cyclones

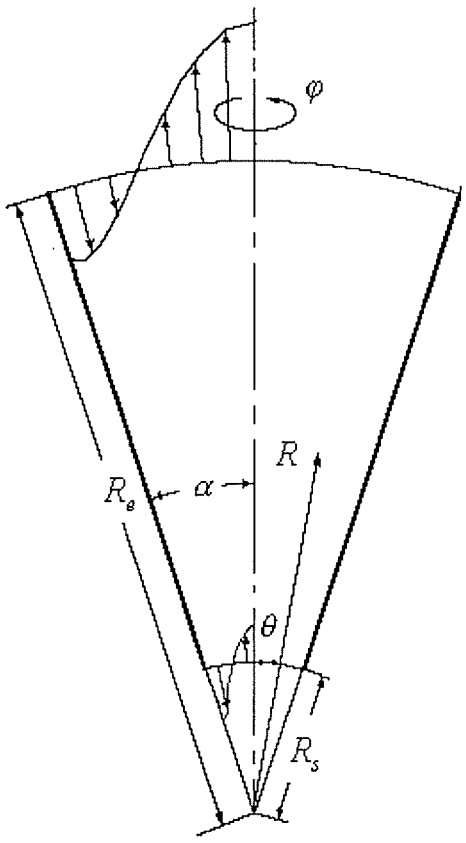

Fig. 3-1 Schematic representation of the calculation domain for a conical cyclone

If series a_i and b_i are determined (I will give the method to determine a_i and b_i in Chapter 8), equation (3-1) will be solved with the boundary conditions: $V_\theta = 0$ on the wall ($\theta = \alpha$) and the axis ($\theta = 0$); V_R will be given on the upper boundary $V_R(R_e,\theta) = f_e(\theta)$ and bottom boundary $V_R(R_s,\theta) = f_s(\theta)$. The streamfunction on the upper boundary can be calculated as $\Psi_e(\theta) = \Psi(R_e,\theta) = \int V_R(R_e,\theta)R_e^2 \sin\theta d\theta = \int f_e(\theta)R_e^2 \sin\theta d\theta$; and on the bottom boundary $\Psi_s(\theta) = \int f_s(\theta)R_s^2 \sin\theta d\theta$.

Conical pattern I

If all the terms on the right side of equation (3-1) are 0, a potential flow will be described.

$$\frac{\partial^2\psi}{\partial R^2} + \frac{\sin\theta}{R^2}\frac{\partial}{\partial\theta}\left(\frac{1}{\sin\theta}\frac{\partial\psi}{\partial\theta}\right) = 0 \qquad (3\text{-}2)$$

The full solution in the conical domain defined by Fig.3-1 for equation (3-2) is

$$\Psi = \Psi_3^* + \Psi_4^*$$

$$\Psi_3^*(R,\theta) = \frac{\Psi(R,\alpha)(1-\cos\theta) + \Psi(R,0)(\cos\theta - \cos\alpha)}{1-\cos\alpha} \qquad (3\text{-}3)$$

$$\Psi_4^* = \sum_{i=1}^{\infty} (A_i R^{-\nu_i+1} + B_i R^{\nu_i}) Z_i(\theta) \qquad (3\text{-}4)$$

Ψ_3^* is a 'direct flow' term. $\Psi(R,\alpha)$ and $\Psi(R,0)$ in equation (3-3) are the stream-functions next to the wall (at $\theta = \alpha$) and on the axis or at the surface of any isolated core , at the upper boundaries. Ψ_3^* describes the solution due to the flow passed through the cyclone from one end to the other, such as the flow in a direct flow gas cyclone (a uni-flow cyclone) or the underflow in a hydrocyclone. It does not introduce vorticity.

Ψ_4^* is the solution of the case with no net flow, and is the sum of a series of eigenfunctions whose detail can be found in the appendix. It can be used to fit any boundary profile. Since the weighting functions in the eigenfunction have high order of R, they change acutely along the axial direction. So the solution of this part has its effect only close to the boundary regions. However it is in such portions that some problems such as shortcut flow attract the designer's attention. Ψ_4^* can be used to describe the secondary flows near the inlet and outlet. This term does not introduce vorticity.

Conical pattern II

The pattern equation is

$$\frac{\partial^2 \Psi}{\partial R^2} + \frac{\sin\theta}{R^2}\frac{\partial}{\partial \theta}\left(\frac{1}{\sin\theta}\frac{\partial \Psi}{\partial \theta}\right) = a_1 \Psi \qquad (3\text{-}5)$$

The full solution in a conical domain defined by Fig.3-1 for equation (3-5) is

$$\Psi = \Psi_3^{**} + \Psi_4^{**}$$

$$\Psi_3^{**}(R,\theta) = \frac{\sin(AR+B)(\Psi(1,\alpha)(1-\cos\theta)+\Psi(1,0)(\cos\theta-\cos\alpha))}{\sin(A+B)(1-\cos\alpha)} \tag{3-6}$$

where

$A = \sqrt{-a_1}$

$$B = arctg[\frac{\Psi(1,\alpha)\sin(AR_s)-\Psi(R_s,\alpha)\sin(A)}{\Psi(1,\alpha)\cos(AR_s)-\Psi(R_s,\alpha)\cos(A)}]$$

$$\Psi_4^{**} = \sum_{i=1}^{\infty} (A_i J_{v_i-0.5}(AR) + B_i Y_{v_i-0.5}(AR)) R^{\frac{1}{2}} Z_i(\theta) \tag{3-7}$$

$J_{v_i-0.5}(AR)$ is the first kind of Bessel function, of $v_{i-0.5}$ order

$Y_{v_i-0.5}(AR)$ is the second kind of Bessel function, of $v_{i-0.5}$ order

$$A_i = \frac{F(R_e)R_e^{-0.5}\ Y_{v_i-0.5}(AR_s) - F(R_s)R_e^{-0.5}\ Y_{v_i-0.5}(AR_e)}{J_{v_i-0.5}(AR_e)\ Y_{v_i-0.5}(AR_s) - J_{v_i-0.5}(AR_s)\ Y_{v_i-0.5}(AR_e)} \tag{3-8}$$

$$B_i = \frac{F(R_s)R_e^{-0.5}\ J_{v_i-0.5}(AR_e) - F(R_e)R_e^{-0.5}\ J_{v_i-0.5}(AR_s)}{J_{v_i-0.5}(AR_e)\ Y_{v_i-0.5}(AR_s) - J_{v_i-0.5}(AR_s)\ Y_{v_i-0.5}(AR_e)} \tag{3-9}$$

$$F(R\ ) = \frac{\int_0^{\alpha} \frac{(\Psi(R,\theta)-\Psi_1^{**}(R,\theta)-\Psi_2^{**}(R,\theta)-\Psi_3^{**}(R,\theta))Z_i(\theta)d\theta}{\sin\theta}}{\int_0^{\alpha} \frac{Z_i^{\ 2}(\theta)d\theta}{\sin\theta}}$$

It can be proved that $\Psi_3^{**} \to \Psi_3^{*}$ and $\Psi_4^{**} \to \Psi_4^{*}$ respectively, when $a_1 \to 0$. But for a_1 nonzero both $\Psi_3^{**}(R,\theta)$ and $\Psi_4^{**}(R,\theta)$ introduce vorticitiy into the cyclones. (Note Ψ_1^{**} and Ψ_2^{**} are defined in parterres VI and VII below.)

Conical pattern III

Bloor and Ingham (1987) gave a particular solution for the equation with just a constant:

$$\frac{\partial^2 \Psi}{\partial R^2} + \frac{\sin\theta}{R^2}\frac{\partial}{\partial \theta}\left(\frac{1}{\sin\theta}\frac{\partial \Psi}{\partial \theta}\right) = a_0 \qquad (3\text{-}10)$$

Their particular solution was

$$\Psi_1^{*} = -0.5a_0R^2\{[\cos^2\alpha + \ln(0.5\tan\alpha) - \cos^2\alpha\cot\alpha]\sin^2\theta - \sin^2\theta\ln(0.5\tan\theta) + \cos\theta - 1\} \qquad (3\text{-}11)$$

I will give the full solution in a conical domain defined by Fig.3-1 for equation (3-10) here. The general solution is

$$\Psi = \Psi_1^{*} + \Psi_3^{*} + \Psi_4^{*}$$

Ψ_1^{*} is given by Bloor and Ingham's solution, which is a particular solution satisfying equation (3-10).

Ψ_3^{*} and Ψ_4^{*} describe the potential flow, which are the solutions satisfying equation (3-2).

Conical pattern IV

I found a particular solution for the following equation (3-12).

$$\frac{\partial^2 \Psi}{\partial R^2} + \frac{\sin\theta}{R^2}\frac{\partial}{\partial \theta}\left(\frac{1}{\sin\theta}\frac{\partial \Psi}{\partial \theta}\right) = b_0R^2\sin^2\theta \qquad (3\text{-}12)$$

The particular solution is

$$\Psi_2^{*} = \frac{b_0R^4}{10}\sin^2\theta\left(1 - \frac{1-5\cos^2\theta}{1-5\cos^2\alpha}\right) \qquad (3\text{-}13)$$

The full solution in a conical domain defined by Fig.3-1 by Fig.3-1 for equation (3-12) is

$$\Psi = \Psi_2^* + \Psi_3^* + \Psi_4^*$$

Conical pattern V

The pattern equation is

$$\frac{\partial^2 \Psi}{\partial R^2} + \frac{\sin\theta}{R^2}\frac{\partial}{\partial \theta}\left(\frac{1}{\sin\theta}\frac{\partial \Psi}{\partial \theta}\right) = a_0 + b_0 R^2 \sin^2\theta \qquad (3\text{-}14)$$

The full solution in a conical domain defined by Fig.3-1 for equation (3-14) is

$$\Psi = \Psi_1^* + \Psi_2^* + \Psi_3^* + \Psi_4^*$$

Conical pattern VI

The pattern equation is

$$\frac{\partial^2 \Psi}{\partial R^2} + \frac{\sin\theta}{R^2}\frac{\partial}{\partial \theta}\left(\frac{1}{\sin\theta}\frac{\partial \Psi}{\partial \theta}\right) = a_0 + a_1 \Psi \qquad (3\text{-}15)$$

The full solution in a conical domain defined by Fig.3-1 for equation (3-15) is

$$\Psi = \Psi_1^{**} + \Psi_3^{**} + \Psi_4^{**}$$

where

$$\Psi_1^{**} = \sum_{i=1}^{\infty} \frac{a_0 C_{ai} \pi R^{\frac{1}{2}}}{2}\left[-J_{\nu_i-0.5}(AR)\int_0^R r^{\frac{1}{2}} Y_{\nu_i-0.5}(Ar)dr + Y_{\nu_i-0.5}(AR)\int_0^R r^{\frac{1}{2}} J_{\nu_i-0.5}(Ar)dr\right] Z_i(\theta) \qquad (16)$$

and

$$C_{ai} = \frac{\int_0^{\alpha} \frac{Z_i(\theta)d\theta}{\sin\theta}}{\int_0^{\alpha} \frac{Z_i^2(\theta)d\theta}{\sin\theta}}$$

Conical pattern VII

The pattern equation is

$$\frac{\partial^2 \Psi}{\partial R^2} + \frac{\sin\theta}{R^2}\frac{\partial}{\partial \theta}\left(\frac{1}{\sin\theta}\frac{\partial \Psi}{\partial \theta}\right) = a_1\Psi + b_0 R^2 \sin^2\theta \qquad (3\text{-}17)$$

The full solution in a conical domain defined by Fig.3-1 for equation (3-17) is

$$\Psi = \Psi_2^{**} + \Psi_3^{**} + \Psi_4^{**}$$

where

$$\Psi_2^{**} = \sum_{i=1}^{\infty} \frac{b_0 C_{bi} \pi R^{\frac{1}{2}}}{2}\left[-J_{v_i-0.5}(AR)\int_0^R r^{\frac{5}{2}} Y_{v_i-0.5}(Ar)dr + Y_{v_i-0.5}(AR)\int_0^R r^{\frac{5}{2}} J_{v_i-0.5}(Ar)dr\right] Z_i(\theta) \qquad (3\text{-}18)$$

and

$$C_{bi} = \frac{\int_0^{\alpha} Z_i(\theta)\sin\theta d\theta}{\int_0^{\alpha} \frac{Z_i^2(\theta)d\theta}{\sin\theta}}$$

Conical pattern VIII

The pattern equation is

$$\frac{\partial^2 \Psi}{\partial R^2} + \frac{\sin\theta}{R^2}\frac{\partial}{\partial \theta}\left(\frac{1}{\sin\theta}\frac{\partial \Psi}{\partial \theta}\right) = a_0 + a_1\Psi + b_0 R^2 \sin^2\theta \qquad (3\text{-}19)$$

The full solution in a conical domain defined by Fig.3-1 for equation (3-19) is

$$\Psi = \Psi_1^{**} + \Psi_2^{**} + \Psi_3^{**} + \Psi_4^{**}$$

3.2.2. Flow patterns in Cylindrical cyclones

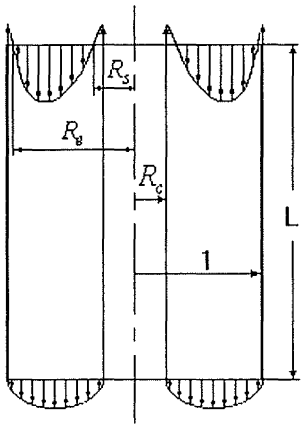

Fig. 3-2 The cylindrical problem domain

The boundary conditions are: $V_r = 0$ on the wall ($R = R_0$) and the surface of central isolated region ($R = R_c$); V_X will be given on the upper boundary $V_X(R,0) = f_0(R)$ and bottom boundary $V_X(R,L) = f_B(R)$. The streamfunctions on the upper boundary can be calculated as $\Psi_0(R) = \Psi(R,0) = \int V_X(R,0)RdR = \int f_0(R)RdR$; and on the bottom boundary as $\Psi_B(R) = \Psi(R,L) = \int V_X(R,L)RdR = \int f_B(R)RdR$

Cylindrical pattern I

For the cylindrical cyclone, the potential flow equation is

$$\frac{\partial^2 \psi}{\partial X^2} + \frac{\partial^2 \psi}{\partial R^2} - \frac{1}{R}\frac{\partial \psi}{\partial R} = 0 \qquad (3\text{-}20)$$

(Cylindrical co-ordinates (X, R, φ))

The full solution of equation (3-20) in the gap between two circular cylinders of radius R_c and R_0 is

$$\Psi = \Psi_3^* + \Psi_4^*$$

where

$$\Psi_3^* = \frac{\Psi_I(R_0)(R^2 - R_c^2) + \Psi_I(R_c)(R_0^2 - R^2)}{R_0^2 - R_c^2} \qquad (3\text{-}21)$$

and

$$\Psi_4^* = \sum_{i=0}^{N} R(A_i e^{-\mu_{1i}X} + B_i e^{\mu_{1i}X}) Z_1(\mu_{1i}R) \qquad (3\text{-}22)$$

Also $Z_1(\mu_{1i}R) = J_1(\mu_{1i}R) - \frac{J_1(\mu_{1i}R_c)}{Y_1(\mu_{1i}R_c)} Y_1(\mu_{1i}R)$

$J_1(\mu_{1i}R)$ is the first kind of Bessel function, of order 1.

$Y_1(\mu_{1i}R)$ is the second kind of Bessel function, of order 1.

μ_{1i} is the ith eigenvalue of equation $J_1(\mu_{1i}R_0) - \frac{J_1(\mu_{1i}R_c)}{Y_1(\mu_{1i}R_c)} Y_1(\mu_{1i}R_0) = 0$.

$$A_i = \frac{-\int_{R_c}^{R_0} (\Psi(R,L) - \Psi_3^*) Z_1(\mu_{1i}R)\, dR + e^{\mu_{1i}L} \int_{R_c}^{R_0} (\Psi(R,0) - \Psi_3^*) Z_1(\mu_{1i}R)\, dR}{(R_0^2 Z_0(\mu_{1i}R_0^2)^2 - R_c^2 Z_0(\mu_{1i}R_c)^2)(e^{\mu_{1i}L} - e^{-\mu_{1i}L})}$$

$$B_i = \frac{\int_{R_c}^{R_0} (\Psi(R,L) - \Psi_3^*) Z_1(\mu_{1i}R)\, dR - e^{-\mu_{1i}L} \int_{R_c}^{R_0} (\Psi(R,0) - \Psi_3^*) Z_1(\mu_{1i}R)\, dR}{(R_0^2 Z_0(\mu_{1i}R_0^2)^2 - R_c^2 Z_0(\mu_{1i}R_c)^2)(e^{\mu_{1i}L} - e^{-\mu_{1i}L})}$$

Ψ_3^* is a 'direct flow' term. $\Psi_I(R_0)$ and $\Psi_I(R_c)$ in equation (3-21) are the stream-functions next to the wall and core at upper boundaries respectively. Ψ_3^* describes the solution due to the flow passed through the cyclone from one end to the other, such as

the flow in a direct flow gas cyclone (a uni-flow cyclone) or the underflow in a hydrocyclone. It does not introduce vorticity.

Ψ_4^* is an eigenfunction expansion. It can be used to fit any boundary profile. Since the weighting functions in the eigenfunction have high order of x in equation (3-22), they change acutely along the axial direction. So the solution of this part has its effect only close to the boundary regions (upper and lower). However it is in such portions that some problems such as shortcut flow attract the designer's attention. Ψ_4^* can be used to describe the secondary flows near the inlet and outlet. This term does not introduce vorticity.

Cylindrical pattern II

The pattern equation is

$$\frac{\partial^2 \psi}{\partial X^2} + \frac{\partial^2 \psi}{\partial R^2} - \frac{1}{R}\frac{\partial \psi}{\partial R} = a_1 \psi \qquad (3\text{-}23)$$

(Cylindrical co-ordinates (X, R, φ))

The full solution of equation (3-23) in the gap between two circular cylinders of radius R_c and R_0 is

$$\Psi = \Psi_3^{**} + \Psi_4^{**}$$

where

$$\Psi_3^{**} = \frac{[\Psi_I(R_0)Y_1(AR_c) - \Psi_I(R_c)Y_1(AR_0)]\ R\ J_1(AR)}{R_0 J_1(AR_0)Y_1(AR_c) - R_c J_1(AR_c)Y_1(AR_0)} + \frac{[\Psi_I(R_0)J_1(AR_c) - \Psi_I(R_c)J_1(AR_0)]\ R\ Y_1(AR)}{R_0 Y_1(AR_0)J_1(AR_c) - R_c Y_1(AR_c)J_1(AR_0)}$$

$$\Psi_4^{**} = \sum_{i=0}^{M-1} R(A_i \sin((A^2 - \mu_{1i}^2)^{\frac{1}{2}} X) + B_i \cos((A^2 - \mu_{1i}^2)^{\frac{1}{2}} X)) Z_1(\mu_{1i} R)$$

$$+ \sum_{i=M}^{N} R(A_i e^{-(\mu_{1i}^2 - A^2)^{\frac{1}{2}} X} + B_i e^{(\mu_{1i}^2 - A^2)^{\frac{1}{2}} X}) Z_1(\mu_{1i} R)$$

where $A^2 = -a_1$

These eigenvalues are related as follows

$$0 < .... \mu_{1i} < \mu_{1i+1} < ... \mu_{1M-1} < A < \mu_{1M} < ... < \mu_{1N} .$$

M is the first i, for which the eigenvalues are larger than A.

$\Psi_I(R_0)$ and $\Psi_I(R_c)$ are the stream-functions next to the wall and core at upper boundaries respectively

When $i < M$

$$A_i = \frac{\int_{R_c}^{R_0} (\Psi - \Psi_1^{**} - \Psi_2^{**} - \Psi_3^{**}) \mid_{X=L} Z_1(\mu_{1i} R) dR - \cos((A^2 - \mu_{1i}^2)^{\frac{1}{2}} L) \int_{R_c}^{R_0} (\Psi - \Psi_1^{**} - \Psi_2^{**} - \Psi_3^{**}) \mid_{X=0} Z_1(\mu_{1i} R) dR}{(R_0^2 Z_0(\mu_{1i} R_0^2)^2 - R_c^2 Z_0(\mu_{1i} R_c)^2) \sin((A^2 - \mu_{1i}^2)^{\frac{1}{2}} L)}$$

$$B_i = \frac{\int_{R_c}^{R_0} (\Psi - \Psi_1^{**} - \Psi_2^{**} - \Psi_3^{**}) \mid_{X=0} Z_1(\mu_{1i} R) dR}{(R_0^2 Z_0(\mu_{1i} R_0^2)^2 - R_c^2 Z_0(\mu_{1i} R_c)^2)}$$

When $M \le i \le N$

$$A_i = \frac{-\int_{R_c}^{R_0} (\Psi - \Psi_1^{**} - \Psi_2^{**} - \Psi_3^{**}) \mid_{X=L} Z_1(\mu_{1i} R) dR + e^{(\mu_{1i}^2 - A^2)^{\frac{1}{2}} L} \int_{R_c}^{R_0} (\Psi - \Psi_1^{**} - \Psi_2^{**} - \Psi_3^{**}) \mid_{X=0} Z_1(\mu_{1i} R) dR}{(R_0^2 Z_0(\mu_{1i} R_0^2)^2 - R_c^2 Z_0(\mu_{1i} R_c)^2)(e^{(\mu_{1i}^2 - A^2)^{\frac{1}{2}} L} - e^{-(\mu_{1i}^2 - A^2)^{\frac{1}{2}} L})}$$

$$B_i = \frac{\int_{R_c}^{R_0}(\Psi - \Psi_1^{**} - \Psi_2^{**} - \Psi_3^{**})\,|_{X=L} Z_1(\mu_{1i}R)dR - e^{-(\mu_{1i}^2 - A^2)^{\frac{1}{2}}L}\int_{R_c}^{R_0}(\Psi - \Psi_1^{**} - \Psi_2^{**} - \Psi_3^{**})\,|_{X=0} Z_1(\mu_{1i}R)dR}{(R_0^2 Z_0(\mu_{1i}R_0^2)^2 - R_c^2 Z_0(\mu_{1i}R_c)^2)(e^{(\mu_{1i}^2 - A^2)^{\frac{1}{2}}L} - e^{-(\mu_{1i}^2 - A^2)^{\frac{1}{2}}L})}$$

Cylindrical pattern III

The pattern equation is

$$\frac{\partial^2 \Psi}{\partial X^2} + \frac{\partial^2 \Psi}{\partial R^2} - \frac{1}{R}\frac{\partial \Psi}{\partial R} = a_0 \qquad (3\text{-}24)$$

The full solution of equation (3-24) in the gap between two circular cylinders of radius R_c and R_0 is

$$\Psi = \Psi_1^* + \Psi_3^* + \Psi_4^*$$

where

$$\Psi_1^* = \frac{0.5a_0[R^2(R_0^2(\ln R - \ln R_0) - R_c^2(\ln R - \ln R_c)) + R_c^2 R_0^2(\ln R_0 - \ln R_c)]}{R_0^2 - R_c^2} \qquad (3\text{-}25)$$

Cylindrical pattern IV

The pattern equation is

$$\frac{\partial^2 \Psi}{\partial X^2} + \frac{\partial^2 \Psi}{\partial R^2} - \frac{1}{R}\frac{\partial \Psi}{\partial R} = R^2 b_0 \qquad (3\text{-}26)$$

The full solution of equation (26) in the gap between two circular cylinders of of radius R_c and R_0 is

$$\Psi = \Psi_2^* + \Psi_3^* + \Psi_4^*$$

where

$$\Psi_2^* = \frac{b_0(R^2 - R_0^2)(R^2 - R_c^2)}{8} \qquad (3\text{-}27)$$

Cylindrical pattern V

The pattern equation is

$$\frac{\partial^2 \Psi}{\partial X^2} + \frac{\partial^2 \Psi}{\partial R^2} - \frac{1}{R}\frac{\partial \Psi}{\partial R} = a_0 + R^2 b_0 \qquad (3\text{-}28)$$

The full solution of equation (3-28) in the gap between two circular cylinders of radius R_c and R_0 is

$$\Psi = \Psi_1^* + \Psi_2^* + \Psi_3^* + \Psi_4^*$$

Cylindrical pattern VI

The pattern equation is

$$\frac{\partial^2 \Psi}{\partial X^2} + \frac{\partial^2 \Psi}{\partial R^2} - \frac{1}{R}\frac{\partial \Psi}{\partial R} = a_0 + a_1 \Psi \qquad (3\text{-}29)$$

The full solution of equation (3-29) in the gap between two circular cylinders of radius R_c and R_0 is

$$\Psi = \Psi_1^{**} + \Psi_3^{**} + \Psi_4^{**}$$

where

$$\Psi_1^{**} = -\frac{a_0}{a_1}[1 + \frac{RJ_1(AR)(R_0Y_1(AR_0) - R_cY_1(AR_c)) - RY_1(AR)(R_0J_1(AR_0) - R_cJ_1(AR_c))}{R_0R_c(J_1(AR_0)Y_1(AR_c) - J_1(AR_c)Y_1(AR_0))}]$$

(3-30)

Cylindrical pattern VII

The pattern equation is

$$\frac{\partial^2\Psi}{\partial X^2} + \frac{\partial^2\Psi}{\partial R^2} - \frac{1}{R}\frac{\partial \Psi}{\partial R} = a_1\Psi + R^2b_0 \qquad (3\text{-}31)$$

The full solution of equation (3-31) in the gap between two circular cylinders of radius R_c and R_0 is

$$\Psi = \Psi_2^{**} + \Psi_3^{**} + \Psi_4^{**}$$

where

$$\Psi_2^{**} = -\frac{b_0}{a_1}[R^2 - \frac{RJ_1(AR)(R_0Y_1(AR_c) - R_cY_1(AR_0)) - RY_1(AR)(R_0J_1(AR_c) - R_cJ_1(AR_0))}{J_1(AR_0)Y_1(AR_c) - J_1(AR_c)Y_1(AR_0)}]$$

(3-32)

Cylindrical pattern VIII

The pattern equation is

$$\frac{\partial^2\Psi}{\partial X^2} + \frac{\partial^2\Psi}{\partial R^2} - \frac{1}{R}\frac{\partial \Psi}{\partial R} = a_0 + a_1\Psi + R^2b_0 \qquad (3\text{-}33)$$

The full solution of equation (3-33) in the gap between two circular cylinders of radius R_c and R_0 is

$$\Psi = \Psi_1^{**} + \Psi_2^{**} + \Psi_3^{**} + \Psi_4^{**}$$

APPENDIX: Details of functions in Ψ_4

In equation (3-4),

$$Z_i(\theta) = p_i^*(\theta) - \frac{p_i^*(0)}{q_i^*(0)} q_i^*(\theta)$$

$$p_i^*(\theta) = \frac{(\nu_i - 1)\int_0^\theta \cos^{\nu_i - 2}(\theta) p_i(\cos\theta) d(\cos(\theta))}{\cos^{\nu_i - 1}(\theta)}$$

$p_i(\cos\theta)$ is the first kind of Legendre function

$$q_i^*(\theta) = \frac{(\nu_i - 1)\int_0^\theta \cos^{\nu_i - 2}(\theta) q_i(\cos\theta) d(\cos(\theta))}{\cos^{\nu_i - 1}(\theta)}$$

$q_i(\cos\theta)$ is the second kind of Legendre function

ν_i is the eigenvalue of equation

$$Z_i(\alpha) = p_i^*(\alpha) - \frac{p_i^*(0)}{q_i^*(0)} q_i^*(\alpha)$$

$$A_i = \frac{R_s^{\nu_i}\left(\int_0^\alpha \frac{10\Psi(R_e,\theta) Z_i(\theta) d\theta}{\sin\theta} + a_0 R_e^2 Z_{1ig} - b_0 R_e^4 Z_{2ig}\right) - R_e^{\nu_i}\left(\int_0^\alpha \frac{10\Psi(R_s,\theta) Z_i(\theta) d\theta}{\sin\theta}\right.}{Z_{ig}(R_e^{-\nu_i+1} R_s^{\nu_i} - R_e^{\nu_i} R_s^{-\nu_i+1})}$$

$$\left. + a_0 R_s^2 Z_{1ig} - b_0 R_s^4 Z_{2ig}\right) + ((\Psi(R,\alpha) - \Psi(R,0)) Z_{3ig} + \Psi(R,0) Z_{4ig})(R_s^{\nu_i} - R_e^{\nu_i})$$

$$B_i = \frac{R_s^{-\nu_i+1}\left(\int_0^{\alpha} \frac{10\Psi(R_e,\theta)Z_i(\theta)d\theta}{\sin\theta} + a_0 R_e^2 Z_{1ig} - b_0 R_e^4 Z_{2ig}\right) - R_e^{-\nu_i+1}\left(\int_0^{\alpha} \frac{10\Psi(R_s,\theta)Z_i(\theta)d\theta}{\sin\theta}\right.}{Z_{ig}(R_e^{\nu_i} R_s^{-\nu_i+1} - R_e^{-\nu_i+1} R_s^{\nu_i})}$$

$$\left. + a_0 R_s^2 Z_{1ig} - b_0 R_s^4 Z_{2ig}\right) + ((\Psi(R,\alpha) - \Psi(R,0))Z_{3ig} + \Psi(R,0)Z_{4ig})(R_s^{-\nu_i+1} - R_e^{-\nu_i+1})$$

$$Z_{ig} = 10\int_0^{\alpha} \frac{Z_i^{\,2}(\theta)d\theta}{\sin\theta}$$

$$Z_{1ig} = \int_0^{\alpha} 5(C_\alpha - \ln(0.5\tan\theta) - \frac{1}{1+\cos\theta})(\sin\theta)Z_i(\theta)d\theta$$

with $C_\alpha = \cos ec^2\alpha + \ln(0.5\tan\alpha) - \cos ec\alpha\cot\alpha$

$$Z_{2ig} = \int_0^{\alpha} (1 - \frac{1-5\cos^2\theta}{1-5\cos^2\theta})(\sin\theta)Z_i(\theta)d\theta$$

$$Z_{3ig} = \int_0^{\alpha} \frac{-10}{(1+\cos\theta)(1-\cos\alpha)}(\sin\theta)Z_i(\theta)d\theta$$

$$Z_{4ig} = \int_0^{\alpha} \frac{-10}{\sin\theta} Z_i(\theta)d\theta$$

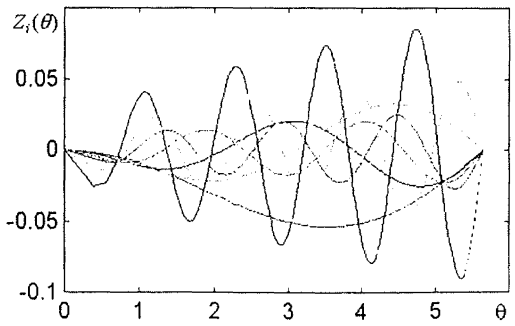

Fig.4-5 Functions $Z_i(\theta)$ vs polar angle θ with α=5.65 degrees

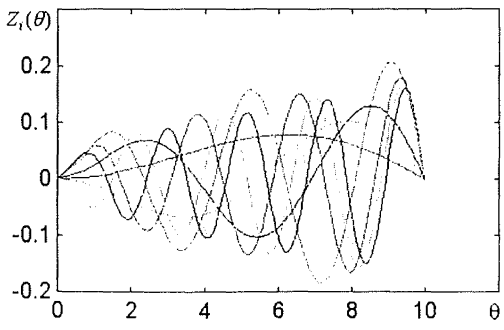

Fig.4-6 Functions $Z_i(\theta)$ vs polar angle θ with α=10 degrees

Chapter 4

A Steady Axisymmetric Reverse Flow With Swirl in a Conical Cyclone

(Conical pattern V)

Part I Theory

ABSTRACT

A mathematical model for the flow in a conical cyclone is developed, which is an exact solution of the equation of motion for steady axisymmetric inviscid flow. The solution consists of four terms representing the effects of circulation, total pressure, 'net flow' and potential flow on the streamfunction respectively. Some particular cases are discussed to show the flexibility and application of the solution.

4.1 INTRODUCTION

Bloor and Ingham (1987) obtained a simple mathematical model for the flow in a conical cyclone, which allows a solution to be obtained in closed form. The flow in the main body of the cyclone is regarded as inviscid but the nature of the fluid entry to the device and the conical geometry ensure that secondary flows develop which make the flow highly rotational. The results of the theory were compared with data from two quite different experimental investigations, and good agreement was obtained over a limited range. Their solution was quite simple, so that it is good for designers. Since this solution can match only a fixed form of velocity distribution at the upstream boundary, it could not be used to analyse the flowfield in the upper portion of cyclones. They recognised that the full solution would be required for more specific boundary conditions. Furthermore, some factors not considered by Bloor and Ingham such as the radial distribution of total pressure, net downflow and existence of a

central region such as an 'air core' will affect the flowfield in cyclones. Thus for a number of reasons, a more general solution for this problem is desirable.

In this chapter a mathematical model for the flow in a conical cyclone is developed, which is an exact solution of the equation of motion for steady axisymmetric inviscid flow with net downflow. Compared with Bloor and Ingham's solution, my solution is a 'flexible' solution for this kind of problem, which consists of four terms representing the effects of non-uniform circulation, non-uniform total pressure, 'net flow' and potential flow on the streamfunction respectively. Some particular cases will be discussed to show the flexibility and application of the solution.

4.2 THEORY

We use spherical polar co-ordinates (r, θ, φ), with corresponding velocity components $(v_r, v_\theta, v_\varphi)$. The origin is at the apex of the cone, the axis is along θ=0 and the surface of the cone boundary is on θ=α. If we introduce the streamfunction ψ, the motion for steady axisymmetric inviscid flow of an incompressible fluid can be described by the vorticity equation (Batchelor 1967, Bloor and Ingham 1987),

$$\frac{\partial^2\psi}{\partial r^2}+\frac{\sin\theta}{r^2}\frac{\partial}{\partial\theta}\left(\frac{1}{\sin\theta}\frac{\partial\psi}{\partial\theta}\right)=-\gamma\frac{d\gamma}{d\psi}+r^2\sin^2\theta\frac{dh}{d\psi} \qquad (4\text{-}1)$$

$$v_r=\frac{1}{r^2\sin\theta}\frac{\partial\psi}{\partial\theta}$$

$$v_\theta=-\frac{1}{r\sin\theta}\frac{\partial\psi}{\partial r}$$

$\gamma = rv_\varphi\sin\theta$ is ($(2\pi)^{-1}$ times) the circulation round any axisymmetrically placed circle, and $h=\frac{p}{\rho}+\frac{1}{2}(v_\theta^2+v_r^2+v_\varphi^2)$ is (ρ^{-1} times) the total pressure. Both γ and h are functions of ψ alone.

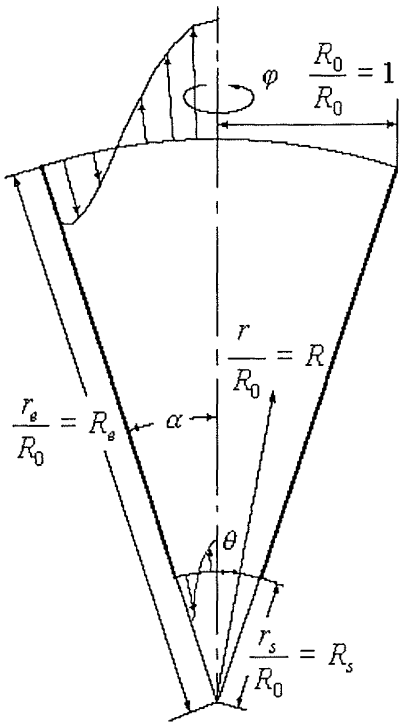

Fig. 4-1 Schematic representation of the calculation domain for a conical cyclone

For convenience, we introduce non-dimensional variables as follows for a conical domain.

$$R = \frac{r}{R_0}, \qquad V_\theta = \frac{v_\theta}{V_{\max 0}}, \quad V_R = \frac{v_r}{V_{\max 0}}, \quad V_\varphi = \frac{v_\varphi}{V_{\max 0}},$$

$$\Psi = \frac{\psi}{V_{\max 0} R_0^2}, \quad \Gamma = \frac{v_\varphi r \sin\theta}{V_{\max 0} R_0}, \quad H = \frac{h}{V_{\max 0}^2}, \quad P = \frac{p}{\rho V_{\max 0}^2}$$

R_0 is the cylindrical radius of the upper boundary of the conical domain, and $V_{\max 0}$ is the absolute magnitude of the maximum velocity vector at the upstream inflow boundary.

r_s is the spherical radius of the lower boundary of the calculation domain.

r_e is the spherical radius of the upper boundary of the calculation domain.

The non-dimensional inviscid equation of steady, rotational symmetric flow is then

$$\frac{\partial^2\Psi}{\partial R^2}+\frac{\sin\theta}{R^2}\frac{\partial}{\partial\theta}\left(\frac{1}{\sin\theta}\frac{\partial\Psi}{\partial\theta}\right)=-\Gamma\frac{d\Gamma}{d\Psi}+R^2\sin^2\theta\frac{dH}{d\Psi} \tag{4-2}$$

$$V_R=\frac{1}{R^2\sin\theta}\frac{\partial\Psi}{\partial\theta} \tag{4-3}$$

$$V_\theta=-\frac{1}{R\sin\theta}\frac{\partial\Psi}{\partial R} \tag{4-4}$$

We can write the terms on the right hand side of equation (4-2) in polynomial form. The first term can be written as,

$$-\Gamma\frac{d\Gamma}{d\Psi}=\sum_0^N a_i\Psi^i \tag{4-5}$$

the second term as

$$R^2\sin^2\theta\frac{dH}{d\Psi}=R^2\sin^2\theta\sum_0^N b_i\Psi^i \tag{4-6}$$

Then equation (4-2) changes to

$$\frac{\partial^2\Psi}{\partial R^2}+\frac{\sin\theta}{R^2}\frac{\partial}{\partial\theta}\left(\frac{1}{\sin\theta}\frac{\partial\Psi}{\partial\theta}\right)=\sum_0^N a_i\Psi^i+R^2\sin^2\theta\sum_0^N b_i\Psi^i \tag{4-7}$$

The general solution for the above equation has not been found.

For many cases, the absolute value of the largest value of dimensionless streamfunction is less than one and we can as an adequate approximation use only the linear main terms.

Bloor and Ingham (1987) found a particular solution for the equation with just a constant:

$$\frac{\partial^2\Psi}{\partial R^2}+\frac{\sin\theta}{R^2}\frac{\partial}{\partial\theta}\left(\frac{1}{\sin\theta}\frac{\partial\Psi}{\partial\theta}\right)=a_0 \tag{4-8}$$

Their particular solution was (which we call Ψ_1^*)

$$\Psi_1^* = -0.5a_0R^2\{[\cos ec^2\alpha + \ln(0.5\tan\alpha) - \cos ec\alpha\cot\alpha]\sin^2\theta - \sin^2\theta\ln(0.5\tan\theta) + \cos\theta - 1\} \tag{4-9}$$

I present here a more flexible solution in a conical domain for equation (4-7) with non-zero coefficients from both series:

$$\frac{\partial^2\Psi}{\partial R^2} + \frac{\sin\theta}{R^2}\frac{\partial}{\partial\theta}\left(\frac{1}{\sin\theta}\frac{\partial\Psi}{\partial\theta}\right) = a_0 + b_0R^2\sin^2\theta \tag{4-10}$$

The 'flexible solution' including all solutions for this problem is

$$\Psi = \Psi_1^* + \Psi_2^* + \Psi_3^* + \Psi_4^* \tag{4-11}$$

where

Ψ_1^* is given by Bloor and Ingham's solution, which is a particular solution satisfying equation (4-10) with $b_0 = 0$, ie for non-zero $\frac{d\Gamma}{d\Psi}$, and zero $\frac{dH}{d\Psi}$.

Ψ_2^* is a particular solution satisfying equation (4-10) with $a_0 = 0$, ie for zero $\frac{d\Gamma}{d\Psi}$, and non-zero $\frac{dH}{d\Psi}$.

$$\Psi_2^* = \frac{b_0R^4}{10}\sin^2\theta\left(1 - \frac{1-5\cos^2\theta}{1-5\cos^2\alpha}\right) \tag{4-12}$$

Ψ_3^* and Ψ_4^* are solutions satisfying equation (4-10) with $a_0 = 0$ and $b_0 = 0$, ie for zero $\frac{d\Gamma}{d\Psi}$ and zero $\frac{dH}{d\Psi}$, but with respectively different boundary conditions.

Ψ_3^* is determined by the net flow given in the upper boundary condition, which specifies values for $\Psi(R,\alpha)$ and $\Psi(R,0)$.

$$\Psi_3^*(R,\theta)=\frac{\Psi(R,\alpha)(1-\cos\theta)+\Psi(R,0)(\cos\theta-\cos\alpha)}{1-\cos\alpha} \qquad (4\text{-}13)$$

Ψ_4^* is the solution of the case with no net flow, and is the sum of a series of eigenfunctions whose detail can be found in the appendix of last chapter.

$$\Psi_4^*=\sum_{i=1}^{\infty}(A_iR^{-\nu_i+1}+B_iR^{\nu_i})Z_i(\theta) \qquad (4\text{-}14)$$

For both Ψ_3^* and Ψ_4^* the tangential vorticity $(\omega_\varphi=-\frac{1}{R\sin\theta}[\frac{\partial^2\Psi}{\partial R^2}+\frac{\sin\theta}{R^2}\frac{\partial}{\partial\theta}(\frac{1}{\sin\theta}\frac{\partial\Psi}{\partial\theta})])$ is 0; both the radial vorticity $(\omega_R=V_R\frac{d\Gamma}{d\Psi})$ and the vorticity in the colatitude direction $(\omega_\theta=V_\theta\frac{d\Gamma}{d\Psi})$ are also 0. So both Ψ_3^* and Ψ_4^* describe potential flows.

By comparing equations (4-2) and (4-10), the relationship between tangential velocity and streamfunction can be found. The result is

$$V_\varphi=\frac{(D-2a_0\psi)^{\frac{1}{2}}}{R\sin\theta} \qquad (4\text{-}15)$$

where D is a constant evaluated from the upstream boundary conditions.

In order to specify boundary conditions and compare more easily this theory with experiment, it is convenient to resolve the two components V_θ and V_R into vertical and radial components of velocity (cylindrical coordinates), denoted by $V_x=V_R\cos\theta-V_\theta\sin\theta$ and $V_r=V_R\sin\theta+V_\theta\cos\theta$ respectively.

Equation (4-10) may be regarded as the simplification of equation (4-2) by the linearization of the terms on the right. The flow cases described by equation (4-10) are only a part of that covered by the full equation (4-2), but these cases are known (see below) to be interesting and important. In order to show the application of the part

solutions Ψ_1^* to Ψ_4^*, some special cases will now be given. We can obtain some by imposing boundary conditions and then simplifying equation (4-2). Batchelor (1967) gave an example of this method. In cases of steady flow in which all the streamlines come from a region where the values of H and Γ for the different streamlines are known, the functions $H(\Psi)$ and $\Gamma(\Psi)$ in equation (4-2) are known. Ψ can then be determined, in principle, as a function of axial position x and cylindrical radius r over the whole field. Batchelor assumed in his case that the fluid far upstream has uniform axial velocity V_{xu}, rotates as a rigid body with angular velocity Ω and with radial velocity $V_r = 0$, and he obtained the relationship between streamfunction and circulation, as well as streamfunction and total pressure. He rewrote these upstream conditions as

$$\Gamma = \frac{2\Omega}{V_{xu}}\Psi, \qquad H = \frac{1}{2}V_{xu}^2 + \frac{2\Omega^2}{V_{xu}}\Psi$$

These relationships remain valid over the whole field.

4.3 EXAMPLES

I will give some examples of boundary conditions leading to values of a_0 and b_0 in equation (4-10) and hence to solutions via Ψ_1^* to Ψ_4^*.

Case I: We can begin with the Bloor and Ingham (1987) example. Though they describe the flow field in spherical polar co-ordinates, they determine the upstream relationships in a *cylindrical* section. It was assumed that the flow is axially symmetric, and enters this region of the cyclone with a 'top hat' profile in the tangential velocity component $V_{\varphi u}$, and uniform (inward to the region) axial velocity V_{xu}. The radial velocity was chosen to ensure that it is zero at the cylindrical wall and that H is a constant. These upstream conditions are

$$\Psi = \frac{1}{2}V_{xu}(R_0^2 - \frac{\Gamma^2}{V_{\varphi u}^2}), \qquad H = \frac{1}{2}(V_{xu}^2 + V_{\varphi u}^2 + V_{ru}^2) + P = \text{constant}$$

where V_{ru} is the cylindrical radial velocity.

Equation (4-2) can then be simplified to

$$\frac{\partial^2 \Psi}{\partial R^2} + \frac{\sin\theta}{R^2}\frac{\partial}{\partial \theta}\left(\frac{1}{\sin\theta}\frac{\partial \Psi}{\partial \theta}\right) = -\frac{V_{u\varphi}^2}{V_{xu}} = \text{constant}$$

This is a special case for equation (4-10), in which $a_0 = -\frac{V_{\varphi u}^2}{V_{xu}}$, $b_0 = 0$.

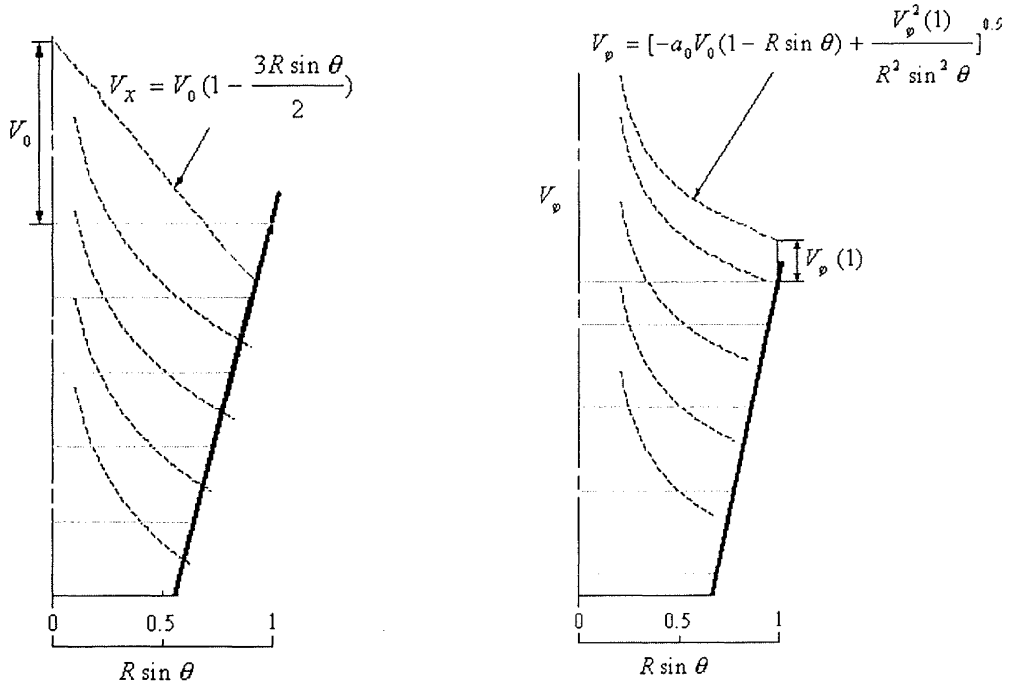

a) **Radial distributions of axial velocity at different levels**

b) **Radial distributions of tangential velocity at different levels**

Fig. 4-2 A flowfield of a particular case satisfying equation (4-8)

Case II: It is noted that equation (4-10) with a_0 non-zero, b_0 zero, ie equation (4-8) describes not only the case given by Bloor and Ingham, but also many others. Assume that at the upstream boundary, (1) axial velocity is $V_{xu} = V_0(1 - \frac{3R_c}{2})$ where R_c = (cylindrical radius)/ R_0; (2) tangential velocity is

$V_{\varphi u} = [-a_0 V_0 (1 - R_c) + \frac{V_\varphi^2(1)}{R_c^{\,2}}]^{0.5}$; (3) Also the radial velocity is chosen to ensure that it is zero at the cylinder wall and that H is a constant. We show below that the relationship between Γ and Ψ satisfies equation (4-8).

The streamfunction at the upstream boundary can be calculated from

$$\Psi = \int R_c V_{xu} dR_c = \int R_c V_0 (1 - \frac{3R_c}{2}) dR_c = \frac{V_0 R_c^{\,2}}{2}(1 - R_c) + c$$

(c is an arbitrary constant)

and

$$\Gamma^2 = R_c^{\,2} V_\varphi^2 = R_c^{\,2}[-a_0 V_0 (1 - R_c) + \frac{V_\varphi^2(1)}{R_c^{\,2}}] = -2a_0(\Psi - c) + c_1$$

(c_1 is an arbitrary constant)

Differentiating Γ^2 with respect to Ψ, we have $\Gamma \frac{d\Gamma}{d\Psi} = -a_0$; taking also H as a constant, $\frac{dH}{d\Psi} = 0$. Bringing these relationships into equation (4-2), equation (4-8) is obtained again.

Fig. 4-2 shows axial and tangential velocities of our particular case expressed *in spherical polar co-ordinates R, θ* with upstream boundary conditions as follows; axial velocity $V_{xu} = V_0 (1 - \frac{3R\ \sin\theta}{2})$, tangential velocity $V_{\varphi u} = [-a_0 V_0 (1 - R\ \sin\theta) + \frac{V_\varphi^2(1)}{R^{\,2} \sin^2\theta}]^{0.5}$, and H = constant.

Case III: Another case defined by equation (4-8) is: Assume that at the upstream boundary, (1) $V_{xu} = c_1 R_c^{\,2} + c_2$, ($c_1$, c_2 are arbitrary constants) where R_c = cylindrical radius/ R_0; (2) $V_{\varphi u} = \frac{c_2}{R_c} + c_1 R_c$; (3) H = constant. The relationships at the upstream boundary can be determined as following;

$$\Gamma = R_c V_{\varphi u} = c_2 + c_1 R_c^2$$

$$\Psi = \int R_c V_{xu} dR_c = \int R_c (c_1 R_c^{\ 2} + c_2) dR_c = \frac{c_1 R_c^{\ 4}}{4} + \frac{c_2 R_c^{\ 2}}{2} + c_3 = \frac{\Gamma^2}{4c_1} + c_3 - \frac{c_2^2}{4c_1}$$

(c_3 is an arbitrary constant)

Differentiating Γ^2 with respect to Ψ, we get $\Gamma \frac{d\Gamma}{d\Psi} = 2c_1$; since H is a constant, so $\frac{dH}{d\Psi} = 0$. Bringing these relationships into equation (4-2), again, equation (4-8) is again obtained. Here $a_0 = -2c_1$.

Case IV: This case is concerned with the constant b_0. We assume that (1) all the fluid particles entering have the same angular momentum, so that the circulation Γ is constant at a value Γ_u; (2) the radial velocity at the upper boundary $V_r = 0$, and (3) the axial velocity there has a radial distribution $V_{xu} = c_1 R_c^{\ 2} + c_2$, ($c_1, c_2$ are arbitrary constants) where R_c = cylindrical radius/ R_0.

Since Γ is constant, the first part on the right of equation (4-2) is zero. Having assumed at entry the cylindrical radial velocity $V_r = 0$, the radial equation of motion reduces here (for a steady flow) to

$$\frac{dP}{dR_c} = \frac{V_\varphi^2}{R_c} = \frac{\Gamma_u^{\ 2}}{R_c^{\ 3}}$$

Integrating the above equation $P = -\frac{\Gamma_u^{\ 2}}{2R_c^{\ 2}} + c_3$ (c_3 is an arbitrary constant)

so that

$$H = \frac{1}{2}(V_x^2 + V_r^2 + V_\varphi^2) + P = \frac{1}{2}(V_{xu}^2 + 0 + \frac{\Gamma_u^{\ 2}}{R_c^{\ 2}}) - \frac{\Gamma_u^{\ 2}}{2R_c^{\ 2}} + c_3 = \frac{1}{2}V_{xu}^2 + c_3 \qquad (4\text{-}16)$$

The streamfunction at the upstream boundary can be calculated from

$$\Psi = \int R_c V_{xu} dR_c = \int R_c (c_1 R_c^{\,2} + c_2) dR_c = \frac{c_1 R_c^{\,4}}{4} + \frac{c_2 R_c^{\,2}}{2} + c_4 = \frac{V_{xu}^2}{4c_1} + c_4 - \frac{c_2^2}{4c_1}$$

(c_4 is an arbitrary constant) (4-17)

Combining (4-16) and (4-17), the relationship between streamfunction and the total pressure at the upstream boundary becomes

$$\Psi = \frac{H}{2c_1} + \text{constant}$$

Since the relationship will stay valid over the whole flowfield, $\frac{dH}{d\Psi} = 2c_1$ over the flow field, and the equation (4-2) can be rewritten as

$$\frac{\partial^2 \Psi}{\partial R^2} + \frac{\sin\theta}{R^2} \frac{\partial}{\partial \theta} \left(\frac{1}{\sin\theta} \frac{\partial \Psi}{\partial \theta} \right) = 2c_1 R^2 \sin^2 \theta$$

This is another special case to be described by equation (4-10), with $a_0 = 0$, $b_0 = 2c_1$.

The result remains valid for any arbitrary constants c_1 and c_2 except $c_1 = 0$. It is useful to show some instances of choice of c_1 and c_2 here. One should note that the centre-line velocity $V_{xu(R_c=0)} = c_2$ and the wall velocity $V_{xu(R_c=1)} = c_1 + c_2$. Then when $V_{xu(R_c=0)} V_{xu(R_c=1)} = c_2(c_1 + c_2) > 0$, all the flow at the upper boundary is in the same direction, and the flow is that of a uni-cyclone. If $V_{xu(R_c=0)} V_{xu(R_c=1)} = c_2(c_1 + c_2) < 0$, the flow of a return flow cyclone is described. There are two options of entry, adjacent to the outer wall, or in the central area. I will consider the normal entry model for cyclone flow, entering adjacent to the wall. In this case, $c_2 > 0$, and three possible flow conditions are considered; a completely returned flow, a return flow with underflow

and a return flow with an upward 'air core', or feed from the base.

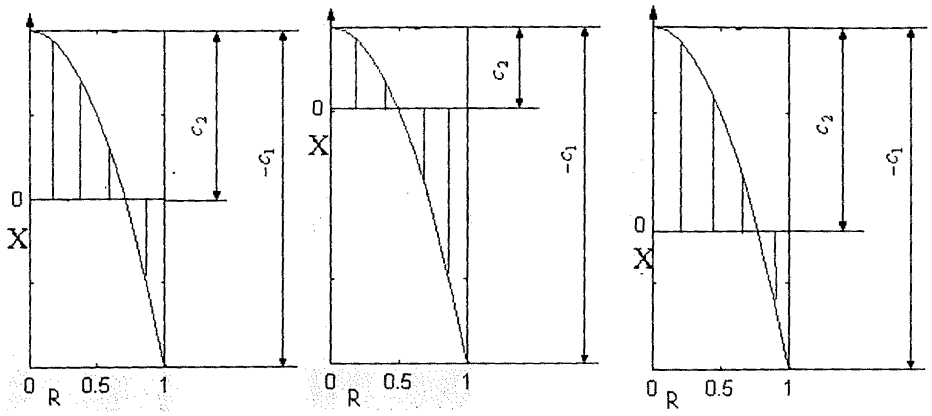

A B C

Fig. 4-3 Examples for choosing c_1 and c_2

As we know, the volumetric flow between the wall and any radius is $Q = 2\pi\Psi$. The input volumetric flow rate

$$Q_I = 2\pi\Psi_I = 2\pi \int_1^{R_c(V_{xu}=0)} R_c V_{xu} dR_c = 2\pi[\frac{c_1 R_c^4}{4} + \frac{c_2 R_c^2}{2}] \Big|_1^{(-\frac{c_2}{c_1})^{0.5}} = \frac{-\pi(c_1 + c_2)^2}{2c_1},$$

where $R_c\big|_{V_{xu}=0} = \left(-\frac{c_2}{c_1}\right)^{0.5}$. The net volumetric flow rate

$$Q_N = 2\pi\Psi_N = 2\pi \int_1^0 R_c V_{xu} dR_c = 2\pi[\frac{c_1 R_c^4}{4} + \frac{c_2 R_c^2}{2}]_1^0 = \frac{-\pi(c_1 + 2c_2)}{2}.$$

So the split flow ratio $S = \frac{Q_N}{Q_I} = 1 - \frac{1}{(1 + \frac{c_1}{c_2})^2}$.

Thus the ratio of c_1 and c_2 is defined by the fractional underflow (positive or negative), and their magnitudes determined by the flow. The three flow conditions can be judged by split flow ratio S,

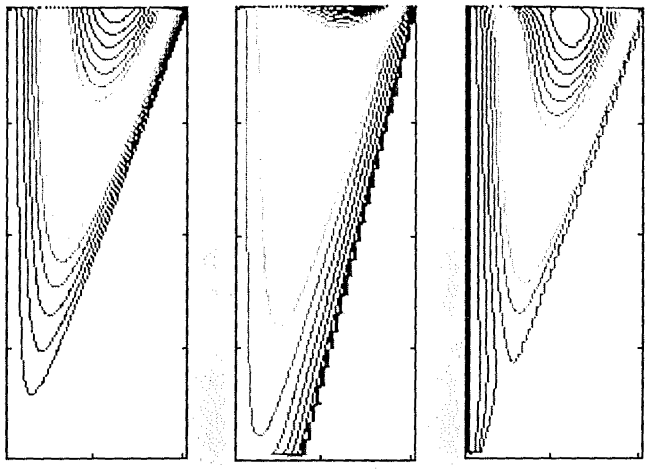

S=0 S>0 S<0

Fig. 4-4 Streamlines of three characteristic flowfields for the cone of a return flow cyclone

(A) S=0, $c_1 = -2c_2$, describing a completely returned flow.

(B) S>0, $c_1 < -2c_2$, describing a return flow hydrocyclone with underflow.

(C) S<0, $c_1 > -2c_2$, describing a return flow cyclone with reverse underflow. This may describe a 'air core'.

Fig. 4-4 shows the typical flow fields corresponding the flow conditions A, B and C respectively.

4.4 DISCUSSION

Now it is understandable that the single constant equation (4-8) describes the flows not only for cases I to III, but also for a family of cases with the same relationship between circulation and stream-function. Another family is defined by equation (4-10) with a_0=0, which includes case IV, with the same relationship between total pressure and stream-function. The larger case family defined by equation (4-10) includes the above two families and their combination.

Solution (4-11) of Ψ_1^* to Ψ_4^* includes all the solutions of equation (4-10) in a conical domain. As to different cases, the flow fields will be different; for different boundary conditions, the solutions of equation (4-10) will be different. For a particular case, the particular boundary conditions are needed to define the problem. At the upper and lower boundaries, the radial distributions of the axial velocity, tangential velocity and total pressure are usually used as the boundary conditions.

Ψ_4^* (equation (4-14)) is the most complex to calculate, and the calculation details are given in the appendix. The fourth term Ψ_4^* in the 'flexible solution' equation (4-11) is an eigenfunction expansion. We can prove that the eigenfunction series is complete, so it can be used to fit any boundary profile. Since the weighting functions in the eigenfunction have high order of R, they change acutely along the R direction. So the solution of this part has its effect only close to the boundary regions. Ψ_4^* is important only near the upper and lower boundaries. However it is in such portions that some problems such as shortcut flow attract the designer's attention. Ψ_4^* can be used to describe the secondary flows near the inlet and outlet. This term describes potential flow, and it does not introduce vorticity.

The third term Ψ_3^* in the 'flexible solution' equation (4-11) is a 'direct flow' term, given by equation (4-13). $\Psi(R,\alpha)$ and $\Psi(R,0)$ in equation (4-13) are the stream-functions along the conical wall and central axis respectively. They are constants, and are determined at the upstream boundary. Ψ_3^* describes the solution due to the flow passed through the cyclone from one end to the other, such as the flow in a direct flow gas cyclone (a uni-flow cyclone) or the underflow in a hydrocyclone (see case IV). It can also be used to describe the 'air core' flow, if the air is flowing upwards with no slippage with the main flow. This third term does not introduce vorticity.

Solution Ψ_1^* ie equation (4-9) describes the main flow characteristic for the cases resulting in equation (4-10). For the constant a_0 in term Ψ_1^*, we can give a more

general form. Since $-\Gamma \frac{d\Gamma}{d\Psi} = a_0$, $\qquad d\Gamma^2 = -2a_0 d\Psi$,

$$\frac{\partial \Gamma^2}{\partial R_c} = -2a_0 \frac{\partial \Psi}{\partial R_c} = -2a_0 R_c V_x$$

So $$a_0 = -\frac{V_\varphi^2 + V_\varphi R_c \frac{\partial V_\varphi}{\partial R_c}}{V_x}, \qquad (4\text{-}18)$$

with evaluations made on the upstream boundary.

Ψ_1^* represents the streamfunction caused by uneven distribution of *circulation* across the streamlines. This distribution introduces vorticity into the flowfield and makes the fluid element rotate or deform. As we know, if no vorticity is introduced into the cyclones, either fluid will flow straight out to the other end or flow in a shortcut manner to the exit finder. It is such element rotation or deformation that makes the streamlines bent, so they can flow deeper into the cyclone. The solution of Ψ_1^* alone cannot match the different boundary conditions, and cannot describe the flowfield near the boundaries.

The method to obtain b_0 in term Ψ_2^* is simple also, but we will not give the derivation here. The result is

$$b_0 = \frac{a_0(V_r^2 + V_x^2 + V_\varphi^2) + 2a_0 P}{C_t - \Gamma^2} \qquad (4\text{-}19)$$

where C_t is a constant and equal to Γ^2 in the case $a_0 = 0$, and V_r is the cylindrical radial velocity. This is also evaluated on the upstream boundary. Practically it is easiest to evaluate this close to the wall (extrapolating the velocities across the boundary layer) since V_r is negligible and a wall pressure tapping will give P.

The second term Ψ_2^* of equation (4-11) represents the streamfunction caused by uneven distribution of *total pressure* across the streamlines. This distribution introduces vorticity into the flowfield and makes the streamlines bent also, so they can flow deeper into the cyclone. But this term flow flows out in shorter paths than those

in Ψ_1^*, because Ψ_2^* declines in R^4 order along the spherical radius R towards the vertex, while the term Ψ_1^* declines in R^2 order.

4.5 CONCLUSION

I find a group of exact inviscid solutions for the swirling flow in a conical cyclone. The solutions are composed of four terms, which represent the effect of circulation gradient, total pressure gradient, net mass flow and potential flow on the flowfield respectively. Some special cases discussed show that these solutions are more flexible than Bloor and Ingham's solution.

Chapter 5

A Steady Axisymmetric Reverse Flow With Swirl in a Conical Cyclone

(Conical pattern V)

Part II: Application to experiment

Abstract

In this chapter, the results of the solution for conical pattern V are compared with experimental results, and good agreement is obtained. The structure of the solution, the secondary flow nears the vortex finder and the characteristics of tangential velocity are discussed.

5.1 INTRODUCTION

In chapter 4, I have given a group of solutions of the equation of motion for steady axisymmetric inviscid flow within a conical cyclone. The solutions are given with or without a central 'air core' and with or without net underflow.

The simplified dimensionless equation of motion we have taken for flow in a conical domain is

$$\frac{\partial^2 \Psi}{\partial R^2} + \frac{\sin\theta}{R^2}\frac{\partial}{\partial \theta}\left(\frac{1}{\sin\theta}\frac{\partial \Psi}{\partial \theta}\right) = a_0 + b_0 R^2 \sin^2\theta \qquad (5\text{-}1)$$

The general solution of the dimensionless streamfunction Ψ for this problem is

$$\Psi = \Psi_1^* + \Psi_2^* + \Psi_3^* + \Psi_4^* \qquad (5\text{-}2)$$

Where Ψ_1^* to Ψ_4^* have been detained in chapter 4.

Here the structure of the solution, the secondary flow near the vortex finder and the characteristics of tangential velocity will be discussed.

5.2 APPLICATION TO EXPERIMENT

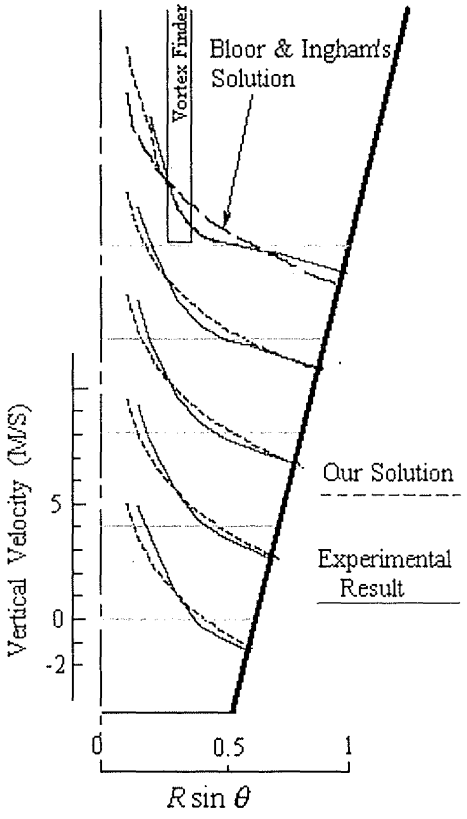

Fig. 5-1 Comparison of the theoretical results with experimental findings of Kelsall
($\alpha = 10$ degrees)
(<0.7% underflow, with air core)

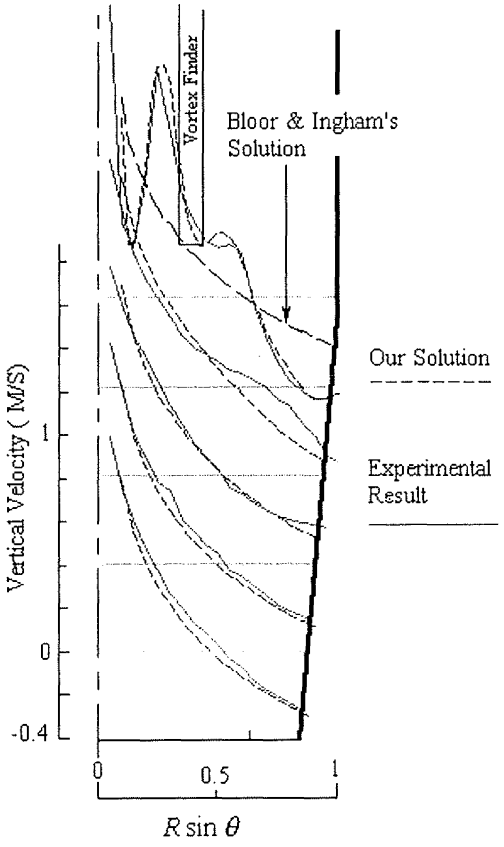

Fig. 5-2 Comparison of the theoretical results with experimental findings of Knowles et al ($\alpha = 5.65$ degrees)
(20% underflow)

Following Bloor and Ingham (1987), I will use the experimental findings of Kelsall (1952) and Knowles et al. (1973) for comparison with our theoretical results. Kelsall used an optical method involving suitable illumination and an ultra-microscope fitted

with a rotating shutter. He measured directly the tangential velocity components of fine aluminium particles suspended in water, at selected positions within a transparent cyclone.

Vertical velocity components at the same positions were obtained by measuring the angle of inclination of particle tracks to the horizontal, and water radial velocity components were calculated from continuity considerations. Particles used were small enough so that tangential and axial velocities were equal to those of the water. Knowles et al. used tracer particles and a cine photography method. They measured three-dimensional flow patterns in a hydrocyclone. The tangential and vertical components of the velocity were read straightforwardly from the records of a view A. Velocities were measured over trails of around 0.1 ms. The radial velocity was determined by a variety of analysis techniques applied to another view B, which was perpendicular to the view A. The measurement of the radial velocity component is usually difficult, and few experimental programmes have been successful in this, since the values of it are usually small, and often comparable to the magnitude of the velocity fluctuations.

Bloor and Ingham compared their theoretical prediction with the axial component of velocity measured at two levels of axial position in the cyclones of Kelsall, which correspond to about 0.4 and 0.85 of the distance between the underflow and the vortex finder, above the underflow. They also gave comparison for the axial velocity component at two levels above the underflow, of 0.86 and 0.96 of the length of the conical section of Knowles's cyclone. I will compare profiles from our theory with all four terms Ψ_1^* to Ψ_4^* included, with all the five experimental profiles under the vortex

finder presented by Kelsall and Knowles. As an approximation we could also use the conical solution *above* the exit tube lip, in the annular region, with the exit tube as a separate flow region, but for simplicity choose not to here.

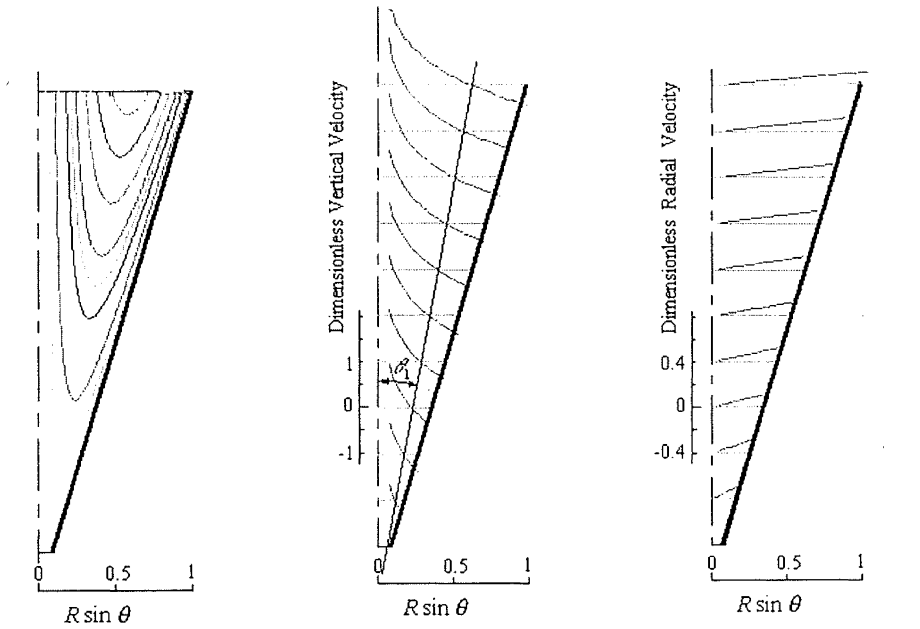

a, Streamlines Pattern **b, Vertical Velocity** **c, Radial Velocity**

Fig. 5-3 First Term Flowfield

Fig. 5-1 shows the comparison of the vertical velocity of the theoretical results with the corresponding experimental findings of Kelsall (1952), and Fig. 5-2 shows that of Knowles (1973). It can be seen that good agreement is obtained for both cases. Many experiments show that the flowfield just below the vortex finder may change acutely, and recirculating or shortcut flow may occur in this region. It is worthwhile to pay attention to this region. My solution can quite accurately represent the flowfield in this region. We can see the differences between my solution, Bloor and Ingham's solution and the corresponding experimental results in this region. With both solutions, a best fit along the upper boundary was obtained by adjusting the model parameters.

The difference between my theory and Bloor and Ingham's result for these examples mainly comes from the fourth term Ψ_4^* of equation (5-2). This term is the sum of a group of eigenfunctions. Any streamfunction at the upper boundary can be theoretically matched with the group of eigenfunctions, if enough eigenfunctions are used.

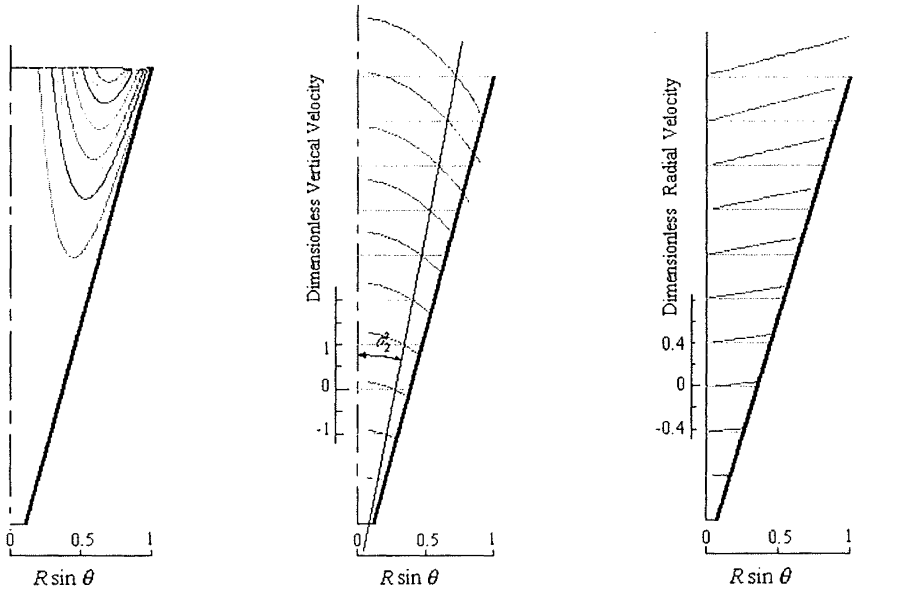

a, Streamlines Pattern **b, Vertical Velocity** **c, Radial Velocity**

Fig. 5-4 Second Term Flowfield

The first term Ψ_1^* of equation (5-2) represents the streamfunction caused by uneven distribution of *circulation* across the streamlines. The second term Ψ_2^* of equation (5-2) represents the streamfunction caused by uneven distribution of *total pressure* across the streamlines. Both these distributions introduce vorticity into the flowfield and make the fluid element rotate or deform, so it can flow deeper into the cyclone. These terms are different from each other not only in their physical sense but also in their forms. Fig. 5-3 and Fig 5-4 show the streamline patterns, the vertical velocity and the radial velocity of first term flow and second term flow respectively. It can be seen from Fig. 5-3 a. and Fig. 5-4 a. that the second term flow flows out in shorter paths, because

the second term declines in R^4 order along the spherical radius R towards the vertex, while the first term declines in R^2 order.

The axial and radial velocities (ie for cylindrical coordinates) for Ψ_1^* and Ψ_2^* terms are respectively

$$V_{1x}^* = a_0(-C_a + \ln(0.5\tan\theta) + \frac{3}{2} - \frac{\cos\theta}{2})$$

$$V_{1r}^* = \frac{a_0(1-\cos\theta)(2-(1-\cos\theta)^2)}{2\sin\theta\cos\theta}$$

$$V_{2x}^* = \frac{b_0 R^2}{5}[1 + \sin^2\theta + \frac{6\cos^2\theta - 2}{1-5\cos^2\theta}]$$

$$V_{2r}^* = \frac{b_0 R^2}{5}[-\cos\theta\sin\theta + \frac{2\cos\theta - 6\sin\theta + 10\cos^2\theta(\sin\theta - \cos\theta)}{1-5\cos^2\theta}]$$

Both vertical and radial velocities of the first term flow are functions of polar angle θ only. Fig. 5-3 b and c show the vertical and radial velocity profiles of the first flow respectively. In contrast, both vertical and radial velocities for the second term flow decline in R^2 order along the spherical radius R towards the vertex. Fig. 5-4 b and c show the vertical and radial velocity profiles of the second flow respectively. The zero vertical velocity envelope of the second term inclines nearer the cyclone wall than does that of the first term. If the half cone angle α of a cyclone is 10 degrees, and angles between these envelopes and axis are θ_1 and θ_2 for the first term flow and second term flow respectively, the ratio of the angles $\frac{\theta_1}{\theta_2}$ is about 0.86.

It is obvious that the *forms* of the first and second terms of equation (5-2) at the upstream boundary will not change with the boundary conditions, but their *scale* will change by the boundary conditions through different values of throughput, and hence a_0, b_0. In general, for a particular cone with cone angle α, there exists a *conical* envelope as the loci of position at which the vertical velocity is zero. The envelope half cone angle is given by $\theta \cong 0.61\alpha$ for the flow described by Ψ_1^* and $\theta \cong 0.71\alpha$ for the flow described by Ψ_2^*. The position of the vortex finder can be arbitrarily placed without affecting the *forms* of the first or second terms of the solution. A recirculating zone may occur near the vortex finder. We can denote the angle of the bottom lip of the vortex finder by θ_e. For the first term flow, when θ_e is less than about 0.61α, the recirculating zone will occur *outside* the vortex finder; when θ_e is more than about 0.61α, the recirculating zone will occur *within* the vortex finder. The case where θ_e is about 0.61α, no recirculating zone occurs. The same situation applies to second term flow, but the critical angle is about 0.71α.

Bloor and Ingham discuss such a recirculating zone (which is outside the zone of their solution), and suggest a viscous mechanism as a driving force. However, as may be apparent from the discussion above, a viscous action within the cyclone body is not necessary for the appearance of a recirculating zone. Such a zone can arise from the radial distributions of circulation and stream function at the upstream boundary, which in turn may come from flow features upstream, perhaps in the inlet duct, and possibly influenced by viscous action. A recirculating zone will reduce the effective flow area and may increase the pressure loss. For these particular solutions, the flow of the first

or second terms only, the only way to avoid a recirculating zone is to locate the vortex finder wall at the position where θ_e is about 0.61α or 0.71α respectively.

If more terms are considered for the flow described by the full solution equation (5-2), the recirculating zone may be dispelled. Any form of the distribution of vertical velocity at the upper boundary can be matched using Ψ_4^*. However this fourth term has its effect only on the upper portion of the cyclone, and below that portion, the flowfield will revert automatically to that when no fourth term was considered. Smith has observed such similarity among flow patterns on a cylindrical cyclone, away from the entrance (Smith 1962), for varying inlet geometries and flows. The "adjusting fluid" corresponding to Ψ_4^* will pass through the upper portion of the cyclone and then flow into the vortex finder. This describes a shortcut flow. The shortcut flow is one of the factors decreasing the separating efficiency, since particles travelling with the fluid have had little time to separate.

Away from the upper boundary, the streamline pattern from equation (5-2) is given by the terms Ψ_1^*, Ψ_2^* and Ψ_3^*. Normally the major term is Ψ_1^*, which has a flow *pattern* independent of a_0. Ψ_2^* added to this will provide a flow pattern weakly dependent on a_0/b_0. Ψ_3^* added will adjust the pattern according to net flow.

a_0 can be calculated following Bloor and Ingham (1987) or Wakelin (1993), a modified calculation can be given by equation (4-18). The comparisons given by Bloor and Ingham show that their method to determine a_0 is suitable for the Kelsall's cyclone. a_0 can also be determined by comparing the vertical velocity profiles in the

main body of cyclones. Fig. 5-5 shows the comparison of experimental data and different flowfields from the different values of a_0 for the Kelsall's cyclone.

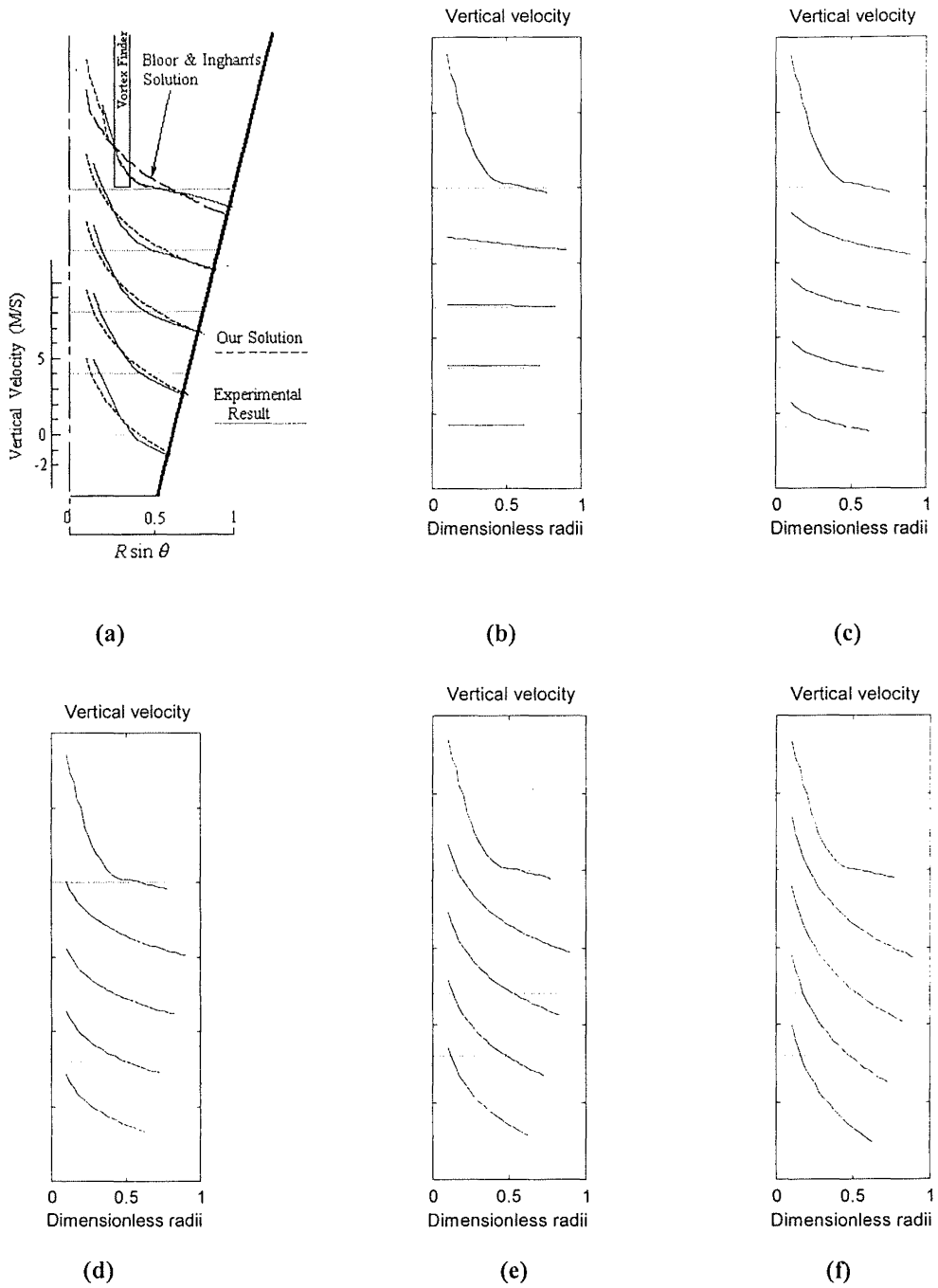

Fig. 5-5 (a) Experimental data and a_0=0.3, (b) a_0=0.0, (c) a_0=0.1, (d) a_0=0.2, (e) a_0=0.3, (f) a_0=0.4

In this comparison, b_0 was taken as zero, and the result is good enough.

If the flow satisfies equation (5-1), then a_0 and b_0 can be determined from the relationships of Γ and H with streamfunction at the upstream boundary. Then the characteristic angle of zero axial flow can easily be estimated. If the flow does not satisfy equation (5-1), the same general principle will apply. In general, to avoid a recirculating zone or a shortcut flow, one needs to match the radius of the vortex finder wall with the characteristic zero vertical velocity radius according to the relationships among circulation, total pressure and streamfunction at the upstream boundary.

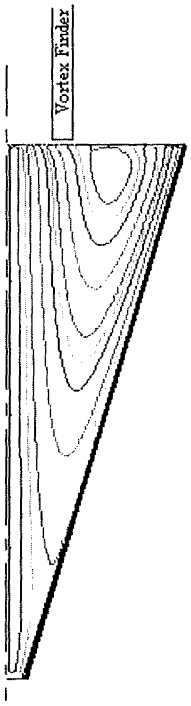

Fig. 5-6 Streamline pattern of Kelsall's Cyclone

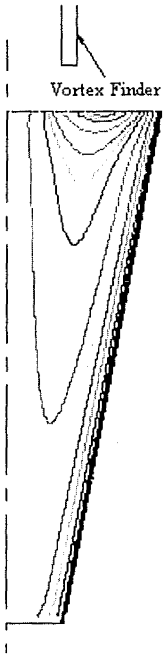

Fig. 5-7 Streamline pattern of Knowles Cyclone

It is useful to study the Kelsall and Knowles et al cyclones in more detail. Fig. 5-6 shows the calculated streamline pattern of Kelsall's cyclone with the four terms of equation (5-2), with fitted a_0, b_0, net flow and using the first 10 terms of Ψ_4^*. There is a whirlpool in the upper portion of the cyclone. Studying the experimental curve just under the vortex finder in Fig. 5-1, we can see that after entering the cyclone, some of the fluid flowing upwards to the vortex finder passes it outside. There is less

recirculating flow outside than indicated by the first term flow (Bloor and Ingham's solution) alone.

Fig. 5-7 shows the calculated streamline pattern of Knowles's cyclone. The lip of the vortex finder is above the examined flow field, as we have limited our calculation to the conical part of their cyclone.

There is a distinguishing difference between the two streamline patterns in Fig 5-6 and Fig. 5-7. Fig. 5-6 shows the streamlines for an all-overflow cyclone with an 'air core', ie. all the fluid entering the cyclone flows out through the upper portion, and a separated 'air core' region flows into the cyclone from a bin and then flows out through the vortex finder. Fig 5-7 shows the streamlines for a split flow cyclone without an 'air core', with about 20% of the fluid entering the cyclone flowing down through the bin (defined by Knowles et al as 20% underflow), and the remainder leaving via the vortex finder. The third term in equation (5-2) is used to describe this 'direct flow' or 'net flow'.

The flows described by either the first or the second terms in equation (5-2) are not 'net flow', since their net mass flow rate in any cross section of the cyclone is zero. In Fig. 5-6, the net flow is the upwards 'air core' flow; In Fig 5-7, it is downwards. The 'net flow' rate should correspond to flows external to the cyclone or be measured in the upper domain boundaries both upstream and downstream. The same net flow applies at the lower boundary to keep the mass balance. The constants $\Psi(R,\alpha)$ and $\Psi(R,0)$ in the third term can be determined with the profile measurement (such as the

distribution of vertical velocity as the boundary condition to calculate the streamfunction Ψ at the boundary).

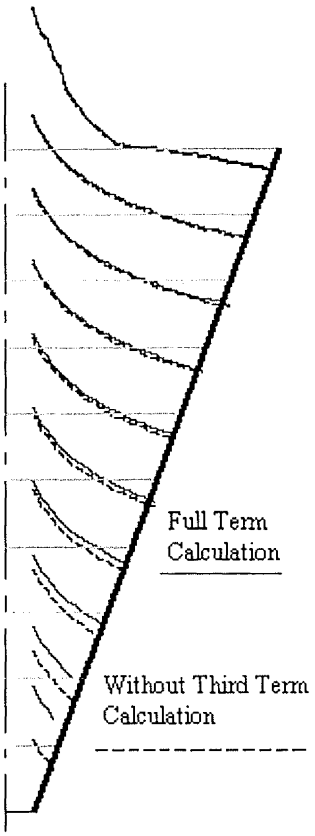

Fig. 5-8 Comparison of calculation with and without third term for Kelsall's cyclone

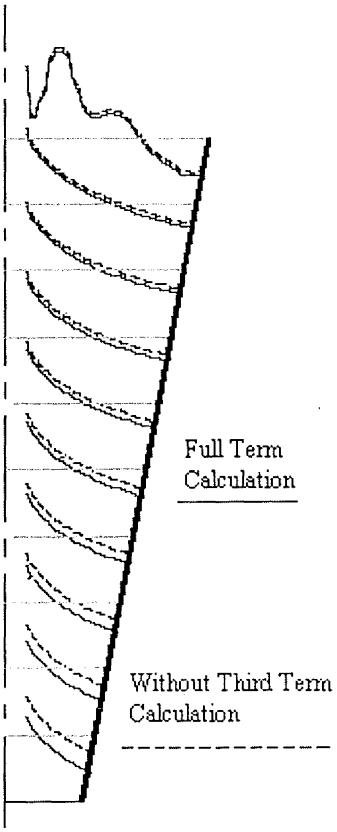

Fig. 5- 9 Comparison of calculation with and without third term for Knowles's cyclone

In Fig. 5-3, Fig. 5-4, Fig. 5-6 and Fig. 5-7 there exist approximately conical envelopes as the loci of positions at which the vertical velocity is zero. All fluid lying between such envelopes and the conical wall of the cyclone moves downwards and fluid between the envelopes and the air/fluid interface or axis moves upwards. Unless a given particle moves inwards through the zero vertical velocity envelope before the underflow opening of the cyclone is reached then the particle will be discharged with the underflow (even then, reentrainment from the bin can occur). By studying Fig. 5-6, it can be found that the zero vertical velocity envelope of Kelsall's cyclone has a higher fraction of the cone radius towards the apex of the cone; from Fig.5-7, it can be

seen that the zero vertical velocity envelope of Knowles's cyclone has a smaller fraction of the cone radius towards the apex of the cone. The difference comes mainly from the net flow difference, ie from Ψ_3^*. This would indicate lower collection efficiency with an air core, under otherwise similar conditions.

Figs. 5-8 and 5-9 show calculated vertical velocity profiles through the whole body of Kelsall's cyclone, and Knowles's cyclone respectively. The solid lines represent the full calculations with four terms, and the dashed lines represent the calculations without the third term. It can be seen that for both cyclones, there is only a little difference of the profiles in the upper part of the cyclones. Since the difference between the full calculations and experimental results is small in the upper part of the cyclones, and the experimental results for the lower 5 profiles of both the cyclones are not available, I do not present experimental results in these comparisons (see Figs.5-1 and 5-2 for this comparison).

The difference due to the third term in the lower part of the cyclones is quite large. For Kelsall's cyclone, the vertical velocity with inclusion of the third term is much higher positive upward than that without the third term in the lower portion; for Knowles's cyclone, the vertical velocity with the third term included is much lower than that without the third term in the lower portion. This is to be expected, since the 'direct flow' in the main body is a small fraction of the whole upflow or downflow, but this fraction enlarges in the lower portion. The change in lower portion flow patterns supports the commonly observed changes in collection efficiency with gas cyclone bin flow; higher efficiency with downflow and lower with upflow (bin leakage).

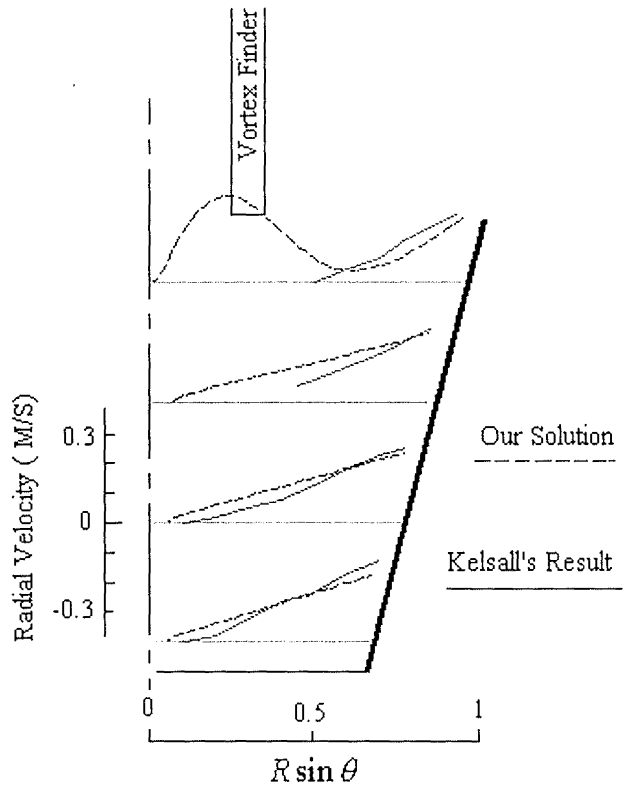

Fig5-10 Comparison of radial velocity profile for Kelsall's cyclone

Fig. 5-10 shows the comparison of radial velocity profiles of Kelsall's cyclone with my theoretical results. The solid lines represent Kelsall's results, and the dashed lines represent my theoretical results. The comparison looks quite good. Kelsall's experimental top curve is not complete, my result shows that near the central area in that level the radial velocity has a peak value, reflecting shortcut flow. Kelsall's visual inspection of this region showed that relatively large solid particles were moving inwards where large outward centrifugal forces were exerted. This implies that the radial velocities were many times greater than those at similar radii for horizontal levels lower in the cyclone. His examination of photographs of solid particles just below the bottom of the vortex finder confirmed that this region was one of high particle loss. At lower levels in the conical portion the radial velocity decreases as radius decreases and becomes zero in the vicinity of the air/fluid interface. Other experimental results with a conical cyclone (Hsieh, 1991) show the same tendency.

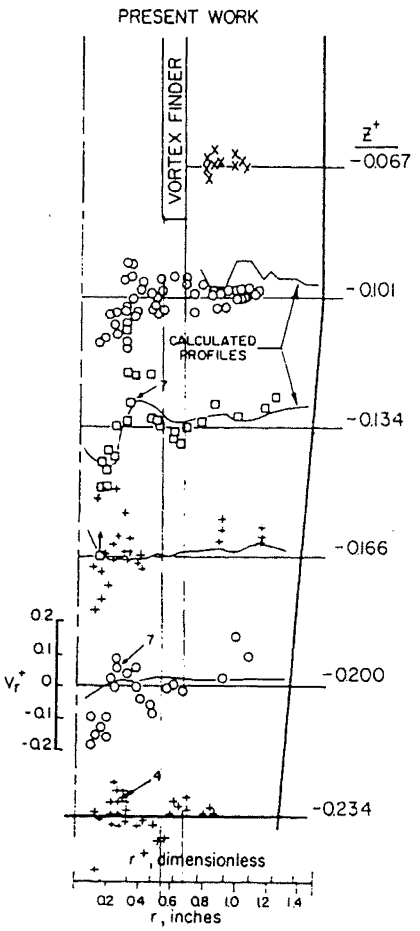

Fig. 5-11 measured radial velocity profiles for Knowles's cyclone

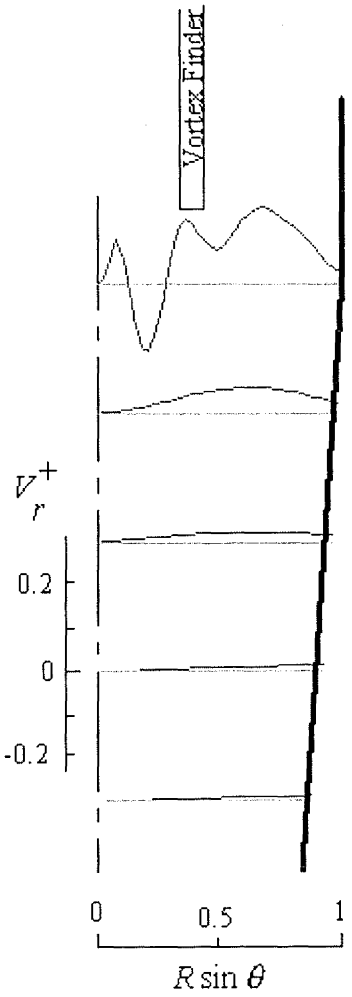

Fig. 5-12 Calculated radial velocity profiles for Knowles's cyclone

Fig. 5-11 shows the experimental radial velocity profiles of Knowles's cyclone, and Fig. 5-12 shows my corresponding theoretical results. Knowles's radial velocity profiles are difficult to interpret unequivocally because of the scatter, although trends in the data can be seen, and the comparison looks reasonable. In general the radial velocity in the main body of the cyclone is small compared to the vertical velocity, and small even compared with the velocity fluctuations. Knowles reported that for $R_c >$ 0.4, V_r was slightly positive, or inward, and constant at all axial locations. For $R_c \cong 0.2$ the data show fluctuation in this radial velocity; sometimes V_r is negative or

outward and sometimes it is positive. My theory is for steady flow, which does not reflect the instantaneous velocities (over 0.1 ms) that Knowles measured. In the upper portion, the profile changes acutely. By combining Fig. 5-2 and Fig. 5-12, it can be seen that the flowfield in the vicinity of the bottom of the vortex finder is quite complicated. The flow entering the vortex finder has two upward vertical velocity peaks: one is the central core domain, the other is an annular domain close to the inner wall of the vortex finder. Between the two peak domains, there is a low vertical velocity valley, which is an annular domain. The fluid moving up below the bottom of the low vertical velocity valley rapidly flows outwards and upwards into the peak velocity domain near the vortex finder wall.

Fig. 5-13 shows the comparison of tangential velocity profiles of Kelsall's cyclone with theoretical results. The solid lines represent Kelsall's experimental results, the dashed lines represent my theoretical results and the point lines represent a free vortex flow. The differences between my theoretical results and the free vortex are small, but the differences between the experimental results and both of the theoretical results are obvious. The latter differences mainly come from the inviscid assumption. Any inviscid flow must follow Kelvin's circulation theorem, which briefly states that the

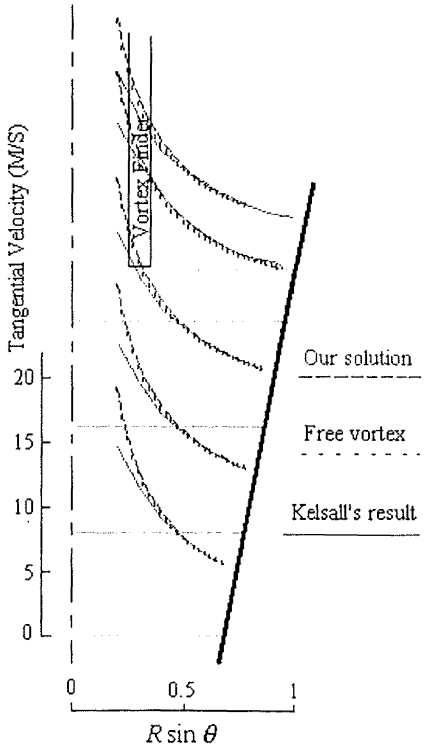

Fig. 13 Comparison of Tangential velocity profiles for Kelsall's cyclone

circulation will not change along the streamlines. For the experimental results the circulation downstream is less than that upstream along the same streamline, so there is a deviation of tangential velocity of the flow from that of a free vortex flow along the streamline. For accurate calculation of tangential velocity, the viscous loss has to be considered.

The tangential velocity has always been thought the most important velocity component. Most previous models have assumed that radial and axial velocities are not linked to the tangential vortex profile. Vatistas (1991) reports that "The main properties of concentrated vortices as represented by the radial distributions of azimuthal velocity and static pressure were found to be common to most vortical flows and not to depend on the method of production." Leibovich (1984), similarly finds that most vortex flows can be approximated as being columnar, with universal profiles.

In support of this, Kelsall's experimental findings showed that within the accuracy of measurement, the loci of constant tangential velocity defined cylindrical envelopes coaxial with the cyclone. He stated that if tangential velocity near the wall of the cyclone was neglected, the relationship between V_φ and radial distance was independent of horizontal position. My solution corroborates this characteristic, but suffers from the inviscid assumption near the vortex core. In equation (4-15) in chapter 4 the first term within the bracket on the right hand side represents the free vortex flow, and if the second term is zero, the tangential velocity is $V_\varphi = \frac{D^{\frac{1}{2}}}{R\sin\theta} = \frac{constant}{R_c}$.

The second term in the numerator of the right hand side of equation (4-15) in chapter 4

represents the modification to the free vortex introduced from the upstream vorticity. When the tangential velocity is small, this term is comparatively large and so the modification is strong. When the tangential velocity is large enough, this modification has little effect, so that the tangential velocity component will change little along the axial direction. In most cyclones, the second term is comparatively small. So the tangential velocity is approximately a function only of radial distance $R\sin\theta$.

From the theory derived in chapter 4, it can be seen that my solution comes from the simplification of equation (4-2) in chapter 4 by the linearization of the terms on the right, and only the first terms of the two series on the right are considered. The solution describes one of the possible flow patterns. Since other assumptions have been made such as the flow being steady, axisymmetric, inviscid, incompressible, and single phase, the solution cannot describe all flow patterns in cyclones. However the solution may be the most common inviscid solution for conical cyclones, and gives the basic characteristic of the flowfield.

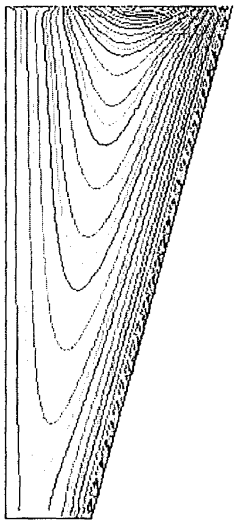

Fig. 5-14 General pattern of streamlines

Fig. 5-14 shows the general pattern of streamlines with both underflows and 'air core' flow. The rates of under flow and 'air core' flow can be determined at the upper boundary, needing in this general case not just the ratio of inflow to overflow, but also the detailed vertical velocity profile. One special case where underflow and 'air core'

flow are equal, is where a closed bin is attached, which allows a wholly recirculated bin flow. This is often about $1/10^{th}$ of the main flow (Abrahamson 1981).

5.3 CONCLUSIONS

The theory presented in chapter 4 has been applied to two well documental experimental studies on hydrocyclones. The following general points were made:

1. In chapter 4, I find a group of exact inviscid solutions for the swirling flow in a conical cyclone. The result of the theory with just two terms describing change of circulation and total pressure with streamfunction are compared with data from two quite different experimental investigations in this part, and good agreement is obtained.

   In summary, if the right hand side terms of the streamfunction form of the momentum equation (equation (4-2) in chapter 4) are zero, and thus no vorticity is introduced into the flowfield, potential flow is described. The solution for this flow will be the third and fourth terms of equation (5-2), Ψ_3^* and Ψ_4^*. The third term flow describes a 'net flow', the fluid will flow through the cyclone. The fourth term flow can describes the complex flowfield near the upper portion of cyclones, the fluid will not flow far into the main body of the cyclones, and will short-circuit through the upper portion. If the right hand side terms in the momentum equation are not zero, the vorticity can be divided into two parts, one of them related to nonuniform distribution of *circulation* across the streamlines, the other related to nonuniform distribution of *total pressure* across the streamlines. In our solution,

these parts correspond to the first (Ψ_1^*) and second terms (Ψ_2^*) of equation (5-2) respectively.

The relationship of streamfunction with circulation and total pressure is determined upstream (determing a_0 and b_0 in the model), and since no friction effect is considered for inviscid flow, the relationship will remain in the whole flowfield.

The existence of non-zero terms on the right of the streamfunction momentum equation means that the uneven distributions of circulation and total pressure in different streamlines introduce vorticity into the flowfield making the fluid elements rotate, and making the fluid flow deep into the cyclone main body.

2. The appearance of 'air core flow upwards', or underflow in hydrocyclones, or net bin withdrawal in gas cyclones, will in many cyclones have little effect on the barrel and upper cone, but have great effect on flow in the lower cone.

3. A recirculating zone and/or shortcut flow may occur in the upper portion of cyclones. In general, to avoid the recirculating zone and the short-circuit flow, one needs to match the radius of the vortex finder wall with the characteristic zero vertical velocity radius according to the relationships among circulation, total pressure and streamfunction at the upstream boundary.

4. Many investigators have reported that tangential velocity profiles within conical cyclones do not vary significantly in the axial direction. My theory indicates this for high relative tangential velocity. However, when the tangential velocity is low, the vorticity entering the cyclone will have great effect on the tangential velocity profile. When relative tangential velocity is high enough, this vorticity will have little effect on the profile, and the tangential velocity will be insensitive to the variations of axial and radial velocities. It will seem self-similar.

Chapter 6

The Further Results for Swirling Flow In a Conical Cyclone

(Conical pattern VIII)

Abstract

A further mathematical model is developed for the flow in a conical cyclone, which is also an exact solution of the equation of motion for steady axisymmetric inviscid flow. The solution consists of four terms corresponding to the terms in my previous solution, where the terms represent the effects of unequal circulation, unequal total pressure, 'net flow' and potential flow on the streamfunction respectively. In this solution, besides the four effects on their corresponding terms, unequal circulation has its effect on all the four terms. A comparison of the two solutions is given. Some particular cases are discussed to show the flexibility and application of the solution.

6.1 INTRODUCTION

In chapters 4 and 5, I have shown some characteristics of the flowfield described by conical pattern V. In this chapter, I will present the full solution in a conical domain for equation (4-2) with non zero coefficients from both series and a linear term of first series, the new term should bring some new characteristics. The pattern equation is

$$\frac{\partial^2 \Psi}{\partial R^2} + \frac{\sin\theta}{R^2}\frac{\partial}{\partial \theta}\left(\frac{1}{\sin\theta}\frac{\partial \Psi}{\partial \theta}\right) = a_0 + a_1\Psi + b_0 R^2 \sin^2\theta \qquad (6\text{-}1)$$

The full solution also includes four terms corresponding to the solutions (4-9), (4-12), (4-13) and (4-14) respectively. The solution is

$$\Psi = \Psi_1^{**} + \Psi_2^{**} + \Psi_3^{**} + \Psi_4^{**} \tag{6-2}$$

where

$$\Psi_1^{**} = \sum_{i=1}^{\infty} \frac{a_0 C_{ai} \pi R^{\frac{1}{2}}}{2} [-J_{v_i-0.5}(AR) \int_0^R r^{\frac{1}{2}} Y_{v_i-0.5}(Ar)dr + Y_{v_i-0.5}(AR) \int_0^R r^{\frac{1}{2}} J_{v_i-0.5}(Ar)dr] Z_i(\theta) \tag{6-3}$$

and

$$C_{ai} = \frac{\int_0^{\alpha} \frac{Z_i(\theta)d\theta}{\sin\theta}}{\int_0^{\alpha} \frac{Z_i^{\,2}(\theta)d\theta}{\sin\theta}}$$

$J_{v_i-0.5}(AR)$ is the first kind of Bessel function, of ($v_{i-0.5}$) order

$Y_{v_i-0.5}(AR)$ is the second of Bessel function, of ($v_{i-0.5}$) order

and

$A = \sqrt{-a_1}$.

Also

$$\Psi_2^{**} = \sum_{i=1}^{\infty} \frac{b_0 C_{bi} \pi R^{\frac{1}{2}}}{2} [-J_{v_i-0.5}(AR) \int_0^R r^{\frac{5}{2}} Y_{v_i-0.5}(Ar)dr + Y_{v_i-0.5}(AR) \int_0^R r^{\frac{5}{2}} J_{v_i-0.5}(Ar)dr] Z_i(\theta) \tag{6-4}$$

and

$$C_{bi} = \frac{\int_0^{\alpha} Z_i(\theta)\sin\theta d\theta}{\int_0^{\alpha} \frac{Z_i^{\,2}(\theta)d\theta}{\sin\theta}}$$

$$\Psi_3^{**}(R,\theta) = \frac{\sin(AR+B)(\Psi(1,\alpha)(1-\cos\theta)+\Psi(1,0)(\cos\theta-\cos\alpha))}{\sin(A+B)(1-\cos\alpha)} \tag{6-5}$$

where

$$B = arctg\left[\frac{\Psi(1,\alpha)\sin(AR_s)-\Psi(R_s,\alpha)\sin(A)}{\Psi(1,\alpha)\cos(AR_s)-\Psi(R_s,\alpha)\cos(A)}\right]$$

Lastly,

$$\Psi_4^{**} = \sum_{i=1}^{\infty} (A_i J_{\nu_i-0.5}(AR)+B_i Y_{\nu_i-0.5}(AR))R^{\frac{1}{2}} Z_i(\theta) \tag{6-6}$$

where

$$A_i = \frac{F(R_e)R_e^{-0.5}\ Y_{\nu_i-0.5}(AR_s)-F(R_s)R_s^{-0.5}\ Y_{\nu_i-0.5}(AR_e)}{J_{\nu_i-0.5}(AR_e)\ Y_{\nu_i-0.5}(AR_s)-J_{\nu_i-0.5}(AR_s)\ Y_{\nu_i-0.5}(AR_e)} \tag{6-7}$$

$$B_i = \frac{F(R_s)R_s^{-0.5}\ J_{\nu_i-0.5}(AR_e)-F(R_e)R_e^{-0.5}\ J_{\nu_i-0.5}(AR_s)}{J_{\nu_i-0.5}(AR_e)\ Y_{\nu_i-0.5}(AR_s)-J_{\nu_i-0.5}(AR_s)\ Y_{\nu_i-0.5}(AR_e)} \tag{6-8}$$

and

$$F(R\ ) = \frac{\int_0^{\alpha} \frac{(\Psi(R,\theta) - \Psi_1^{**}(R,\theta) - \Psi_2^{**}(R,\theta) - \Psi_3^{**}(R,\theta))Z_i(\theta)d\theta}{\sin\theta}}{\int_0^{\alpha} \frac{Z_i^{\ 2}(\theta)d\theta}{\sin\theta}}$$

6.2 THEORY

It is expectable that $\Psi_1^{**}(R,\theta) \to \Psi_1^{*}(R,\theta)$, $\Psi_2^{**}(R,\theta) \to \Psi_2^{*}(R,\theta)$, $\Psi_3^{**}(R,\theta) \to \Psi_3^{*}(R,\theta)$ and $\Psi_4^{**}(R,\theta) \to \Psi_4^{*}(R,\theta)$ respectively, when $a_1 \to 0$. For equation (6-1) will become equation (4-10), when $a_1 = 0$. We will show that each term $\Psi_i^{**}(R,\theta)$ of the solution (6-2) will approach the corresponding term $\Psi_i^{*}(R,\theta)$ of solution (4-11), if a_1 is small enough.

Although equation (6-3) of term $\Psi_1^{**}(R,\theta)$ seems much different from equation (4-9) of term $\Psi_1^{*}(R,\theta)$, their value will close to each other, when a_1 is small enough.

Since $Y_v(R) = \frac{\cos(v\pi)J_v(R) - J_{-v}(R)}{\sin v\pi}$, the equation (6-3) can be simplified into

$$\Psi_1^{**} = \sum_{i=1}^{\infty} \frac{a_0 C_{ai} \pi R^{\frac{1}{2}}}{2\sin[(v_i - 0.5)\pi]} [J_{v_i-0.5}(AR)\int_0^R r^{\frac{1}{2}} J_{-v_i+0.5}(Ar)dr - J_{-v_i+0.5}(AR)\int_0^R r^{\frac{1}{2}} J_{v_i-0.5}(Ar)dr]Z_i(\theta)$$

(6-9)

Since $J_v(AR)=\sum_{k=0}^{\infty}\frac{(-1)^k}{\Gamma(k+1)\Gamma(v+k+1)}(\frac{AR}{2})^{v+2k}$, if AR is small enough, the following equations can be obtained

$$J_v(AR)\approx\frac{1}{\Gamma(v+1)}(\frac{A}{2})^v R^v \tag{6-10}$$

$$J_{-v}(AR)\approx\frac{1}{\Gamma(-v+1)}(\frac{A}{2})^{-v} R^{-v} \tag{6-11}$$

Bring equation (10), (11) into equation (9),

$$\begin{aligned}\Psi_1^{**}&\approx\sum_{i=1}^{\infty}\frac{a_0C_{ai}\pi R^{\frac{1}{2}}}{2\sin[(v_i-0.5)\pi]\Gamma(v_i+0.5)\Gamma(-v_i+1.5)}[R^{v_i-0.5}\int_0^R r^{-v_i+1}dr-R^{-v_i+0.5}\int_0^R r^{v_i}dr]Z_i(\theta)\\&=\sum_{i=1}^{\infty}\frac{\sin[(v_i+0.5)\pi]a_0C_{ai}R^2}{2\sin[(v_i-0.5)\pi](-v_i-0.5+1)}[\frac{1}{-v_i+2}-\frac{1}{v_i+1}]Z_i(\theta)\\&=\sum_{i=1}^{\infty}\frac{-a_0C_{ai}R^2}{2(-v_i+0.5)}[\frac{1}{-v_i+2}-\frac{1}{v_i+1}]Z_i(\theta)\\&=\sum_{i=1}^{\infty}\frac{a_0C_{ai}R^2}{(-v_i+2)(v_i+1)}Z_i(\theta)\end{aligned} \tag{6-12}$$

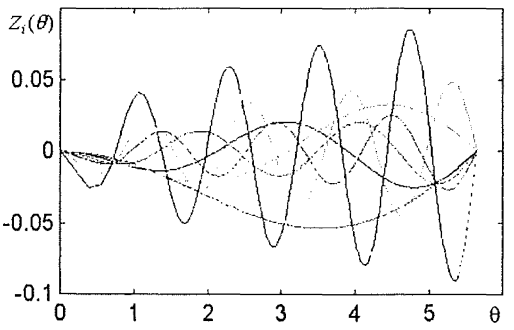

Fig. 6-1 Functions $Z_i(\theta)$ vs polar angle θ with α=5.65 degrees

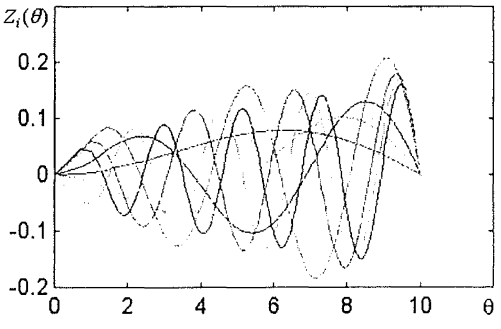

Fig. 6-2 Functions $Z_i(\theta)$ vs polar angle θ with α=10 degrees

In fact equation (4-9) Ψ_1^* can also be expanded by the same series of eigenfunction $Z_i(\theta)$,

$$\Psi_1^* = \sum_{i=1}^{\infty} \frac{a_0 C_{ai} R^2}{(-v_i + 2)(v_i + 1)} Z_i(\theta) \qquad (6\text{-}13)$$

The coefficients C_{ai} and eigenvalues v_i in the equations (6-12) and (6-13) are exactly the same. For the cone boundary angle $\alpha = 10°$, the first ten eigenvalues are 22.5, 40.7, 58.8, 76.8, 94.9, 112.9, 130.9, 148.9, 166.9, 184.9 successively; and 39.4, 71.6, 103.7, 135.7, 167.6, 199.5, 231.4, 263.2, 295.1, 326.9 for $\alpha = 5.65°$. Fig. 6-1 and Fig. 6-2 give the values of $Z_i(\theta)$ $(i = 1 \sim 10)$ for θ up to arbitrary α, with values of α equal to 5.65 degrees in Fig. 6-1, 10 degrees in Fig.6-2. So the approximate expansion (Assuming a_1 is small enough) of equation (6-3) equals to the exact expansion of equation (4-9) with the same series of eigenfunction $Z_i(\theta)$.

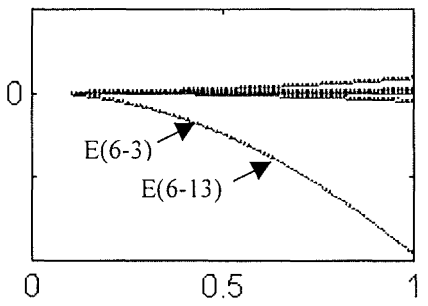

Fig.3a

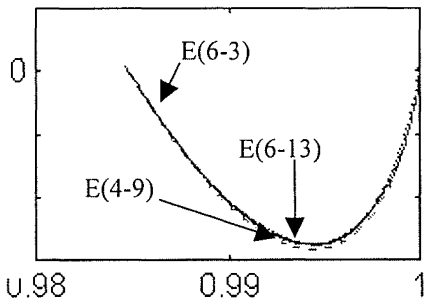

Fig. 3b

Fig. 3 Comparison of equations (4-9), (6-3) and (6-13) (both using first ten terms) with $\alpha = 10°$, A=1.

Fig. 6-3a shows the comparison of the first ten weighting functions in equation (6-3)

$$\left|\frac{a_0 C_{ai}\pi R^{\frac{1}{2}}}{2}[-J_{v_i-0.5}(AR)\int_0^R r^{\frac{1}{2}}Y_{v_i-0.5}(Ar)dr + Y_{v_i-0.5}(AR)\int_0^R r^{\frac{1}{2}}J_{v_i-0.5}(Ar)dr]\right|_{i=1\sim10}$$ and in

equation (6-13) $\left|\frac{a_0 C_{ai} R^2}{(-v_i+2)(v_i+1)}\right|_{i=1\sim10}$ with $\alpha = 10°$, A=1.

Fig. 3b shows the comparison of equations (4-9), (6-3) and (6-13) (both using first ten terms) at R=1 with $\alpha = 10°$, A=1.

$$\Psi_1^* = -0.5a_0R^2\{[\sec^2\alpha + \ln(0.5\tan\alpha) - \sec\alpha\cot\alpha]\sin^2\theta - \sin^2\theta\ln(0.5\tan\theta) + \cos\theta - 1\} \tag{4-9}$$

$$\Psi_1^{**} = \sum_{i=1}^{\infty} \frac{a_0 C_{ai}\pi R^{\frac{1}{2}}}{2}[-J_{v_i-0.5}(AR)\int_0^R r^{\frac{1}{2}}Y_{v_i-0.5}(Ar)dr + Y_{v_i-0.5}(AR)\int_0^R r^{\frac{1}{2}}J_{v_i-0.5}(Ar)dr]Z_i(\theta) \tag{6-3}$$

$$\Psi_1^* = \sum_{i=1}^{\infty} \frac{a_0 C_{ai} R^2}{(-v_i+2)(v_i+1)} Z_i(\theta) \tag{6-13}$$

In this case, the corresponding weighting functions in equations (6-3) and (6-13) are almost overlapping; the streamfunction by equations (6-3) and (6-13) (both using first ten terms) at R=1 are also almost overlapping, in fact the streamfunction by equations (6-3) and (6-13) (both using first ten terms) are almost overlapping in the whole calculation domain when A=1. The simplification of equation (6-3) by equation (6-13) is quite accurate when A=1.

The first term is the main term in the expansion equations (6-12) or (6-13). The first ten ratios of the weighting functions divided by their first term in equation (6-13)

$[\frac{C_{ai}}{(-v_i+2)(v_i+1)} / \frac{C_{a1}}{(-v_1+2)(v_1+1)}]_{i=1\sim10}$ are [1.0000 -0.0893 0.0509 -0.0168

0.0085 -0.0034 0.0037 -0.0015 0.0018 -0.0006] successively for $\alpha = 10°$ and [1.0000 0.1929 0.1779 0.0587 0.0535 0.0189 0.0171 0.0037 0.0022 -0.0008] for $\alpha = 5.65°$. The ratios oscillate while declining when $\alpha = 10°$ and progressing decline when $\alpha = 5.65°$. Generally speaking, the absolute values of the tenth ratios for both series are less 0.001.

The expansion error of equation (6-13) to equation (4-9) comes from the calculation of eigenvalues v_i and eigenfunction $Z_i(\theta)$. The accuracy of eigenvalues v_i is only ± 0.1 at the moment, but the result is still acceptable in this stage.

To expand the equation (4-9), the first ten terms of equation (6-13) are good enough. The accuracy of expansion of equation (6-3) with equation (6-12) will depend on the constant A.

Fig. 4a shows the comparison of the first ten weighting functions in equations (6-3) and (6-13) with $\alpha = 10°$, A=5. Fig. 4b shows the comparison of equations (4-9), (6-3) and (6-13) (both using first ten terms) at R=1 with $\alpha = 10°$, A=5.

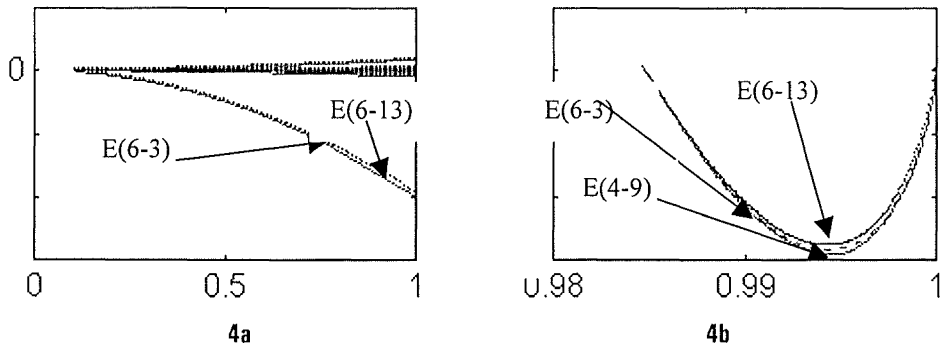

Fig. 4 Comparisons of equations (4-9), (6-3) and (6-13) with $\alpha = 10°$, A=5.

It can be seen that the equation (6-12 or 6-13) is still a good expansion of equation (6-3) even for A as high as 5.

In the equations (4-9) and (6-13), the parameter a_1 (ie A) does not appear. This is expected since the equations (4-9) and (6-13) are the solutions of equation (6-1) with a_1 = 0. When a_1 is small enough, the equation (6-3) can be expanded by equation (6-12) very accurately (Figs.3a and 4a), which is also not related to a_1. That means a_1 is insensitive for the solution equation (6-3) with a_1 being small enough. But a_1 will have a great effect on the solution (6-3), when a_1 is larger enough. I will show the effect in the following calculation.

Fig. 5a shows the comparison of the first ten weighting functions in equations (6-3) and (6-13) with $\alpha = 10°$, A=10. Fig. 5b shows the comparison of equations (4-9), (6-3) and (6-13) (both using first ten terms) at R=1 with $\alpha = 10°$, A=10.

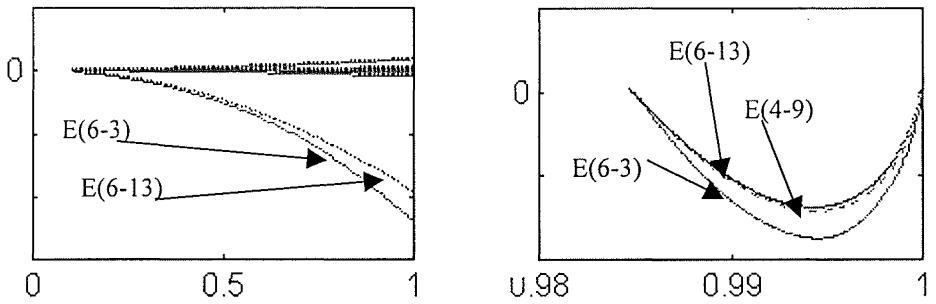

Fig. 5 Comparison of equations (4-9), (6-3) and (6-13) with $\alpha = 10°$, A=10.

In this case, there is an obvious difference between equation (6-3) and its approximate expansion equation (6-13), The difference is almost that between the solutions (4-9) and (6-3), which is the difference bringing by a_1. The term a_1 makes the streamfunction steeper, more fluid flows turning out from upper portion.

Fig. 6a shows the comparison of the first ten weighting functions in equations (6-3) and (6-13) with $\alpha = 10°$, A=20. Fig. 6b shows the comparison of equations (4-9), (6-3) and (6-13) (both using first ten terms) at R=1 with $\alpha = 10°$, A=20.

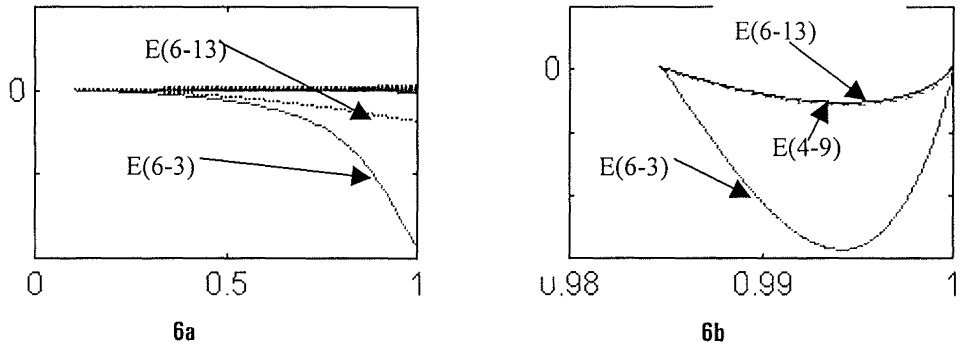

Fig. 6 Comparison of equations (4-9), (6-3) and (6-13) with $\alpha = 10°$, A=20.

The difference between equation (6-3) and its approximate expansion equation (6-12) (equals to the exact expansion of equation (4-9)) is so large that the deviation is about 5 times. They describe the different flowfields with great difference in separate performance, though the flowfield described by equation (6-1) is still a single return flow field. The factor described by term a_1 makes the most fluid flows turning out from upper portion.

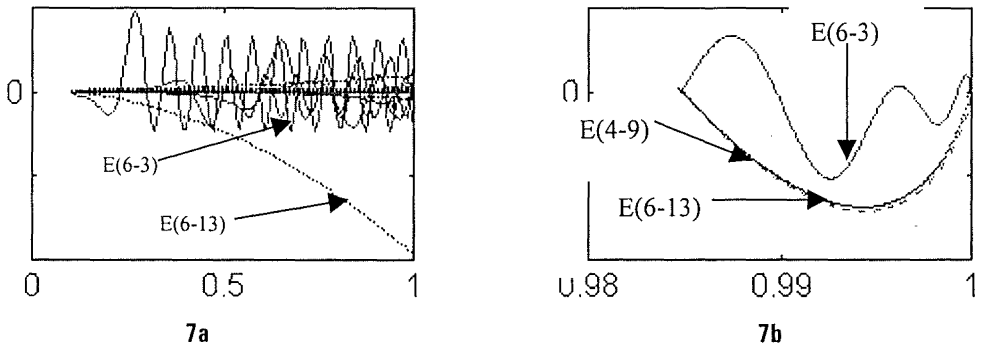

Fig. 7 Comparison of equations (4-9), (6-3) and (6-13) with $\alpha = 10°$, A=100.

Fig. 7a shows the comparison of the first ten weighting functions in equations (6-3) and (6-13) with $\alpha = 10°$, A=100. Fig. 7b shows the comparison of equations (4-9), (6-3) and (6-13) (both using first ten terms) at R=1 with $\alpha = 10°$, A=100.

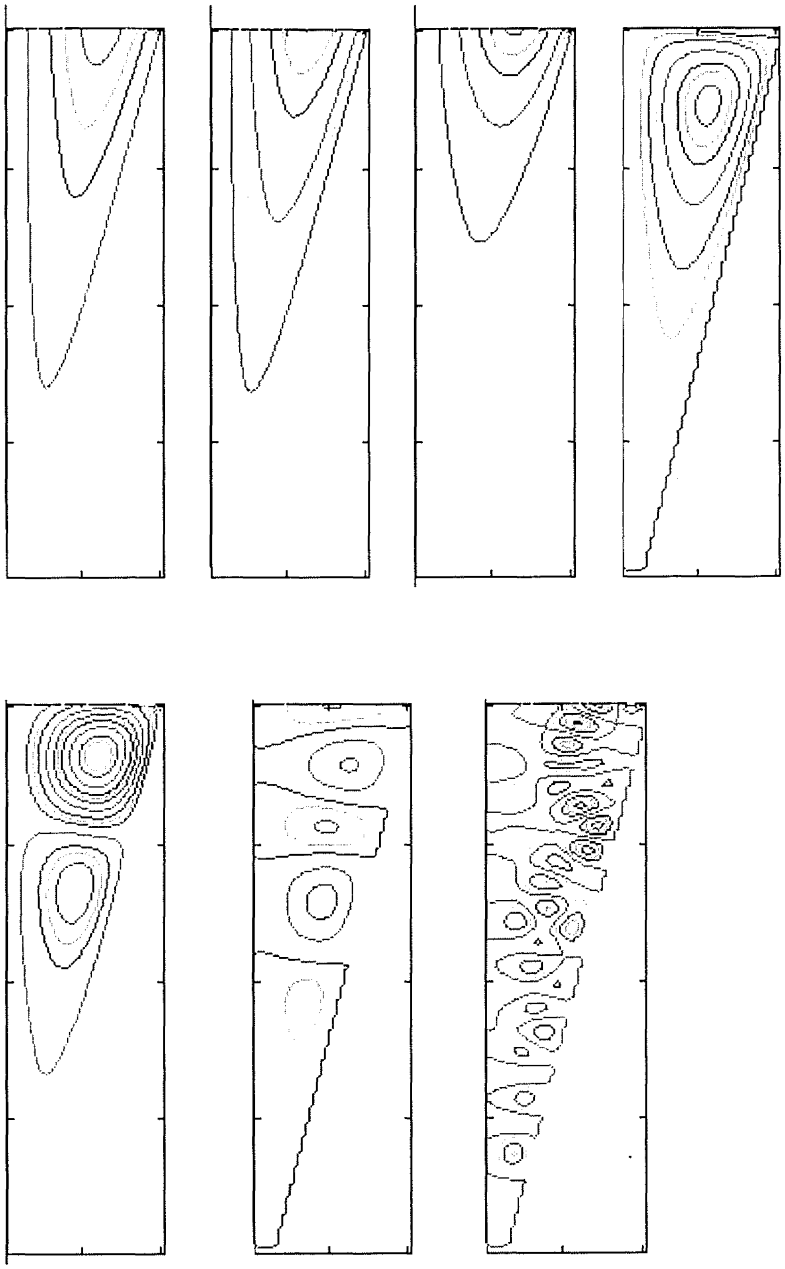

Fig.8 Deviating process with A increasing from 1 to 100.

In this case, first ten weighting functions in equations (6-3) and (6-13) are totally different. They describe different flowfields. The flowfield described equation (6-3) is planless and jumbled.

Briefly speaking, as coefficient A increasing, the flowfield described by equation (6-3) Ψ_1^{**} is deviating from that described by equation (4-9) Ψ_1^{*}.

Fig. 8 shows the deviating process with A increasing from 1 to 100.

When coefficient A is less than 5, the flowfield described by equation (6-3) is overlapped with that by equation (4-9).

When coefficient A is 20, the flowfield described by equation (6-3) becomes steeper than that by equation (4-9). More fluid flows turning out from upper potion.

As coefficient A increasing, a whirlpool will form. If coefficient A keep to increase, more whirlpools will occur. At last, a planless and jumbled flowfield will fill the cyclone.

In practical design, the cases with very high coefficient A have been avoided. But Smith (1962) has observed the multi-whirlpools phenomena during his research.

As above discuss I can prove that when $a_1 \to 0$, $\Psi_2^{**}(R,\theta) \to \Psi_2^{*}(R,\theta)$. If AR is small enough, the following equations can be obtained

$$\Psi_2^{**} \approx \sum_{i=1}^{\infty} \frac{b_0 C_{bi} \pi R^{\frac{1}{2}}}{2\sin[(v_i - 0.5)\pi]\Gamma(v_i + 0.5)\Gamma(-v_i + 1.5)} [R^{v_i - 0.5} \int_0^R r^{-v_i + 3} dr - R^{-v_i + 0.5} \int_0^R r^{v_i + 2} dr] Z_i(\theta)$$

$$= \sum_{i=1}^{\infty} \frac{\sin[(v_i + 0.5)\pi] b_0 C_{bi} R^4}{2\sin[(v_i - 0.5)\pi](-v_i - 0.5 + 1)} [\frac{1}{-v_i + 4} - \frac{1}{v_i + 3}] Z_i(\theta)$$

$$= \sum_{i=1}^{\infty} \frac{-b_0 C_{bi} R^4}{2(-v_i + 0.5)} [\frac{1}{-v_i + 4} - \frac{1}{v_i + 3}] Z_i(\theta)$$

$$= \sum_{i=1}^{\infty} \frac{b_0 C_{bi} R^4}{(-v_i + 4)(v_i + 3)} Z_i(\theta)$$

The last equation is the same as the expansion of equation (4-12) $\Psi_2^* = \sum_{i=1}^{\infty} \frac{b_0 C_{bi} R^4}{(-v_i+4)(v_i+3)} Z_i(\theta)$.

As coefficient A increasing, the flowfield described by equation (6-4) Ψ_2^{**} is deviating from that described by equation (4-12) Ψ_2^*. With coefficient A increasing, a whirlpool will form. If coefficient A keep to increase, more whirlpools will occur. At last, a planless and jumbled flowfield will fill the cyclone.

It can be proved that when $a_1 \to 0$, $\Psi_3^{**}(R,\theta) \to \Psi_3^*(R,\theta)$ and $\Psi_4^{**}(R,\theta) \to \Psi_4^*(R,\theta)$. I will prove only the latter very roughly.

Since when r is small enough, the first kind of Bessel function $J_v(r) \approx c_v r^v$ and the second kind of Bessel function $Y_v(r) \approx cI_v r^v + cII_v r^{-v}$,

$$\Psi_{4i}^{**} = (A_i^* J_{v_i-0.5}(AR) + B_i^* Y_{v_i-0.5}(AR)) R^{\frac{1}{2}} Z_i(\theta)$$

$$\approx (A_i^* c_{v_i-0.5}(AR)^{v_i-0.5} + B_i^* (cI_{v_i-0.5}(AR)^{v_i-0.5} + cII_{v_i-0.5}(AR)^{-v_i+0.5})) R^{\frac{1}{2}} Z_i(\theta)$$

$$= [(A_i^* c_{v_i-0.5} + + B_i^* cI_{v_i-0.5})(AR)^{v_i-0.5} + B_i^* cII_{v_i-0.5}(AR)^{-v_i+0.5}] R^{\frac{1}{2}} Z_i(\theta)$$

$$= (A_i R^{-v_i+1} + B_i R^{v_i}) Z_i(\theta)$$

From above calculations, We can see that if coefficient A is under 5 the solution of equation (6-1) can almost overlap the solution of equation (4-10). All the comparisons, analysis and conclusions in Chapter 4 and 5 will valid for the solution if A is under 5. The solution of equation (6-1) should fit the experimental findings of Kelsall (1952) and Knowles et al. (1973) very well. Furthermore the solution should fit more flexible

experimental findings than that of equation (4-10), since some steeper flowfields can be described by the solution.

Unlike terms a_0 and b_0 possessing their Owen solutions Ψ_1^* and Ψ_2^*, the term a_1 does not possess its Owen solution. It has its effect into the effects of other terms. Term a_1 will introduce vorticity into the cyclones, solutions Ψ_3^{**} and Ψ_4^{**} does not describe potential flow.

6.3 CONCLUSION

1. I find a group of exact inviscid solutions for the reverse swirling flow in a conical cyclone. It can fit the experimental findings of Kelsall (1952) and Knowles et al. (1973) very well. Furthermore the solution should fit more complex experimental findings than that of equation (4-10).

2. More characteristics of the flowfield of cyclones can be described by the introducing of term a_1. It represents a kind of vorticity introduced into cyclones. When term a_1 is small enough, it is insensitive to the flowfield. When term a_1 increase to some value, the flowfield becomes steeper than that by equation (4-9). More fluid flows turning out from upper potion. As term a_1 increasing, a whirlpool will form. If term a_1. keep to increase, more whirlpools will occur. At last, a planless and jumbled flowfield will fill the cyclone. The multi-whirlpools phenomena have been comfirmed by the observation of Smith (1962) during his research.

Chapter 7

A Steady Axisymmetric Reverse Flow With Swirl in Cylindrical Cyclones

(Cylindrical pattern II)

7.1 introduction

In this chapter a mathematical model for the flow in a cylindrical cyclone is developed, which is an exact solution of the equation of motion for steady axisymmetric inviscid flow with or without a central 'air' core. The theoretical results are compared with experimental data from Smith (1962). The effect on the flow pattern of vorticity introduced into the inlet stream by circulation profile is discussed.

Most previous models have assumed that radial and axial velocities are not linked to the tangential vortex profile. Vatistas (1991) reports that the main properties of concentrated vortices as represented by the radial distributions of azimuthal velocity and static pressure were found to be common to most vortical flows and not to depend on the method of production. Leibovich (1984) similarly finds that most vortex flows can be approximated as being columnar, with universal profiles. In this paper, the interdependence of axial velocity and radial velocity with tangential velocity will be discussed.

7.2 THEORY

We use cylindrical co-ordinates (x, r, φ), with corresponding velocity components (v_x, v_r, v_φ). The equations of motion for steady axisymmetric inviscid flow of incompressible fluid are

$$v_x \frac{\partial v_x}{\partial x} + v_r \frac{\partial v_x}{\partial r} = -\frac{1}{\rho}\frac{\partial p}{\partial x} \tag{7-1}$$

$$v_x \frac{\partial v_r}{\partial x} + v_r \frac{\partial v_r}{\partial r} - \frac{v_\varphi^2}{r} = -\frac{1}{\rho}\frac{\partial p}{\partial r} \tag{7-2}$$

$$v_x \frac{\partial v_\varphi}{\partial x} + v_r \frac{\partial v_\varphi}{\partial r} + \frac{v_\varphi v_r}{r} = 0 \tag{7-3}$$

The equation of continuity is

$$\frac{\partial v_x}{\partial x} + \frac{1}{r}\frac{\partial (r v_r)}{\partial r} = 0 \tag{7-4}$$

Further, if we introduce the streamfunction ψ, the above equations can be written as

$$\frac{\partial^2 \psi}{\partial x^2} + \frac{\partial^2 \psi}{\partial r^2} - \frac{1}{r}\frac{\partial \psi}{\partial r} = -C\frac{dC}{d\psi} + r^2 \frac{dh}{d\psi} \tag{7-5}$$

Where $v_x = \frac{1}{r}\frac{\partial \psi}{\partial r}$

$v_r = -\frac{1}{r}\frac{\partial \psi}{\partial x}$

$C = r v_\varphi$ is ($(2\pi)^{-1}$ times) the circulation round a symmetrically placed circle, and h is (ρ^{-1} times) the total pressure $h = \frac{p}{\rho} + \frac{1}{2}(v_x^2 + v_r^2 + v_\varphi^2)$. Both C and h are functions of ψ alone.

For convenience, we introduce nondimensional variables as follows for a cylindrical domain

$R = \frac{r}{R_0}$, $X = \frac{x}{R_0}$,

$$V_x = \frac{v_x}{V_{x0}} \qquad V_r = \frac{v_r}{V_{x0}} \qquad V_\varphi = \frac{v_\varphi}{V_{x0}}$$

$$\Psi = \frac{\psi}{V_{x0} R_0^2} \qquad \Gamma = \frac{v_\varphi r}{V_{x0} R_0} \qquad H = \frac{h}{\rho V_{x0}^2}$$

Where R_0 is the radius of the cylinder, and V_{x0} is the maximum axial velocity at upstream boundary.

The nondimensional inviscid equation of steady, rotational symmetric rotating flow is then

$$\frac{\partial^2 \Psi}{\partial X^2} + \frac{\partial^2 \Psi}{\partial R^2} - \frac{1}{R}\frac{\partial \Psi}{\partial R} = -\Gamma \frac{d\Gamma}{d\Psi} + R^2 \frac{dH}{d\Psi} \tag{7-6}$$

The relationships among Γ, H and Ψ may be specified at the upstream boundary, as given by Batchelor (1967) for a special case. We will do this in a more general form according to swirling velocity V_φ, axial velocity V_x and total pressure at the upstream boundary. To establish the relationship between Γ and Ψ, the swirling velocity V_φ and axial velocity V_x at the upstream boundary are needed:

$$\Gamma(R) = RV_\varphi(R) \tag{7-7}$$

$$\Psi(R) = \int_{R_s}^{R} r^* V_x(r^*) dr^* + \Psi_0 \tag{7-8}$$

In the above two equations, the range of R from which range the fluid enters the domain is between R_s and R_e, as in Fig. 1. For cyclones, usually $R_e = 1$ and is most often larger than the gas exit radius R_x. If we eliminate R from equations (7-7) and (7-8), Γ becomes a function of Ψ.

Furthermore if we write the first term on the right hand side of equation (7-6) in polynomial form, it can be written as

$$-\Gamma \frac{d\Gamma}{d\Psi} = \sum_0^N a_i \Psi^i \tag{7-9}$$

We can do the same for the second term on the right hand side of equation (7-6)

$$\frac{dH}{d\Psi} = \sum_{0}^{N} b_i \Psi^i \tag{7-10}$$

Then equation (7-6) changes to

$$\frac{\partial^2 \Psi}{\partial X^2} + \frac{\partial^2 \Psi}{\partial R^2} - \frac{1}{R}\frac{\partial \Psi}{\partial R} = \sum_{0}^{N} a_i \Psi^i + R^2 \sum_{0}^{N} b_i \Psi^i \tag{7-11}$$

The analytical general solution for the above equation has not been found.

As defined, the dimensionless streamfunction Ψ has a maximum value of 0.5. In many cases, especially return flows, the maximum value in the field is much less than this, and we can discuss the linear main term at this stage. In this chapter a narrower pattern will be investigated. The pattern equation is:

$$\frac{\partial^2 \Psi}{\partial X^2} + \frac{\partial^2 \Psi}{\partial R^2} - \frac{1}{R}\frac{\partial \Psi}{\partial R} = a_1 \Psi \tag{7-12}$$

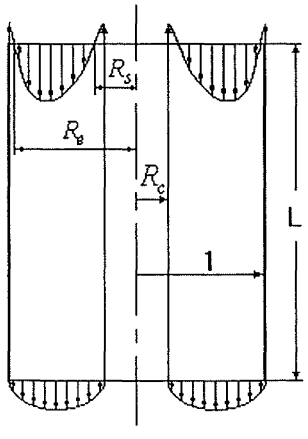

Fig. 7-1 The general problem domain

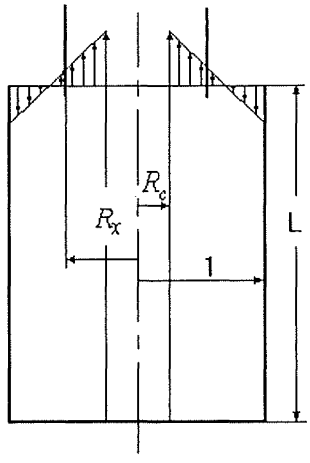

Fig. 7-2 The problem domain for a cylindrical return flow cyclone

The domain we are considering is the gap between two circular cylinders as in Fig. 7-1, the inner one having radius R_c, the outer one having radius 1. If R_c is zero, the domain will be a cylinder. The domain within the core radius R_c does not exchange fluid with the outer domain being considered here. The need for such an inner domain can be seen from a number of experimental studies (Stairmand, 1951; Smith, 1962; Ogawa, 1984; Wakelin, 1993), which show reverse flow and circulation within a core cell. R_s and R_e are the radii dividing upflow and downflow, and R_x is the radius of the exit tube.

Following Batchelor (1967), we write

$$\Psi(X,R) = RF(X,R)$$

whence the equation (7-12) becomes

$$\frac{\partial^2 F}{\partial X^2} + \frac{\partial^2 F}{\partial R^2} + \frac{1}{R}\frac{\partial F}{\partial R} + (A^2 - \frac{1}{R^2})F = 0$$

where $A^2 = -a_1$

The above equation can be solved by separation of variables.

Using this method, the analytical solution of equation (7-12) is

$$\Psi = \sum_{i=0}^{M-1} R(A_i \sin((A^2 - \mu_{1i}^2)^{\frac{1}{2}} X) + B_i \cos((A^2 - \mu_{1i}^2)^{\frac{1}{2}} X)) Z_1(\mu_{1i} R)$$

$$+ \sum_{i=M}^{N} R(A_i e^{-(\mu_{1i}^2 - A^2)^{\frac{1}{2}} X} + B_i e^{(\mu_{1i}^2 - A^2)^{\frac{1}{2}} X}) Z_1(\mu_{1i} R) \qquad (7\text{-}13)$$

Where $Z_1(\mu_{1i} R) = J_1(\mu_{1i} R) - \frac{J_1(\mu_{1i} R_c)}{Y_1(\mu_{1i} R_c)} Y_1(\mu_{1i} R)$

$J_1(\mu_{1i} R)$ is the first kind of Bessel function, of order 1.

$Y_1(\mu_{1i} R)$ is the second kind of Bessel function, of order 1.

μ_{1i} is the ith eigenvalue of equation $J_1(\mu_{1i}R_0) - \frac{J_1(\mu_{1i}R_c)}{Y_1(\mu_{1i}R_c)} Y_1(\mu_{1i}R_0) = 0$ (7-13a), and these eigenvalues are related as follows

$$0 < .... \mu_{1i} < \mu_{1i+1} < ... \mu_{1M-1} < A < \mu_{1M} < ... < \mu_{1N} .$$

The M th eigenvalue is the first larger than A.

The corresponding velocities are

$$V_x = \frac{1}{R}\frac{\partial \Psi}{\partial R} = \sum_{i=0}^{M-1} (A_i \sin((A^2 - \mu_{1i}^2)^{\frac{1}{2}} X) + B_i \cos((A^2 - \mu_{1i}^2)^{\frac{1}{2}} X))\mu_{1i} Z_0(\mu_{1i} R)$$

$$+ \sum_{i=M}^{N} (A_i e^{-(\mu_{1i}^2 - A^2)^{\frac{1}{2}} X} + B_i e^{(\mu_{1i}^2 - A^2)^{\frac{1}{2}} X})\mu_{1i} Z_0(\mu_{1i} R) \qquad (7\text{-}14)$$

$$V_r = -\frac{1}{R}\frac{\partial \Psi}{\partial X} = -\sum_{i=0}^{M-1} (A^2 - \mu_{1i}^2)^{\frac{1}{2}} (A_i \cos((A^2 - \mu_{1i}^2)^{\frac{1}{2}} X) - B_i \sin((A^2 - \mu_{1i}^2)^{\frac{1}{2}} X)) Z_1(\mu_{1i} R)$$

$$- \sum_{i=M}^{N} (\mu_{1i}^2 - A^2)^{\frac{1}{2}} (-A_i e^{-(\mu_{1i}^2 - A^2)^{\frac{1}{2}} X} + B_i e^{(\mu_{1i}^2 - A^2)^{\frac{1}{2}} X}) Z_1(\mu_{1i} R) \qquad (7\text{-}15)$$

$$V_\varphi = \frac{(A^2 \Psi^2 + D)^{\frac{1}{2}}}{R} \qquad (7\text{-}16)$$

The arbitrary constants a_1, A_i and B_i can be specified from boundary conditions. For example, taking the flow depicted in Fig. 7-1, if the axial velocities at both the upper boundary (X=0) and lower boundary (X=L) are given, arbitrary constants A_i and B_i can be calculated as follows.

When $i < M$

$$A_i = \frac{2\int_{R_c}^{1} RV_x \mid_{X=L} Z_0(\mu_{1i} R) dR - 2\cos((A^2 - \mu_{1i}^2)^{\frac{1}{2}} L) \int_{R_c}^{1} RV_x \mid_{X=0} Z_0(\mu_{1i} R) dR}{\mu_{1i}(Z_0(\mu_{1i})^2 - R_c^2 Z_0(\mu_{1i} R_c)^2) \sin((A^2 - \mu_{1i}^2)^{\frac{1}{2}} L)} \qquad (7\text{-}17)$$

$$B_i = \frac{2\int_{R_c}^{1} RV_x \mid_{X=0} Z_0(\mu_{1i}R)dR}{\mu_{1i}(Z_0(\mu_{1i})^2 - R_c^2 Z_0(\mu_{1i}R_c)^2)} \tag{7-18}$$

When $M \le i \le N$

$$A_i = \frac{2(\int_{R_c}^{1} RV_x \mid_{X=0} Z_0(\mu_{1i}R)dR - e^{-(\mu_{1i}^2 - A^2)^{\frac{1}{2}}L} \int_{R_c}^{1} RV_x \mid_{X=L} Z_0(\mu_{1i}R)dR)}{\mu_{1i}(Z_0(\mu_{1i})^2 - R_c^2 Z_0(\mu_{1i}R_c)^2)(1 - e^{-2(\mu_{1i}^2 - A^2)^{\frac{1}{2}}L})} \tag{7-19}$$

$$B_i = \frac{2(\int_{R_c}^{1} RV_x \mid_{X=0} Z_0(\mu_{1i}R)dR - e^{(\mu_{1i}^2 - A^2)^{\frac{1}{2}}L} \int_{R_c}^{1} RV_x \mid_{X=L} Z_0(\mu_{1i}R)dR)}{\mu_{1i}(Z_0(\mu_{1i})^2 - R_c^2 Z_0(\mu_{1i}R_c)^2)(1 - e^{2(\mu_{1i}^2 - A^2)^{\frac{1}{2}}L})} \tag{7-20}$$

We will now discuss the case approximating a return flow cyclone, when fluid enters a cylinder with swirl through an annular area from the top, and then leaves through the top central area. There is the core in the cylinder as discussed above, and the bottom of the cylinder is closed (Fig. 7-2, Fig. 7-3 and Fig. 7-4).

At the cylinder walls and bottom, the stream function has the same value. We can choose Ψ_0 in equation (7-8), so that the boundary conditions become:

(1) $\Psi(R_c, X) = 0$

(2) $\Psi(1, X) = 0$

(3) $\Psi(R, L) = 0$

Since at the inlet and outlet boundaries a Dirichlet condition is used (Ψ is given along the boundaries), it is necessary to ensure the net mass flow is zero:

$$\int_{R_c}^{R_x} RV_x \mid_{X=0} dR + \int_{R_x}^{1} RV_x \mid_{X=0} dR = 0$$

Since the axial velocity at the bottom is zero, with substituting A_i, B_i from equations (7-17)-(7-20), equation (7-13) is simplified to

$$\Psi = \sum_{i=0}^{M-1} R \frac{2\int_{R_c}^{1} RV_x \mid_{X=0} Z_0(\mu_{1i}R)dR}{\mu_{1i}(Z_0(\mu_{1i})^2 - R_c^2 Z_0(\mu_{1i}R_c)^2)} \left(\frac{\sin((A^2-\mu_{1i}^2)^{\frac{1}{2}}(L-X))}{\sin((A^2-\mu_{1i}^2)^{\frac{1}{2}}L)}\right) Z_1(\mu_{1i}R)$$

$$+ \sum_{i=M}^{N} R \frac{2\int_{R_c}^{1} RV_x \mid_{X=0} Z_0(\mu_{1i}R)dR}{\mu_{1i}(Z_0(\mu_{1i})^2 - R_c^2 Z_0(\mu_{1i}R_c)^2)} \left(\frac{e^{(\mu_{1i}^2-A^2)^{\frac{1}{2}}(L-X)} - e^{-(\mu_{1i}^2-A^2)^{\frac{1}{2}}(L-X)}}{e^{(\mu_{1i}^2-A^2)^{\frac{1}{2}}L} - e^{-(\mu_{1i}^2-A^2)^{\frac{1}{2}}L}}\right) Z_1(\mu_{1i}R) \quad (7\text{-}21)$$

By inputting the upstream boundary velocities V_φ, V_x and the downstream boundary velocity V_x, both at X=0, the problem is determined. In fact, since we are considering the linearised problem at this stage, the *forms* of the profiles of axial velocity and tangential velocity are not independent. We can input either the V_φ or V_x profile along the upstream boundary, and the other velocity will be determined by adjusting arbitrary coefficients A and D. The relationship between V_φ and V_x on the upstream boundary is, from equation (7-16),

$$V_\varphi = \frac{(A^2\Psi^2 + D)^{\frac{1}{2}}}{R} = \frac{(A^2\left(\int_R^1 RV_x dR\right)^2 + D)^{\frac{1}{2}}}{R} \qquad (7\text{-}22)$$

Having specified V_x along the upstream boundary, V_φ is thus still dependent on the choice of A and D.

7.3 RESULTS AND DISCUSSION

In this section, the theoretical results are compared with the experimental findings of Smith (1962) and Ogawa (1983).

Smith's apparatus is shown in Fig. 7-3. The inlet of the cylindrical cyclone was formed by eight logarithmic-spiral blades between two flat disks. The upper disk formed the roof of the cyclone. The spiral blades projected through slots in the upper disk so that the inlet area could be adjusted by a vertical motion of the top disk. Room air was drawn into the inlet.

The circumferential and axial velocity components were determined by measuring the total velocity and its direction in a plane normal to the diameter. It was assumed that the radial velocity was everywhere small enough so that the velocity could be considered normal to the radius.

Ogawa's return flow cyclone is shown in Fig. 7-4, and was made of transparent plastics.

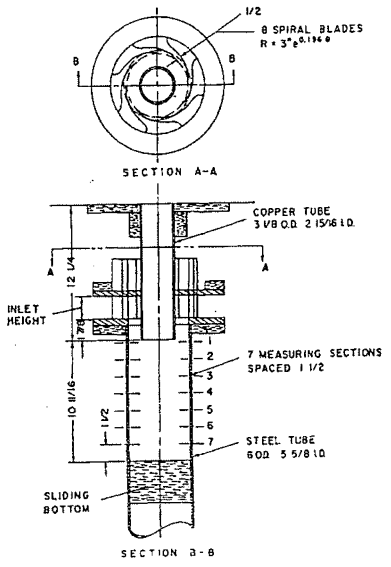

Fig.7- 3 Smith's experimental cyclone

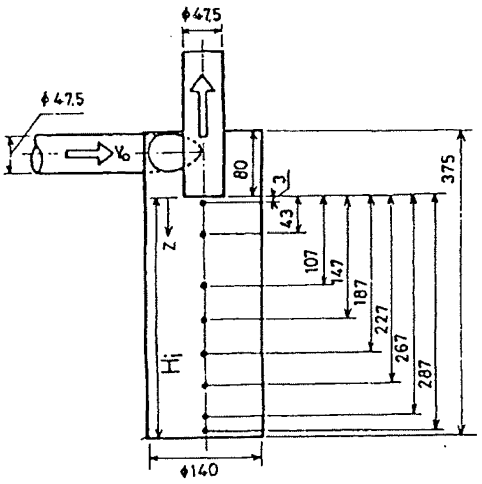

Fig.7- 4 Ogawa's experimental cyclone

Smith did a complete determination of the velocity distribution with two different inlet heights, noted as case 1 and case 2. For case 1 the inlet height was 2 in, and for case 2 it was 0.5 in. Before the detailed comparisons of velocities with experiments are made, it is useful to show a typical streamline pattern of the flow in the cross-plane. Figs. 7-5 and 7-7 show the experimental streamlines for cases 1 and 2 of Smith respectively. Figs. 7-6 and 7-8 show the corresponding calculated results for Smith's two cases. We can see that in Smith's cases 1 and 2, the streamlines do not enter the central core regime; this is quite common for the high efficiency cyclones that develop considerable high tangential velocity.

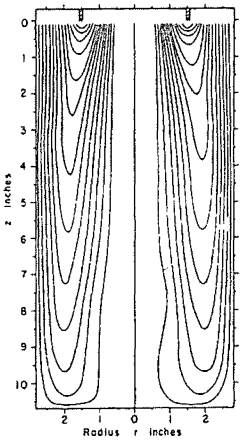

Fig. 7-5 Smith's experimental streamlines for case 1

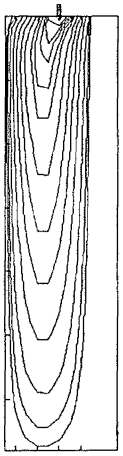

Fig. 7-6 Caculated streamlines for Smith's case 1

Stairmand (1951) gave some pictures describing the central core in his cyclones of "high efficiency" design. In hydrocyclones, a gas or vapour central core may appear. The characteristics of the core have not been fully studied. In this work I do not calculate the flowfield of the 'air core', and think that its flowfield is separated from that of the main body of the cyclone. The radius of the air core was made equal to that from experiments (Figs.7-5 and 7-7), and was checked by net mass balance. The axial velocities at the boundaries were taken directly from the experiments (Figs. 7-9 and 7-11).

Both Smith's experiments and my theoretical calculations show that in the lower half of the cyclone the flow pattern in the two cases is quite similar in spite of the large difference between the patterns in the upper half. Smith inferred from his experiment that the flow in the lower part of the cyclone has unique characteristics; if the inlet design does not match these characteristics, the flow makes a rapid adjustment in the upper part of the cyclone.

The measurements show that in case 1, a large portion of the flow moves radially in, over the first few inches below the end of the exit pipe. The surface of zero axial velocity begins at the bottom edge of the exit and then moves out to a characteristic position in the lower part. The theoretical results show the same tendency, but show a faster movement to the characteristic position. The difference may be due to the simplification of linearization in equation (7-11). Another possibility for the difference may rise from Smith's assumption, which he made while doing his measurements, that the radial velocity was everywhere small enough. The calculation shows the radial velocity at the inlet is quite significant. Since the axial velocity near the cylinder wall at entry is smaller than that in the vicinity of the main body and that downstream (Fig. 7-9), some fluid moves out from the main body to compensate for the deficiency.

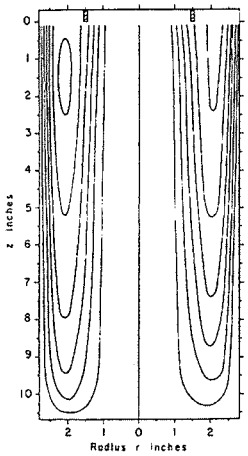

Fig. 7-7 Smith's experimental streamlines for case 2

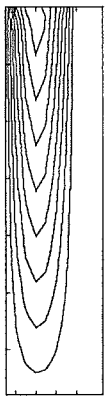

Fig. 7-8 Caculated streamlines for Smith's case 2

Experimental streamlines in case 2 show that there is virtually no radial flow in the upper portion of the cyclone. The surface of zero axial velocity is at the characteristic radius at every measuring section. This surface does not immediately join the bottom of the exit, and there is an upflow just outside the exit pipe. This means some entered flow will return back to the inlet annulas, which may increase the efficiency of dust collection.

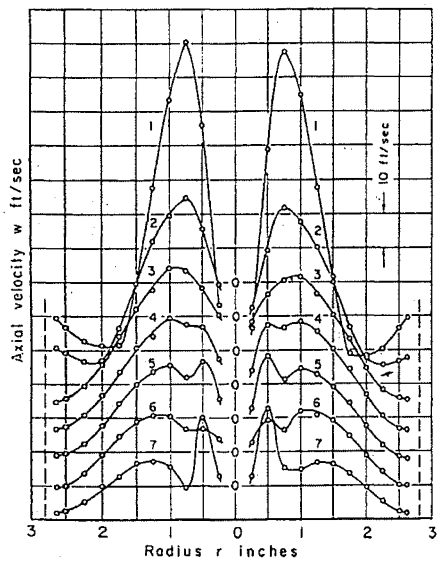

Fig. 7-9 Smith's experimental axial velocity versus radius profiles for case 1. Numbers above curves refer to measuring sections in Fig. 7-1

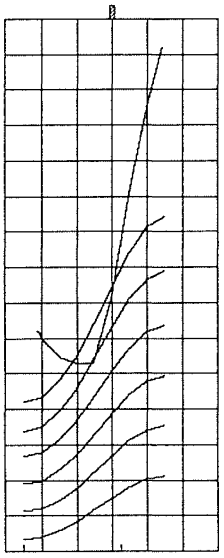

Fig. 7-10 Calculated axial velocity corresponds to that in Fig. 7-8

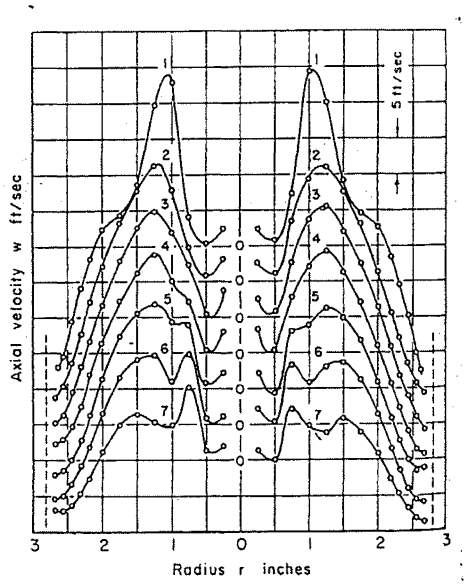

Fig. 7-11 Smith's experimental axial velocity versus radius streamlines for case 2. Numbers above curves refer to measuring sections in Fig.7-1

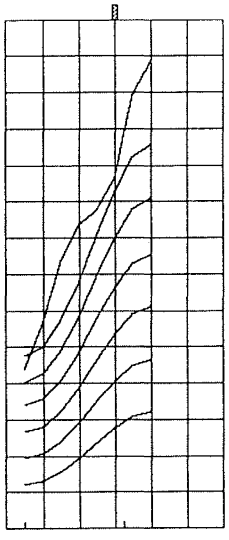

Fig. 7-12 Calculated axial velocity corresponds to that in Fig. 7-10

Figs. 7-9 and 7-11 show Smith's experimental distributions of axial velocity along radial direction at different heights. Figs. 7-10 and 7-12 show the corresponding theoretical results. The calculations corroborate the properties on which the measurements are based.

In the upper portion the axial velocity components vary acutely; in the lower portion they tend to have a common appearance. Along the axial direction, the magnitude of axial velocity component will decrease gradually, then reach zero at the bottom of the cylinder.

At the bottom of the cyclone the experimental axial velocities show an upward hump, and this may be caused by drainage from the boundary layer along the bottom. The main body of the fluid is essentially inviscid and in rapid rotation, the centrifugal force being balanced by a radially inward pressure gradient. This pressure gradient also imposes itself throughout the thin viscous boundary layer on the bottom of the cylinder, where it is stronger than required, for the fluid in the boundary layer rotates much less rapidly. That fluid therefore spirals inward and eventually turns up and out of the boundary layer.

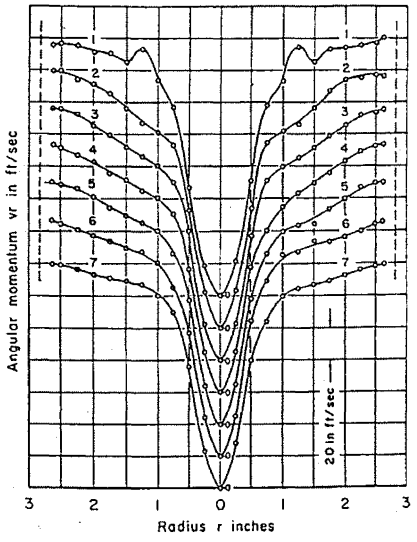

Fig. 7-13 Smith's experimental angular momentum versus radius streamlines for case 1. Numbers above curves refer to measuring sections in Fig.7-1

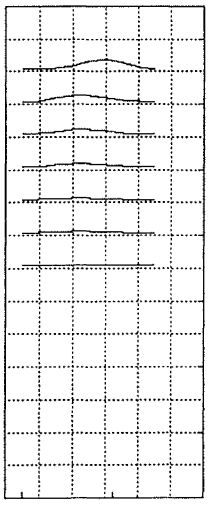

Fig. 7-14 Calculated angular momentum corresponds to that in Fig. 7-13

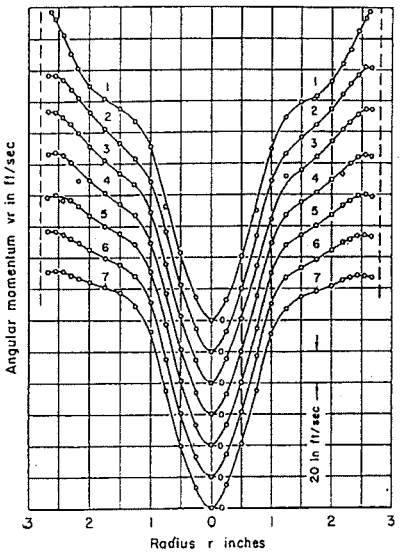

Fig. 7-15 Smith's experimental angular momentum versus radius streamlines for case 2. Numbers above curves refer to measuring sections in Fig.7-1

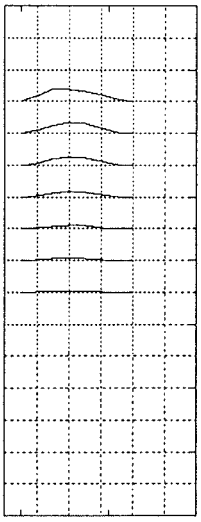

Fig. 7-16 Calculated angular momentum corresponds to that in Fig. 7-15

Figs. 7-13 and 7-15 show Smith's experimental distributions of angular momentum along radial direction at different heights. Figs.7- 14 and 7-16 show the corresponding theoretical results, finishing at the core radius.

There is a pronounced difference between experimental and theoretical results in the distributions of angular momentum. The difference comes from inviscid assumption. Out of the boundary layer, the experimental angular momentum decreases obviously with decreasing radius and then breaks and decreases with r^2. In contrast, the theoretical results follow Kelvin's circulation theorem, which briefly states that the circulation will not change along the streamline.

In equation (7-22) the second term in the right hand side represents the free vortex flow, and if the first term is zero, the tangential velocity is $V_\varphi = \frac{\Gamma}{R}$. The first term in the numerator of the right hand side of equation (7-22) represents the modification to the free vortex introduced from the upstream vorticity. When the tangential velocity is small, this term is comparatively large and so the modification is strong. When the tangential velocity is large enough, this modification has little effect, so that the

tangential velocity component will not change approximately along axial direction. It then tends to be self-similar (Gupta 1984).

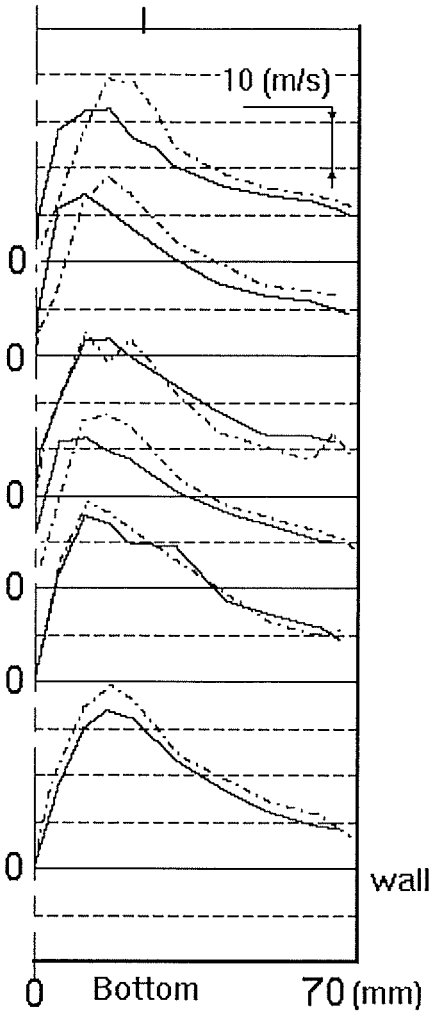

Fig. 7-17 Distributions of the tangential velocities at each height beneath the edge of the inner pipe for axial(------) and return flow (.....)cyclones of Ogawa.

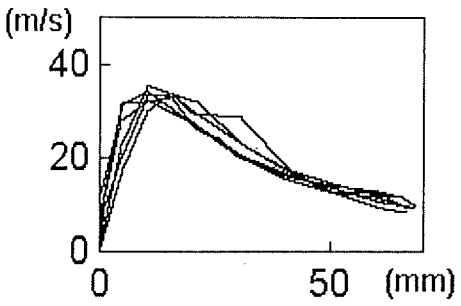

Fig.7-18 Compare with the tangenti velocities at each heights for axial flc cyclones.

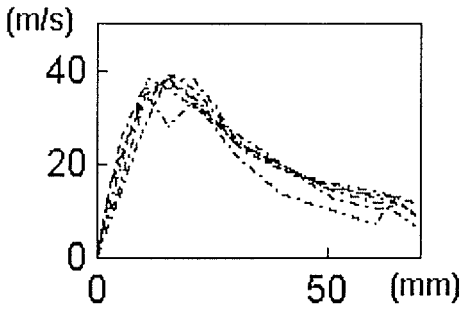

Fig. 7-19 Comparison of tangential velocities at different heights for return flow cyclones. (Ogawa)

Figs. 7-17, 7-18 and 7-19 show the distributions of the tangential velocities at each height beneath the edge of the inner pipe for two types of cyclones (axial flow and return flow). The dotted lines indicate the return flow cyclone. This experiment

confirms that in cylindrical cyclones, when the tangential velocity is large enough, it can be self-similar, and is insensitive to the axial velocity given at the upstream boundary.

Next, we try to explain the characteristics that Smith found from his experiments, with the structure of the theoretical solution. Equation (7-12) is a typical elliptic partial differential equation. The most important feature of this kind of equation is that a disturbance introduced at an interior point influences all other points in the domain. The closed bottom boundary condition will influence the flow pattern heavily. When $\mu_{1i} \geq A$, each term in solution (7-21) will have a similar structure as follows

$$F_i(X) = \frac{2R\int_{R_c}^{1} RV_x \mid_{X=0} Z_0(\mu_{1i}R)dR}{\mu_{1i}(Z_0(\mu_{1i})^2 - R_c^2 Z_0(\mu_{1i}R_c)^2)} \left(\frac{e^{(\mu_{1i}^2-A^2)^{\frac{1}{2}}(L-X)} - e^{-(\mu_{1i}^2-A^2)^{\frac{1}{2}}(L-X)}}{e^{(\mu_{1i}^2-A^2)^{\frac{1}{2}}L} - e^{-(\mu_{1i}^2-A^2)^{\frac{1}{2}}L}}\right) Z_1(\mu_{1i}R) \quad (7\text{-}23)$$

At the upstream and downstream boundaries (X=0), the maximum value of each of the above terms F_i is obtained, then the value continuously decreases with increasing depth, and at the bottom the values of each of the terms is zero. If the index coefficient $(\mu_{1i}^2 - A^2)^{\frac{1}{2}}$ is large enough, the value of the term (7-23) will decrease very sharply along the axial direction. Fig. 7-20 shows the relationships between F_i and X, while $A \to \mu_{11}$. The values of the terms other than i=1 will reach near to zero, if the depth is more than 20 % of cylinder length.

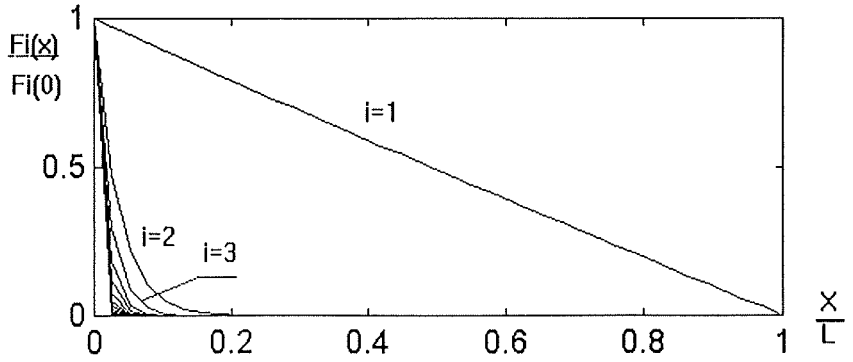

Fig. 7-20 ND-values of Fi for terms I versus nondimensional length.

To make things clearer, we investigate the potential flow first. If the right hand side of equation (12) is zero, a potential flow is defined. With the boundary condition of Smith's case 1, the corresponding potential flow pattern is shown in Fig 21. The irrotational returned flow with closed bottom boundary will move radially inward in the vicinity of the inlet, then flow up through the exit pipe. When vorticity at the upstream boundary is introduced by the distribution of tangential velocity, the elemental fluid volume will deform, and can be driven to flow deeply into the lower part of the cyclone. The constant A measures the degree of vorticity introduced with the inflow.

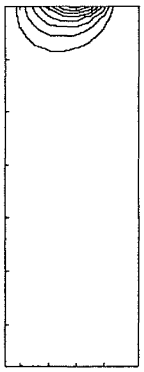

Fig. 7-21 Potential flow with boundary condition of Smith's case 1

When A is near any μ_{1i}, the index coefficient $(\mu_{1i}^2 - A^2)^{\frac{1}{2}}$ is near zero, and the corresponding term of equation (7-23) can be simplified by taking the limit. In this case, the value of the term will decrease gradually along the axial direction.

$$\lim_{\mu_{1i}\to A} \frac{2R\int_{R_c}^{1} RV_x \mid_{X=0} Z_0(\mu_{1i}R)dR}{\mu_{1i}(Z_0(\mu_{1i})^2 - R_c^2 Z_0(\mu_{1i}R_c)^2)} \left(\frac{e^{(\mu_{1i}^2-A^2)^{\frac{1}{2}}(L-X)} - e^{-(\mu_{1i}^2-A^2)^{\frac{1}{2}}(L-X)}}{e^{(\mu_{1i}^2-A^2)^{\frac{1}{2}}L} - e^{-(\mu_{1i}^2-A^2)^{\frac{1}{2}}L}}\right) Z_1(\mu_{1i}R)$$

$$= \frac{2R\int_{R_c}^{1} RV_x \mid_{X=0} Z_0(\mu_{1i}R)dR}{\mu_{1i}(Z_0(\mu_{1i})^2 - R_c^2 Z_0(\mu_{1i}R_c)^2)} \left(1 - \frac{X}{L}\right) Z_1(\mu_{1i}R)$$

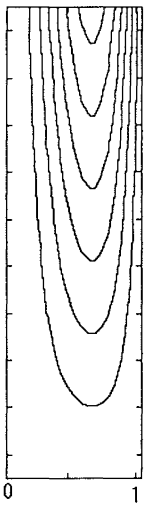

Fig. 7-22 Flow pattern for i=1

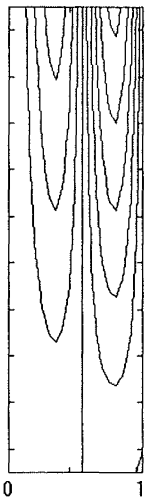

Fig. 7-23 Flow pattern for i=2

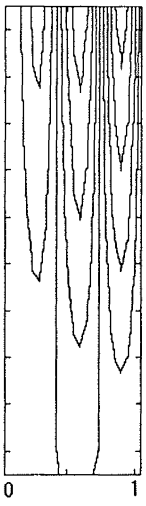

Fig. 7-24 Flow pattern for i=3

Figs. 7-22 to 7-24 show some simple characteristic flow patterns according to A→ μ_{1i}. The first pattern is suitable as a main term to describe the flow in returned cyclones. With increasing tangential velocity, while the constant A tends to approach the first eigenvalue, only the first term of equation (7-21) can have a considerable value in the lower portion of the cyclone; the other terms have their major values only in the upper portion of the cyclone. In the upper portion all terms of equation (7-21) have their effect, whereas in the lower portion only the first term has its effect.

7.4 CONCLUSION

1. I found a group of exact inviscid solutions for the reverse swirling flow in a cylinder, which shows natural features of the flow similar to those from experimental investigations. The results of this model show reasonable agreement with experiments by Smith (1962).

2. My model corroborates Smith's (1962) observation that the flow in the lower part of the cyclone has unique characteristics; if the inlet pattern does not match these

characteristics, the flow makes a rapid adjustment in the upper part of the cyclone. I give an explanation of the characteristics from the structure of the theoretical solution.

3. Many investigators reported that the tangential velocity profile does not vary significantly in the axial direction. My theory shows that this result can be tenable in a certain range. When tangential velocity is low, the vorticity which is a function of axial distance and radius will have a great effect on the tangential velocity profile; when tangential velocity is high enough, the vorticity would have little effect on it, the tangential velocity will be insensitive to the variations of axial and radial velocities, and it will seem self-similar.

Chapter 8

Some Analytical Results and Design Considerations

In the last 4 chapters, I studied the characteristics of the flowfield in cyclones. For more characteristics, more patterns (more a_i and b_i terms) need to be studied. In general, the patterns can be determined by upstream boundary conditions: a_i can be calculated from the distributions of tangential and axial velocities at the upstream boundary, and b_i can be calculated from that of total pressure.

At the upstream boundary, circulation in the cylindrical coordinates is

$$\Gamma(R) = RV_{\varphi}(R) \tag{8-1}$$

and stream-function can be calculated as

$$\Psi_0(R) = \Psi(R,0) = \int V_X(R,0)RdR = \int f_0(R)RdR \tag{8-2}$$

Combine equations (8-1) and (8-2) by eliminating R, the relationship formula for vorticity by circulation and streamfunction can be

$$-\Gamma\frac{d\Gamma}{d\Psi} = F_{vorc}(\Psi) \tag{8-3}$$

Equation (8-3) can be represented as a polynomial approximation by interpolation or spline approximation $-\Gamma\frac{d\Gamma}{d\Psi} = \sum_0^N a_i\Psi^i$. Then the series a_i can be calculated. The more the interpolation points, the higher accuracy and the more a_i terms. Series b_i can be calculated in the same way. Through the calculations of a_i and b_i, the flow patterns of

experimental cyclones can be diagnosed. So we can decide on which combination of terms are important for a particular cyclone.

The analytical solutions with higher order of a_i and b_i have not been well studied. To study the flowfield characteristics of higher order of a_i and b_i, numerical method may be a good choice. The relationships between these a_i, b_i and flowfield characteristics can be discussed as in chapter 6 but numerically.

Here some findings will be highlighted and developed further. Application to practical design will be discussed.

8.1 SOME ANALYTICAL RESULTS

8.1.1 Flow patterns

For varying geometry and dimensions, the flow field of a cyclone should vary. Perhaps since the performance of normal cyclones used for same application is approached, their flowfields seem similar. This encourages people to describe the flowfield with a simple, unified model. "Simple functional forms are desired" Wakelin (1993). When some people find a model of a vortex flowfield, they tend to use it for most cyclones without discussing conditions of the cyclones. For example, the axial velocity is expressed as a linear function of axial distance in some models, and some experimental findings confirmed this expression, but some not. However this model tends to be used generally. By fitting the velocity profiles, many empirical expressions of flowfields have been made.

I found and studied a group of flow patterns of cyclones, which are a group of the exact solutions of the Euler equation with different vorticity distributions. More patterns can be obtained by finding the solutions raised by more terms a_i and b_i in the vorticity distributions, and more characteristics may be studied. But so far, I have already given some important analytical findings, which can guide the design of cyclones.

1. Some models were compared with some different experimental findings. The comparisons confirmed that the inviscid models could be used to describe the flowfield of normal cyclones outside of the core and wall boundary layers. So they may be used to study the characteristics of the flowfields.

2. The flowfields can be classified by several kinds of patterns. The flow with axial velocity decreasing linearly along axial distance is one of them. The flowfields described include: shortcut flow, direct flow, the flow with the axial velocity decreasing linearly along axial distance, the flow with the axial velocity decreasing along axial distance at different rates, multi-whirlpools flow and jumbled flow.

3. The distribution of vorticity across streamlines determines the flow patterns. It is very important to control this distribution to obtain the required flowfields.

8.1.2 Tangential velocity (mathematical proof and explanation from first principle)

Many investigators have reported that tangential velocity profiles within the main body of cyclones do not vary significantly in the axial direction, whilst radial and axial velocities do not influence the tangential profile. All my pattern models in this work indicate this result for high Swirl Number. However, when relative tangential velocity is low, the radial and axial velocities will have great effect on the tangential velocity profile. When the tangential velocity is high enough, it will be insensitive to the variations of axial and radial velocities, and seem self-similar. My models indicate that this insensitivity does not reciprocate. Small variation in distributions of tangential velocity will strongly influence the axial and radial velocities.

This finding can be simply explained from energy conservation law as follows:

Since the total pressure $h=\frac{p}{\rho}+\frac{v_\varphi^2}{2}+\frac{v_x^2}{2}+\frac{v_r^2}{2}$ should not change very much along a streamline in the main body of a cyclone, we can assume here for convenience that it is a constant. Also, we assume that static pressure is a constant along the axial direction in a streamline, and radial velocity can be neglected for its small value. So along a streamline parallel the axis, at two points 1 and 2, $\frac{v_{\varphi 1}^2}{2}+\frac{v_{x1}^2}{2}=\frac{v_{\varphi 2}^2}{2}+\frac{v_{x2}^2}{2}=$ constant. For a normal cyclone, $v_\varphi \approx 5v_x$, then $\frac{v_{\varphi 2}^2}{v_{\varphi 1}^2}-1=\frac{v_{x1}^2-v_{x2}^2}{v_{\varphi 1}^2}\approx\frac{v_{x1}^2-v_{x2}^2}{25v_{x1}^2}=0.04[1-\frac{v_{x2}^2}{v_{x1}^2}]$. When axial velocity increases by 100% ($\frac{v_{x2}}{v_{x1}}=2$), we get $\frac{v_{\varphi 2}}{v_{\varphi 1}}=0.938$ (tangential velocity decreases 6%); While axial velocity decreases by 100% to zero ($\frac{v_{x2}}{v_{x1}}=0$), we get $\frac{v_{\varphi 2}}{v_{\varphi 1}}=1.02$ (tangential velocity increases by 2%).

The significance of this conclusion in velocity modelling is that a simple, unified equation may be expected to model the tangential velocity profile for the purpose of design, and while the effects of v_x and v_r may be neglected, the effects of viscous friction (h changing) and pressure (p changing) may be more important. Perhaps, that is why Burgers' tangential velocity equation has been found to have a good agreement with experimental results.(Wakelin 1993).

For design, a dynamic force balance on a particle should be studied. The centrifugal force, determined by tangential velocity, will make the particle move outward, the fluid moving inward with its radial velocity will drag the particle to the central region. A small variation of tangential velocity profile will not change the centrifugal force very much, but may change the radial velocity thoroughly. The designer should choose the tangential velocity profile more for radial velocity considerations than for centrifugal force.

8.1.3 "Air core" (mechanism and calculation)

It is easy to observe a "air core' in a high efficiency hydrocyclone. The fluid coming from the main body of the hydrocyclone will not flow into the "air core". When people study the flowfield in a hydrocyclone, the "air core" will be well recognised. There should be a "air core" (a central isolated region) in a high efficiency gas cyclone also, and the fluid coming from the main body of the cyclone will also not flow into the isolated region. Since the central isolated region cannot be easily observed, the fact has not been generally recognised. Normally, when people analyse or model the flowfield, even when recording the experimental results, they describe the flowfield as a whole as a matter of course. My theory indicates that a central isolated region will occur inevitably in a high efficiency gas cyclone. Wakelin's observation of reverse flow in the centre (reverse to the general exit flow) supports this statement. (Wakelin, 1993). The streamlines measured by Smith's (1962) showed the central isolated region very clearly in his gas cyclone.

The total pressure h is again assumed as a constant along a streamline near to the wall boundary layer, and circulation C assumed constant also. At point 1, near to the wall boundary at upper boundary, and point 2, in the same streamline as point 1 but on the isolated surface (surface of the air core),

$h = \frac{p_1}{\rho} + \frac{v_{\varphi 1}^2}{2} + \frac{v_{x1}^2}{2} + \frac{v_{r1}^2}{2} = \frac{p_2}{\rho} + \frac{v_{\varphi 2}^2}{2} + \frac{v_{x2}^2}{2} + \frac{v_{r2}^2}{2} =$ constant, and since $v_{r1} = v_{r2} = 0$, and

$C = r v_\varphi =$ constant, $\frac{p_1}{\rho} + \frac{C^2}{2r_1^2} + \frac{v_{x1}^2}{2} = \frac{p_2}{\rho} + \frac{C^2}{2r_2^2} + \frac{v_{x2}^2}{2}$,

$$r_2 = \left[\frac{1}{\frac{2\Delta p - \rho v_{x2}^2 + \rho v_{x1}^2}{\rho C^2} + \frac{1}{r_1^2}}\right]^{0.5} \qquad (8\text{-}4)$$

where $\Delta p = p_1 - p_2$, v_{x1} and v_{x2} can be calculated with the pattern equations given previously.

From equation (8-4), we can reckon that the larger the circulation on the streamline near to wall boundary layer, the larger the radius of the isolated region. Only when the

circulation in the streamline is zero, the radius of central region can be zero, then no central region occurs. This is possible if the vortex strength is low. If the circulation on the streamline near to the wall boundary layer is low enough, the radius of the "air core" should be very small, and very near the axis. The streamlines through the boundary layer will *form* the central core, and the axis will begin from a point on the wall or on the bottom. The central core can absorb some rotationed energy through the boundary surface of the core, and this will make the radius smaller. The "boundary layer core" can remain. If the circulation on the streamline near to the wall boundary layer is high enough, the radius of the "air core" should be large. The "boundary layer core" will absorb some rotation energy from the main body, and will be broken up to spin with the main body.

Another inference is that the larger the pressure difference, the smaller the radius. When the collection bin or exit tube are open to air, the pressure difference is smaller, and the radius will be larger. When collection bin and exit tube are closed, the pressure difference will be larger (the limit of p_2 is absolutely vacuum), and the radius will be smaller.

For a certain flow pattern in the main body, several flow patterns of the central isolated region may be matched according to the tangential velocity, and the structures of collection bin and exit tube. If the bin is open, a direct flow can pass through the central region from bin to exit tube; if the exit tube is open to the air and the bin is closed, a return flow cell with down flow inside and up flow outside may be formed. If both bin and vortex finder are closed, a bubble or several bubbles or a return flow cell may be formed.

A further calculation of central isolated region is complex, if the viscous action is considered. I have found some solutions to deal these conditions. I will not introduce them here.

The estimation of the radius of a central isolated region is important for efficiency prediction, and sometimes the flow pattern of the central region may have some effect on separation performance if the re-entrainment of particles from the collection bin

occur. The internal flow pattern of the central region will affect the pressure drop of cyclone heavily.

8.1.4 Shortcut flow and eddy flows

The flow that goes from the upper stream boundary region directly into the vortex finder is called as "shortcut flow". This flow will not go into the main body of a cyclone. Some people thought that this flow most credibly originated from boundary layer flow passing radially inward across the cyclone roof. My theory indicates that the boundary layer flow may be one of the reasons for shortcut flow, but not the only one. Some shortcut flows can be described by term Ψ_4^* in chapter 5 and the term can describe only potential flow, which cannot be boundary layer flow. Some experimental findings can support this statement, since some cyclones such as Smith's (1962a) have no roof, but have the shortcut flow. The term Ψ_4^{**} in chapter 6 can describe the shortcut flow for both potential flow and flows with vorticity.

For a desired cyclone performance, a certain flow pattern is required. The pattern is determined by the distribution of vorticity across the streamlines. This vorticity makes fluid elements rotate, and then they follow different flow tracks. People have previously looked for the required flow pattern by experiments. The required pattern may possess some characteristics, such as the locus of zero vertical velocity, which cannot often match the upper boundary. Some "adjusting flow" is then needed to match the flowfield of the main body and the upper boundary. The "adjusting flow" will not go into the main body of the cyclone, and may form a shortcut flow if it goes to vortex finder very directly.

In some cyclones, a vertical upward flow can exist in the region outside of the radius of the outer wall of the vortex finder. This exists in the form of a recirculating eddy or eddies. This can be regarded as the result of a non-match of the main flow field and the position of the vortex finder.

In the bottom of cyclones, a "fast adjusting flow" can also be found from my calculations. This flow is also due to Ψ_4^*, and it can effect lower boundary region only.

In general, to avoid the recirculating zone or the short-circuit flow, one needs to match the radius of the vortex finder wall with the locus of zero vertical velocity according to the relationships among circulation, total pressure and streamfunction at the upstream boundary.

8.2 A CONCEPT OF OPTIMUM DESIGN AND A DESIGN PROCEDURE

8.2.1 An optimum structure for clarification

For clarification, all the particles should be separated from the fluid. A dynamic force balance on the particle itself determines the motion of a particle. By balancing the centrifugal force against the radial drag force we can obtain the particle slip velocity. If the particle slip velocity + fluid radial velocity = zero, the particle will move in a circle. If the value of the slip velocity is larger than that of the fluid radial velocity, the particle will move toward the cyclone wall. If the value of the slip velocity is smaller than that of the fluid radial velocity, the particle will move toward the central area.

If the radial velocity is zero in the whole flowfield of a cyclone, the particles will, theoretically, be totally separated. The 'cylindrical flow' in which radial velocity is zero does exist, but this concept has not been used to design return flow cyclones. Since the fluid in a return flow cyclone will flow from outside vortexes to inside vortexes, radial velocity must not be zero in the whole flowfield. For cylindrical cyclones, if we make radial velocity zero in the upper portion, the radial velocity should be larger than normal in the lower portion. For conical cyclones, it is impossible to find a main portion in which the radial velocity is zero.

My concept for an 'optimum' cyclone for clarification is to establish a flowfield in the upper cylindrical portion with a radial velocity of zero. In the lower conical portion the radial velocity should change uniformly along the spherical radius. Some underflow is needed to carry the particle to the bin. This kind of flowfield appears to exist, and it is described by the combination of my flow patterns (Conical pattern III & Cylindrical pattern III). In these two patterns, the motion equations are the same except at different coordination. They have the same relationships between total pressure, circulation and streamfunction, so they can match each other.

For this optimum cyclone, any particles that are heavier than the fluid will move towards the cyclone wall in the cylindrical portion. No particles can escape into the vertex finder from this portion. If the portion is long enough, all the particles will move into a region close to the wall, where streamlines are almost parallel to the wall. In the conical portion, the particles will separate from the streamlines they were in, to the next line toward the wall. A good design should ensure that few particles from the upstream region would escape into the core region from this section. At the entrance of the bin, some fluid carries the particles into the bin. The return flow from the bin will carry very small particles. According to Abrahamson (1978), collection in the bin must depend on particle agglomeration. These small particles may move towards the wall when travelling through the conical portion, they must move towards the wall when travelling through the cylindrical portion. They can then travel between the upstream outside vortex and the downstream inner vortex. When this kind of motion is repeated many times a dust cloud is formed. By increasing the density of this cloud of small particles, the particles will contact and agglomerate. When they become large enough, they will be separated. This idea first published by Abrahamson in 1978 with measures on bins.

Since the particle trajectories can be calculated if the flowfield is given, dimensions can be theoretically determined for optimum performance.

The optimum structures are different for different purposes, and we can choose the appropriate optimum structures following the same way.

8.2.2 A design procedure for clarification

A design procedure for clarification will be described sketchily as follows.

1. Choose the inlet structure according to the requirement of clarification, normally the structure for conical pattern III & cylindrical pattern III. (Since I find that the flow patterns are determined by the inlet structures, I have been thinking how to realise the structures for a long time. This work has exceeded the requirement for a PhD, so I will introduce and develop further this work later.)

2. Calculate the trajectory of a minimum size of particle to be separated, from the bottom of vortex finder to the cylindrical portion wall, to obtain the relationship of the radius R_{cy} and the length L_{cy} of the cylindrical portion. After the particle has travelled a distance of L_{cy} along the axial direction, it will touch the wall.

3. Determine the radius R_{cy} and conical angle α by the saltation velocity according to the flow rate.

4. Determine the radius of the entrance and structure of bin according to the solid flow characteristics of particle and re-entrancement.

5. Determine the radius of vortex finder according to the pattern characteristics such as the locus of zero vertical velocity. Some "adjusting flow" may be needed if the effect on efficiency of "shortcut flow" can be controlled or neglected.

6. Calculate the radius of the central isolated region, then go step 2 to modify the calculation until a closed result is obtained.

Further optimum choice may be made between L_{cy}, R_{cy} and α. Since a particle may keep going to the wall in the conical portion, it is possible to decrease L_{cy}.

The dimensions calculated should satisfy separation performance. To decrease pressure drop, lower velocity may be chosen. The re-iteration can start from step 3, an optimum process can be made between pressure drop, capital (materials), space and mainenance (wear). For a more complete optimisation process, the performance of the inlet should also be considered.

My theory and calculation are based on the inviscid flow. For the real flow, some vorticity will be introduced from wall boundaries into the flowfield, and the flow patterns may be changed. A modification to the structures can be made with CFD. Other factors, such as flow instability, boundary layer, re-entrancement, effect between particles and between particle and fluid may need to be studied if they show their disturbance in the design. Fortunately, many researchers have achieved some results about the effects of practical factors on the performance of cyclones. All the knowledge could be gathered to enrich our understanding of the real flow in cyclones.

After the design method becomes mature, it can be programmed into software. So what will be left for the design engineers? —Input the data required for design to their computers, then pick up the design drawings from the printers.

In last 3 years, I have been trying to find the relationships between geometry (especially inlet geometry) and flow patterns. The final result has not been found, but some knowledge on flowfields in cyclones can be summarised.

- The distribution of vorticity over streamlines determines the flow patterns. It is very important to control this distribution in the upstream region to obtain the required flowfields.
- The 'Natural length' should be controlled by inlet geometry.
- In most efficiency prediction models, the radial velocity profiles are desirably assumed as a function of radius alone. These kind of flowfields are obtainable, but not the best.

- The tangential velocity profiles have been proved as self-similar at high Swirl Number from first principles.
- In general, to avoid the recirculating zone and the short-circuit flow, one needs to match the radius of the vortex finder wall with the locus of zero vertical velocity according to the relationships among circulation, total pressure and streamfunction at the upstream boundary. Or a new cyclone geomitry may be suggested.
- Most 'slot-entry' cyclones can be described by conical pattern V.
- More patterns with high order of a_i and b_i have been studied numerically, and a_0 and b_0 have been proved as main terms.
- A new concept cyclone with zero radial velocity in the upper separate region is proposed.

References

Abrahamson, J., (1981) "Mechanisms of dust collection in cyclones". *Ch. in Progress in Filtration and separation*, Vol. 2 ed. by R. J. Wakeman, Elsevier, Amsterdam pp1-74.

Batchelor, G.K., (1967), *An introduction to Fluid dynamics*. Cambridge Univ. Press London, (U.K.).

Barth, W., (1956), "Design and layout of the cyclone separator on the basic of new investigations" *Brenn. Warme Kraft,* **8** , p1-9.

Beeckmans, J. M., (1972), "Steady-state model of the reverse-flow cyclone", *J. Aerosol Sci,* **3**, 491.

Beeckmans, J. M., (1973), "A two-dimensional turbulent diffusion model of the reverse-flow Cyclone", *J. Aerosol Sci,* **4**, 329-336.

Bellamy-Knights, P. G., (1970), "An unsteady two-cell vortex solution of the Navier-Stokes equation", *J. Fluid. Mech*, **41**, 673.

Bhattacharyya, P. (1980), "Theoretical study of the flow field inside a hydrocyclone with vortex finder diameter greater than that of apex opening, I. Laminar case, II. Turbulent case". *Appl. Sci. Res.*, **36**, 197-225.

Bloor, M.I.G. and Ingham, D.B., (1975), "Turbulent spin in a cyclone" *Trans. Instn. Chem. Engrs.*, **53**, p1-6 .

Bloor, M.I.G. and Ingham, D.B., (1987), "The flow in industrial cyclones" *Journal of Fluid Mechanics*, **178** , p 507-519 .

Bradley , D. and Pulling, D. J., (1959) "Flow patterns in the hydraulic cyclone and their interpretation in terms of performance". *Trans. Instn. Chem. Eng.*, **37** , 34-45.

Burgers, J. M., (1948) "A mathematical theory illustrating the theory of turbulence", *Advances in Appl. Mech.*, **1**, 198.

Dabir, B., and Petty, C. A., (1986), "The measurements of mean velocity profiles in a hydrocyclone using laser Doppler anemometry". *Chem Eng Commun.*, **48**, 377-388.

Day, W. R. & Grichar, C. N. "Hydrocyclone Separation. In Schweitzer, P. A". *Handbook of separation Techniques for Chemical Engineers.*, McGraw-Hill Book Company, p4-135.

Dietz, P. W., (1981), "Collection efficiency of cyclone separators", *AIChE J.*, **27**, 888-892.

Dirgo, J. & Leith, D. Design of cyclone separators.***

Donaldson, C. P. & Sullivan, R. D., (1960), *In Proceedings of the 1960 Heat Transfer Fluid Dynamics Inst*, Stanford Univ Press, Stanford, CA.

Gupta, A.K., Lilley, D.G. and Syred, N., (1984), *Swirl Flow*, Abacus Press, p 301

Hoffmann, A. C. and others, (1996), "Effect of the dust collection system on the flowpattern and separation efficiency of a gas cyclone", *The Canadian Journal of Chemical Engineering*, **74**, 464-470.

Hejma, J., (1971), "Influence of turbulence on the separation process in a cyclone" *Staub-Reinhalt. Luft*, **31**, no7.

Hsieh, K.T. and Rajamari, R.K., (1991), "Mathematical model of the hydrocyclone based on physics of fluid flow". *A.I.Ch.E. J.*, **37** no.5, 735-746.

Iozia, D. L. And Leith, D., (1989), "Effect of cyclone dimensions on gas flow patterns and collection efficiency". *Aerosol Science and Technology*, **10**, 491- 500.

Jackson, R., (1963), "Mechanical equipment for removing grit and dust from gases".

The British Coal Utilisation Resear Association, p108

Kelsall, D.F., (1952), "A study of the motion of solid particles in a hydraulic cyclone" *Trans. Instn. Chem. Engrs.*, **30**

Knowles, S. R., Woods, D. R. and Feuerstein, I. A., (1973), "The velocity distribution within a hydrocyclone operating without an air core". *Can. J. Chem. Eng.*, **51**, 262-271.

Leibovich, S., (1984), "Vortex stability and breakdown: Survey and Extension". *AIAA J.*, **22**, 1192-1206.

Mayer E.W. and Powell K.G., (1992), "Similarity solutions for viscous vortex cores". *J. Fluid Mech.*, **238**, 487-507.

Mager, A., (1972), "Dissipation and breakdown of a wing-tip vortex", *Journal of Fluid Mechanics*, **55**, 609-28,

Ogawa, A., (1984), "Estimation of the collection efficiencies of the 3 types of cyclone dust collectors from the standpoint of the flow patterns in the cylindrical cyclone", *J.S.M.E. Bull*, **27** n222, p64.

Ogawa, A., (1987), "Theoretical consideration of the pressure drop of the cylindrical cyclone dust collectors", *Nihon University publication*, Japan

Ohashi, H. and Maeda, S., (1958), "Motion of water in a hydraulic cyclone". *Chem. Eng. Japan*, **22**, 200-210.

Pervov, A.A., (1974), *Chem. & Petrol. Eng.*, **10**, p898.

Phillips, H., (1991), "Modified Burgers equation for tangential velocity modelling". personal comm from SPS Harwell to J. Abrahamson.

Reyna, L.G. & Menne, S., (1988), "Numerical prediction of flow in slender vortices",

Computers Fluids, **16 (3):**, 239-256.

Rietema, K., (1961), "Performance and design of hydrocyclones: I. General considerations; II Pressure drop in the hydrocyclone; III. Separating power of the hydrocyclone; IV. Design of hydrocyclone". *Chem. Eng. Sci.*, **15**, 298-325.

Rott, N., (1958), "On the viscous core of a line vortex", *ZAMP*, **9**, 543

Sevilla, E. M. & Branion R. M. R., (1997), "The fluid dynamics of hydrocyclones", *Journal of pulp and paper science*, **23**, J85-J97.

Smith, J.L., (1962), "An experimental study of the Vortex in the Cyclone Separator" *J. Basic Eng. Trans. A.S.M.E.*, **84D**, p602.

Soo, S.L., (1989), *Particulates and continuum multiphase fliud dynamics.* Hemisphere Publishing Corporation.

Stairmand, C.J., (1951), "The design and performance of cyclone separators" *Trans. Instn. Chem. Engrs.*, **29**, p356.

Swift, P. **** Steam Heat. Eng. 38: 453***, 1969.

ter Linden, A.J., (1953), "Cyclone dust collectors for Boilers" *Trans. ASME*, **75**, p433.

THE OXFORD ENGLISH DICTIONARY, (1933), Clarendon, Oxford University Press.

THE NEW SHORTER OXFORD ENGLISH DICTIONARY, (1993), Oxford, Clarendon Press.

Tran, T.V., (1981), "Experimental and theoretical studies on gas cyclone separators operating at high efficiency", unpublished PhD thesis, Uni Minnesota.

Vatistas, G.H.; Kozel, V & Mih, W.C., (1991) "A simpler model for concentrated vortices", *Expts in Fluids*, **11**, p73.

Wakelin, R.F., (1993), "Vortex breakdown in dust-collecting return-flow cyclones", Christchurch, Canterbury University, (Thesis: Ph.D: Chemical and Process Engineering).

Wolbert, D. and others, (1995), "Efficiency estimation of liquid-liquid hydrocyclones using trajectory analysis", *AIChE Journal,* **41**, 1395-1402.

Yoshida, H. and others, (1991), "Size classification of submicron powder by air cyclone and three-dimensional analysis", *Journal of chemical engineering of Japan,* **24**, 641-647.

Zhou, L. and others, (1988), "Study of structure parameters of cyclones", *Chem Eng Res Des*, **66**, 114-121.

Zhou, L.X. & Soo, S.L., (1990), "Gas-solid flow and collection of solids in a cyclone separator", *Powder Technology,* **63**, 45-53.